

Project Progress

ID 5281

Application of remote sensing to hydrology and water resources management

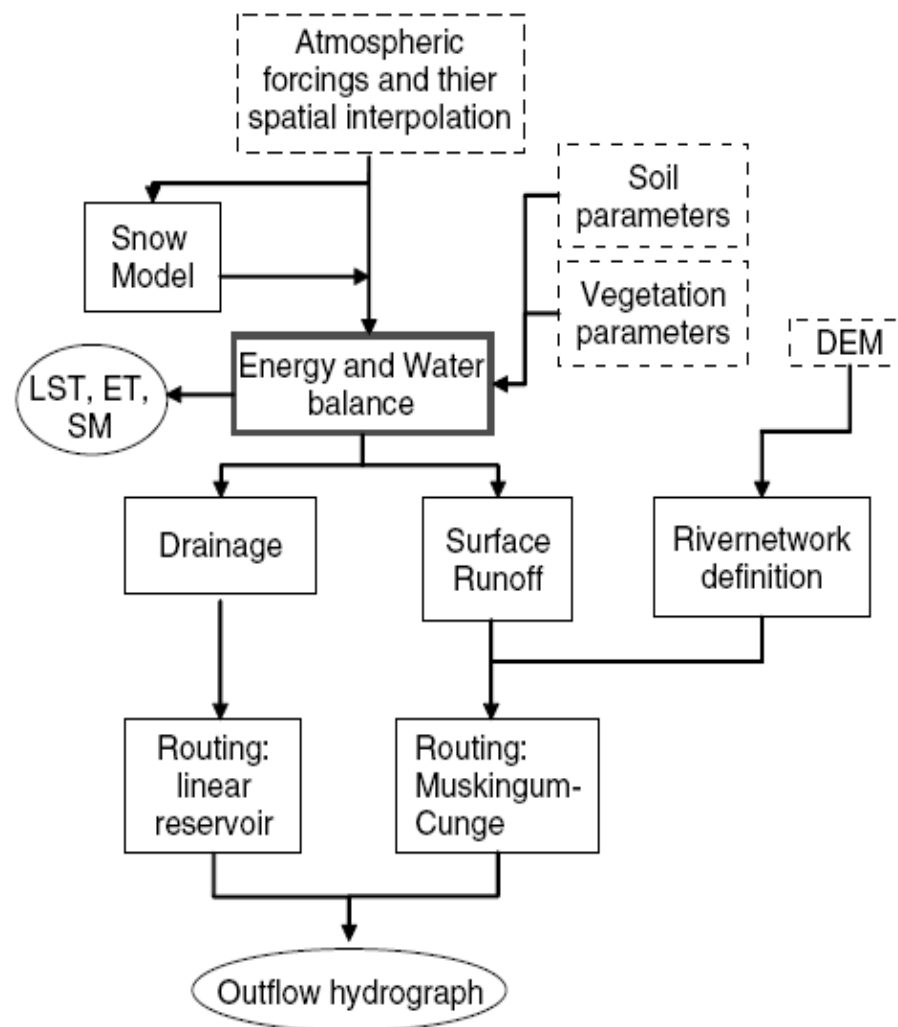
21 June 2011

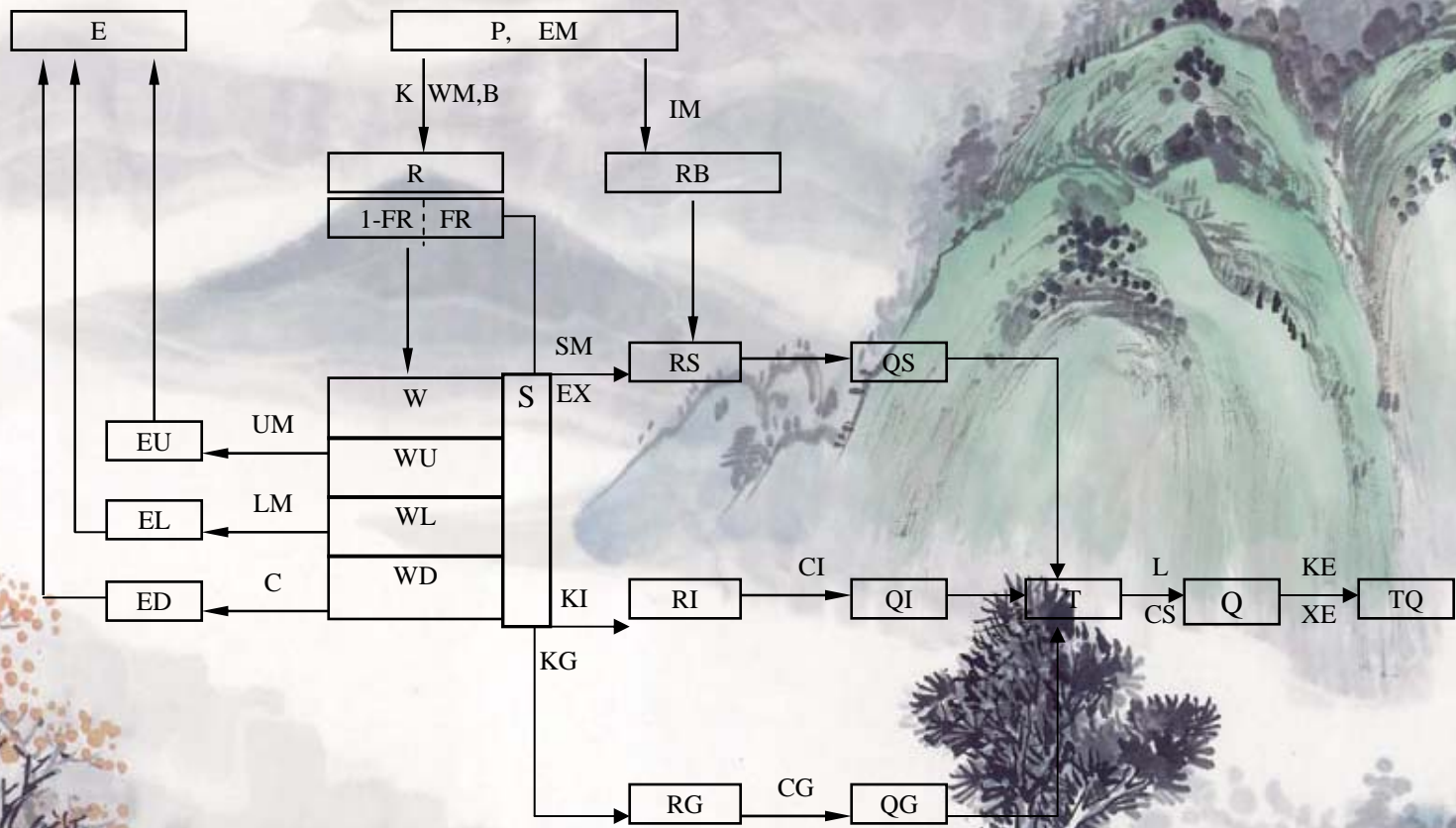
Main Results

- 1) Preparation for distributed hydrological model application in the Changjiang River Basin**
- 2) Quantitative soil erosion model**
- 3) Analysis of effect of operation of Three Gorge Hydropower Plant on downstream area**
- 4) Water pollution monitoring and assessment**
- 5) Assimilation of remotely sensed for flood extent**

1) Preparation for distributed hydrological model application in the Changjiang River Basin

Through FEST-EWB model, introduction of energy balance into the Xinanjiang Distributed Model which is very widely used in China and based on water balance in order to further improve the accuracy for real-time hydrological forecasting and water resources assessment

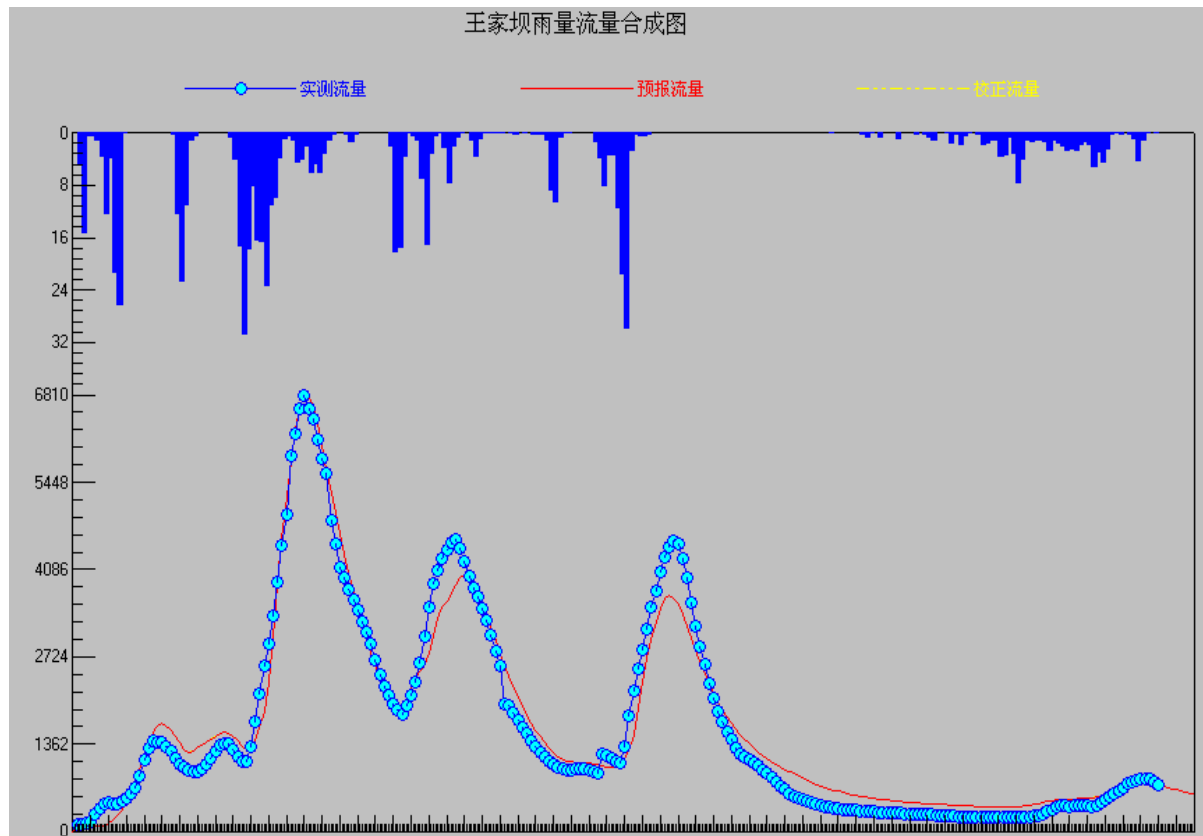




Flow chart of the Xinanjiang Model

Inputs, outputs and state variables are written within the blocks, while the parameters are written outside of blocks.

Comparison between predicted and observed hydrograph at Wangjiaba Station, Huaihe River



Preparation

- 1) Test area: Daning River Watershed, located in the upstream of the Changjiang River**
- 2) Data: hydrological, topographic, meteorological data and historical data of remote sensing images.**
- 3) Document for application of Chinese National Project**
- 4) Expenditure for visit of Italy experts**

2) Quantitative soil erosion model

**Improvement of parameter arithmetic in RUSLE
(revised universal soil loss equation)**

**Determination of parameters in regions with
different soil (brown earth, loess, red soil, black
soil, calcic cinnamon soil)**

Soil erosion monitoring network and management system for whole country

全国水土保持监测网络和信息系統

水利部水土保持监测中心
北京地拓科技发展有限公司

水土保持公务管理信息系統	预防监督管理系統	<p style="color: green; font-size: 1.2em;">水土保持公务管理系统分为： 项目管理系统和预防监督管理系統</p>
水土保持监测预报信息系統	项目管理系统	
水土保持WebGIS系統		
维护管理系统		
水土保持辅助规划设计		
退出		



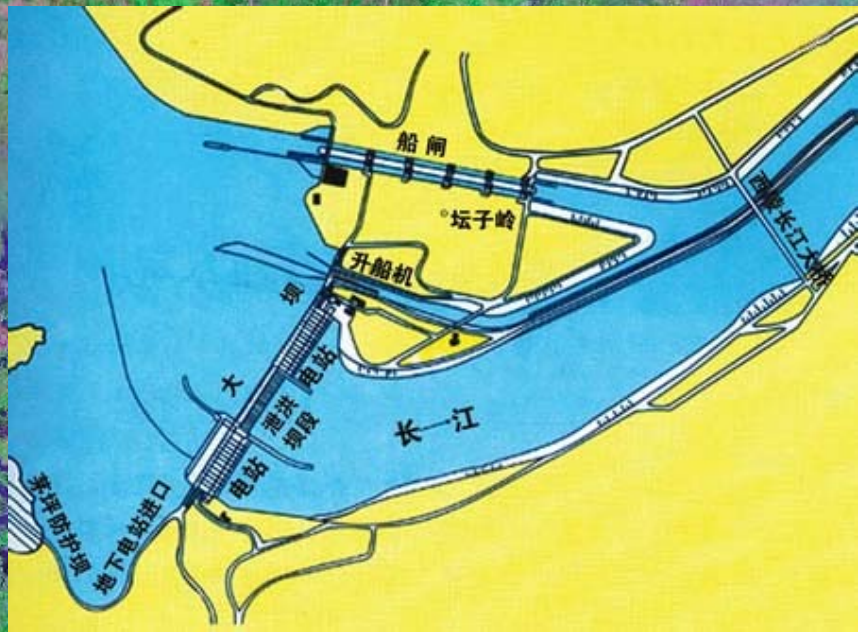


3) Analysis for effect of operation of Three Gorge Hydropower Plant on downstream area

Drought

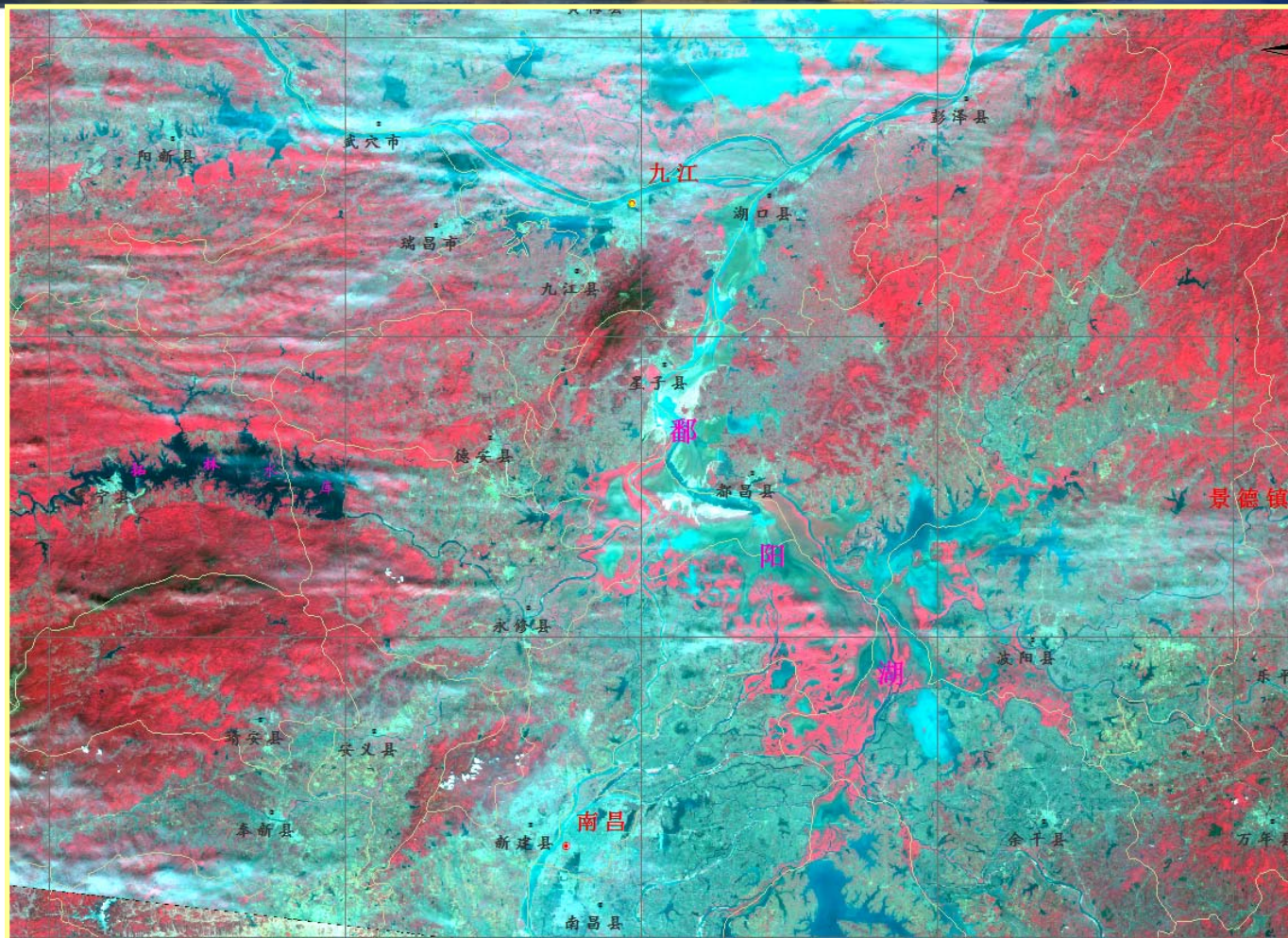
It is important to distinguish the climatic change of the downstream basin with the effect from operation of Three Gorge Hydropower Plant

Three Gorge Dam



Dongting Lake

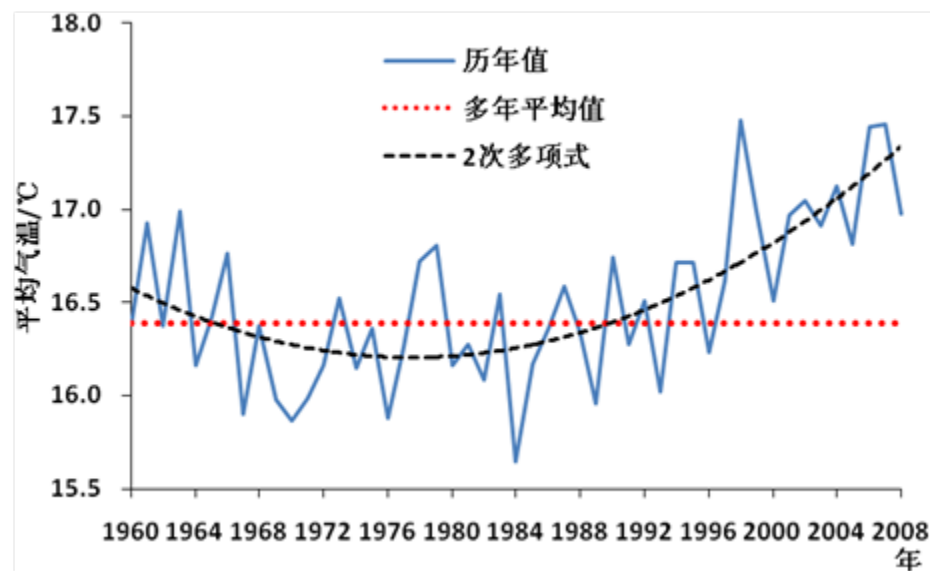
Poyang Lake



The Poyang Lake on April 23th by HJ-1A

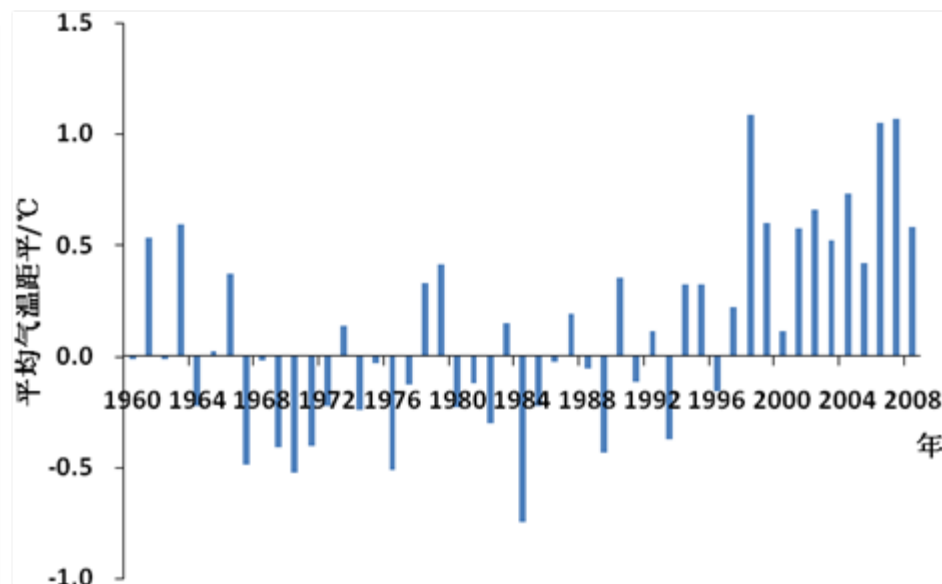
Temperature

Yearly mean temperature

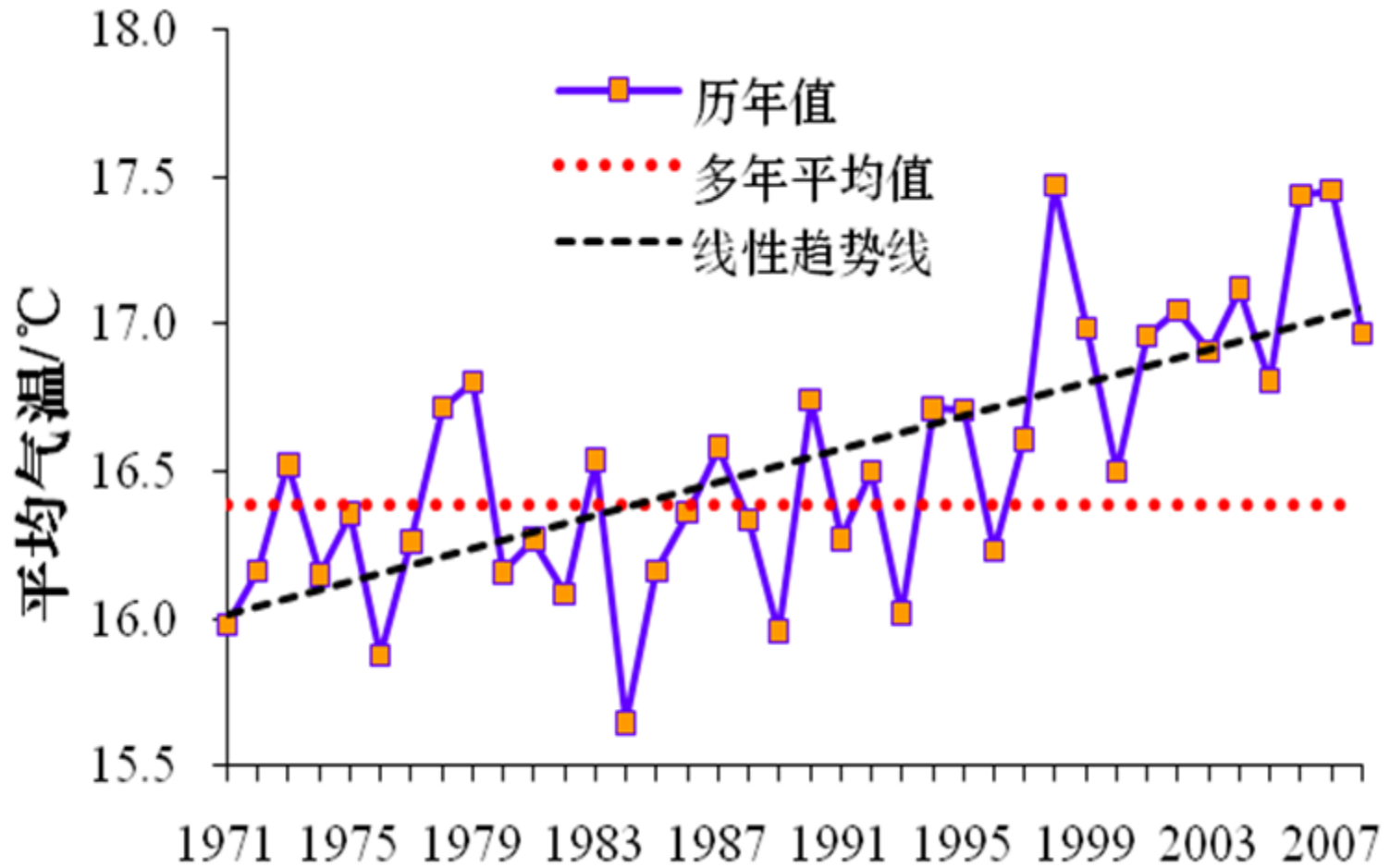


(year)

Yearly mean temperature anomaly



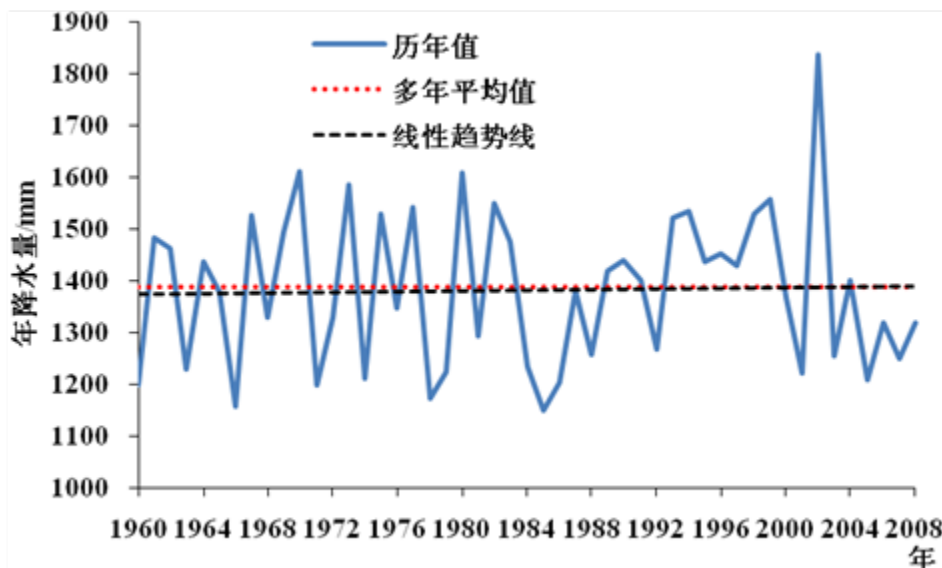
(year)



Temperature variation

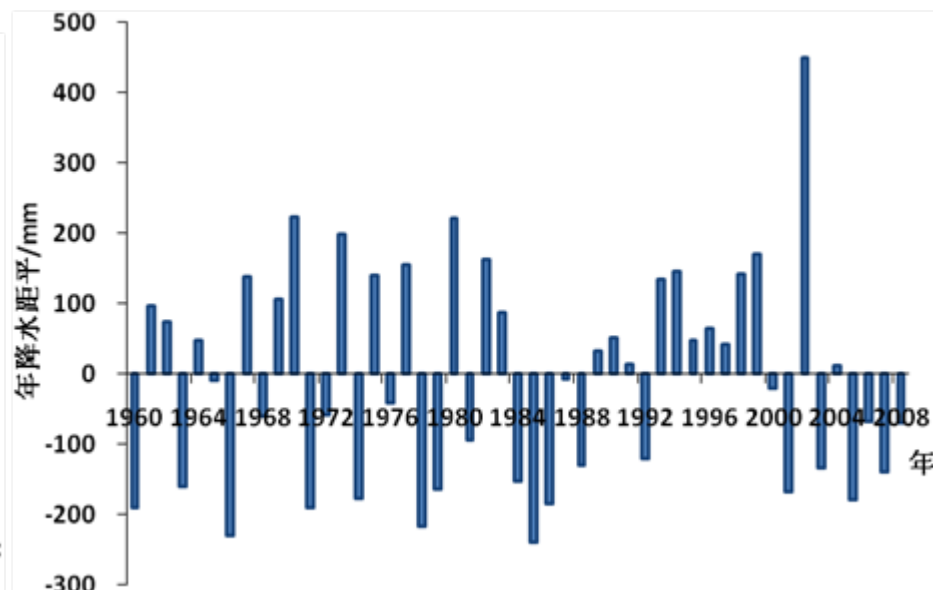
Precipitation

Annual precipitation



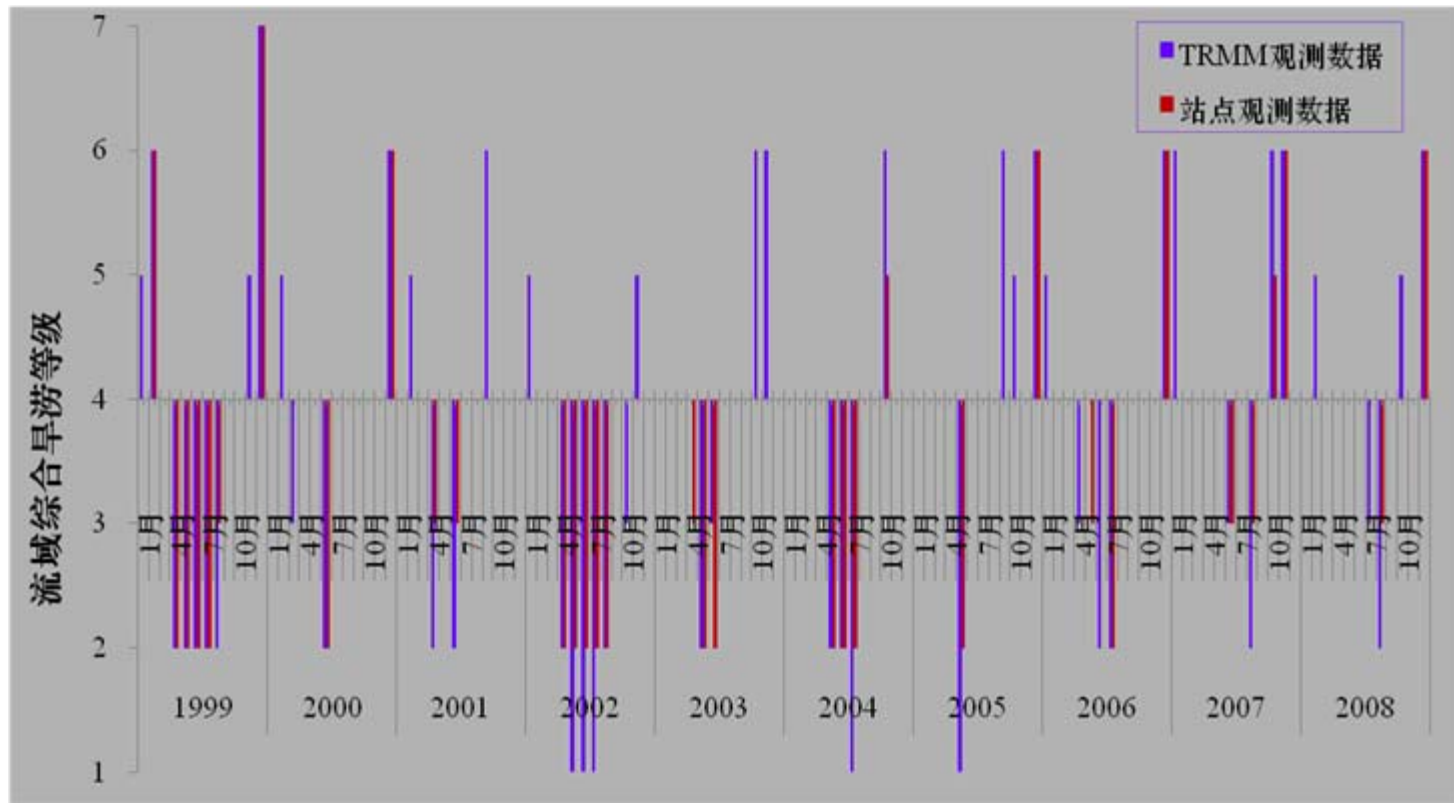
(year)

Annual precipitation anomaly



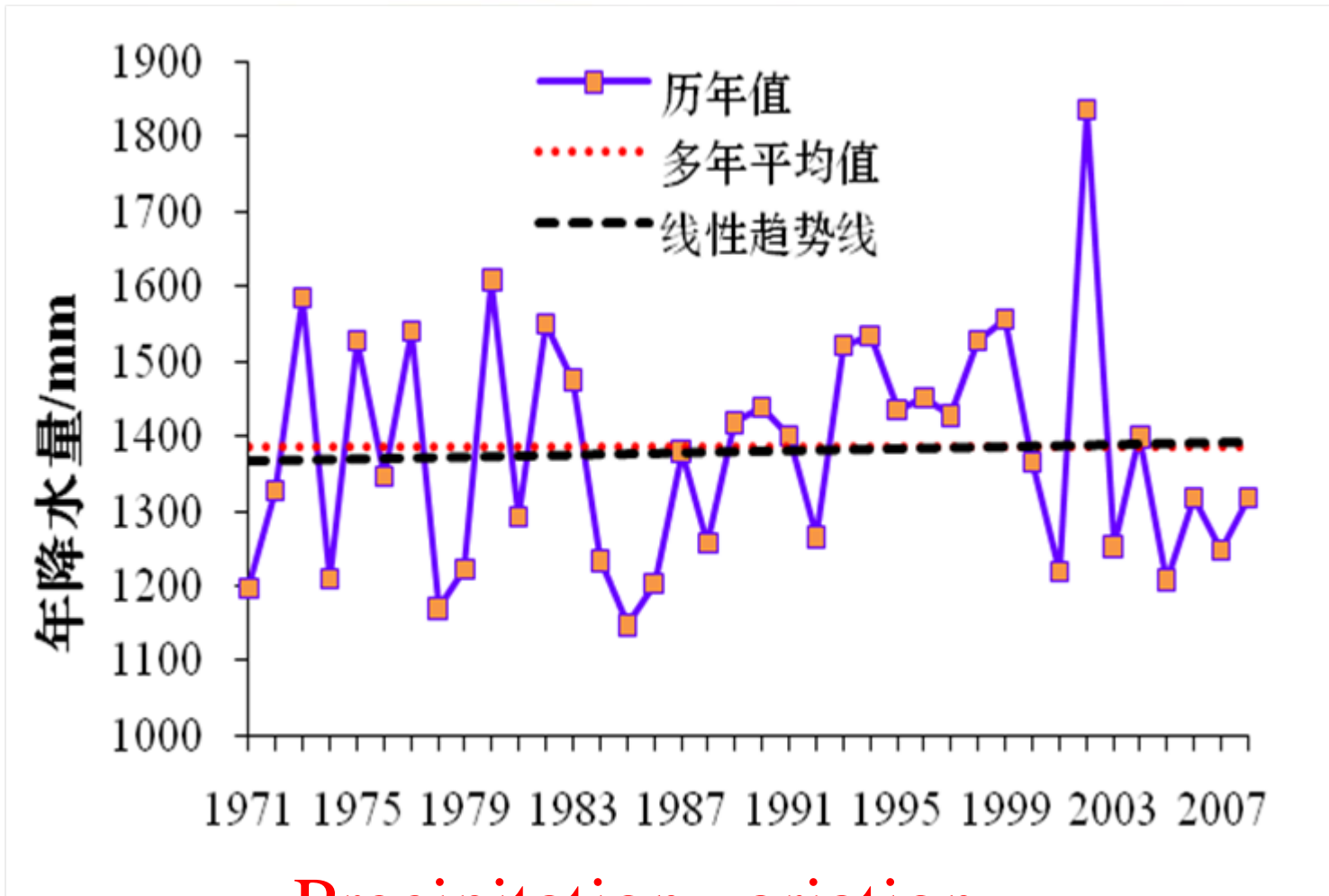
(year)

Spatial-temporal characteristics of precipitation in the Dongting Lake Basin from 1960 to 2008



Flood

Drought



Precipitation variation

In this spring and early summer (from January 1st to May 8th), the rainfall in downstream area (Hubei, Hunan, Jiangsi, Anhui, Jiangsu, Zhejiang, Shanghai) is only 242mm, 245mm less than the average one, being the minimum in recent 60 years.

Due to serious drought in downstream area of the Three Gorge Dam, such as the Hubei, Jiangsi, and Jiangsu provinces, the Three Gorge Hydropower Plant released a lot of water for drought relief. The release discharge increased to 12000m³/s. In fact, without the Three Gorge Reservoir, the drought would be more serious.

Conclusion

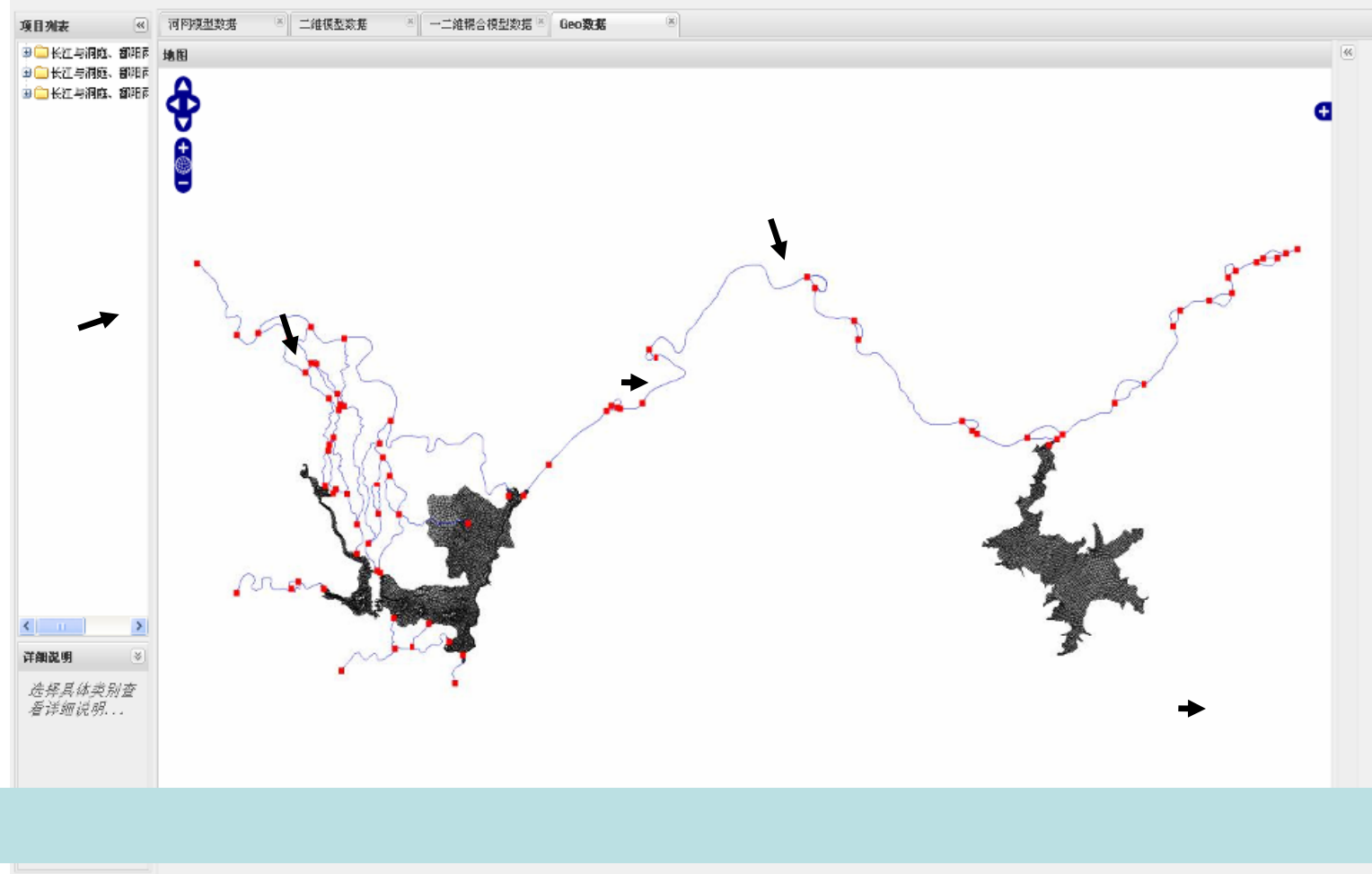
The rule of the Three Gorge Reservoir is flood control, power generation and navigation, but it still plays certain role to drought relief for downstream area.

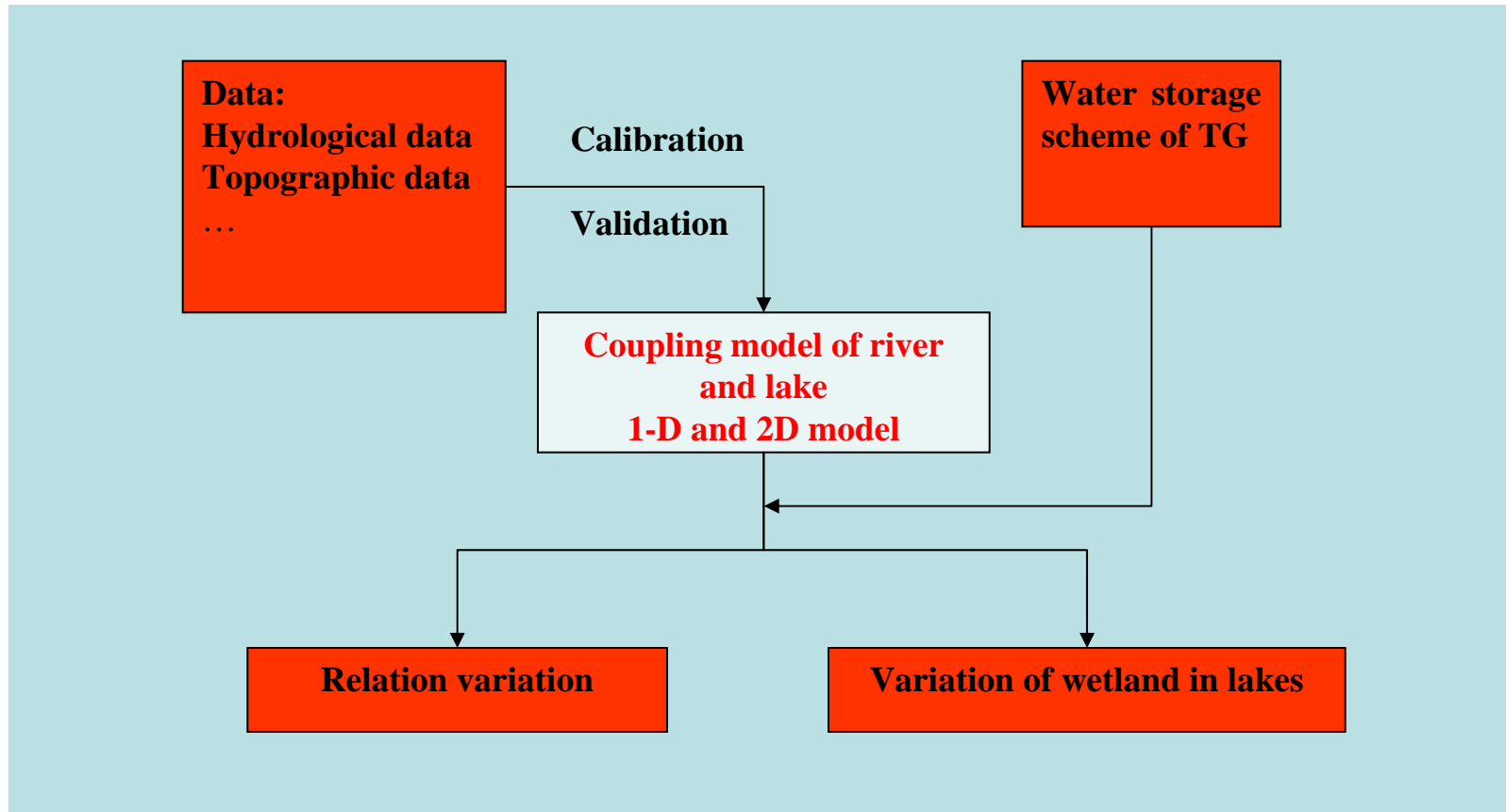
Also, during this period, the water surface areas of the Poyang Lake and the Dongting Lake decreased rapidly, being 1/3 as normal. The most important reason of course is the drought. Through hydrodynamic calculation, the reason can be concluded as follows.

- (1) Due to sand mining on outlet of lake, the bed slope and the discharge from the lake to the Changjiang River increased.
- (2) The control of reservoirs in branches decreased the inflow of the lakes.
- (3) The water level of the Changjiang River was low, it can not back the water from lake to river.
- (4) The water released from the Three Gorge Reservoir is clear water with lower sediment concentration, the scour and filling conditions are changed in the Changjiang River.

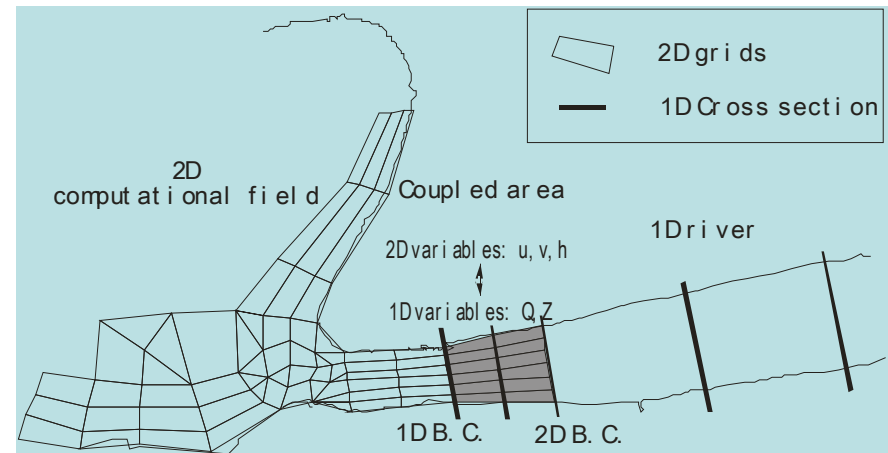


水环境动力模型系统





- **Key issue:**
Linkage of 1-D and 2-D models



$$Q = \sum h(un_x + vn_y)$$

$$Z = \bar{z}$$

$$\frac{\partial Q}{\partial t} + \frac{\partial}{\partial x}(uQ) + gA \frac{\partial \zeta}{\partial x} + gA \frac{Q|Q|}{A^2 C^2 R} + \frac{Q}{A} q = 0$$

$$\frac{\partial AS}{\partial t} + \frac{\partial}{\partial x}(QS) = \frac{\partial}{\partial x} \left(AD \frac{\partial S}{\partial x} \right) - AKS + C_2 q$$

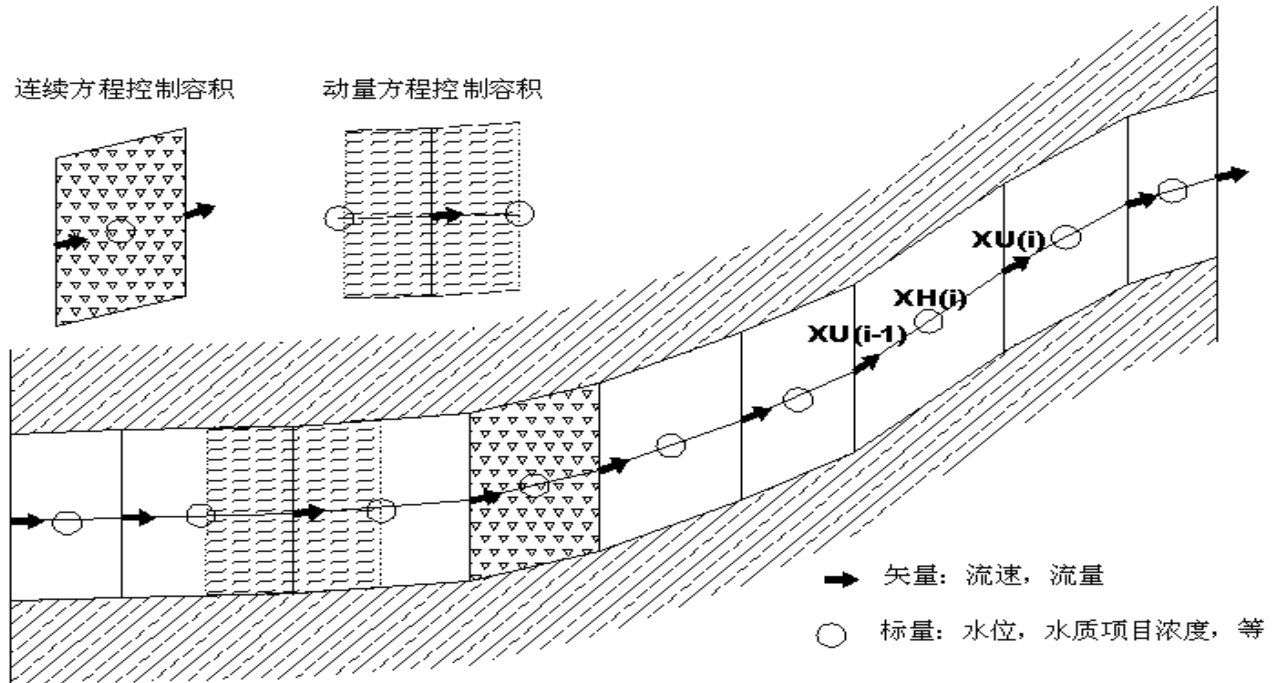
$$\frac{\partial Q}{\partial x} + B \frac{\partial \zeta}{\partial t} = q$$

Equation

Section

连续方程控制容积

动量方程控制容积



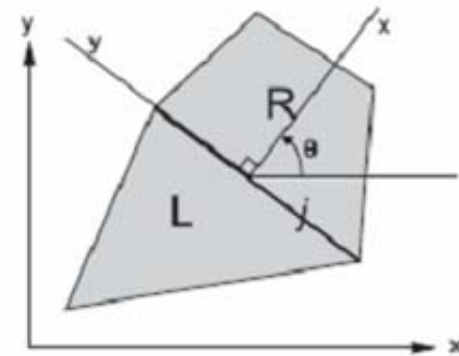
2D flood model

2D shallow water equations

$$\frac{\partial h}{\partial t} + \frac{\partial hu}{\partial x} + \frac{\partial hv}{\partial y} = 0$$

$$\frac{\partial hu}{\partial t} + \frac{\partial hu u}{\partial x} + \frac{\partial hv u}{\partial y} = -gh \frac{\partial Z}{\partial x} + \frac{1}{\rho} \left(\frac{\partial h \tau_{xx}}{\partial x} + \frac{\partial h \tau_{yx}}{\partial y} \right) + \frac{1}{\rho} (\tau_{zxs} - \tau_{zxb}) + fvh$$

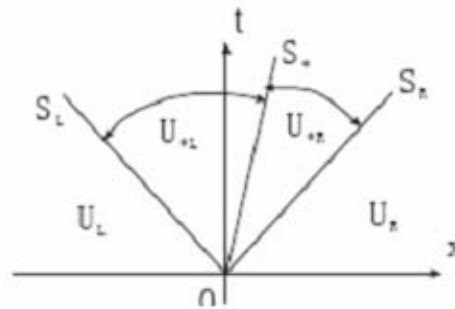
$$\frac{\partial hv}{\partial t} + \frac{\partial hu v}{\partial x} + \frac{\partial hv v}{\partial y} = -gh \frac{\partial Z}{\partial y} + \frac{1}{\rho} \left(\frac{\partial h \tau_{xy}}{\partial x} + \frac{\partial h \tau_{yy}}{\partial y} \right) + \frac{1}{\rho} (\tau_{zys} - \tau_{zyb}) - fuh$$

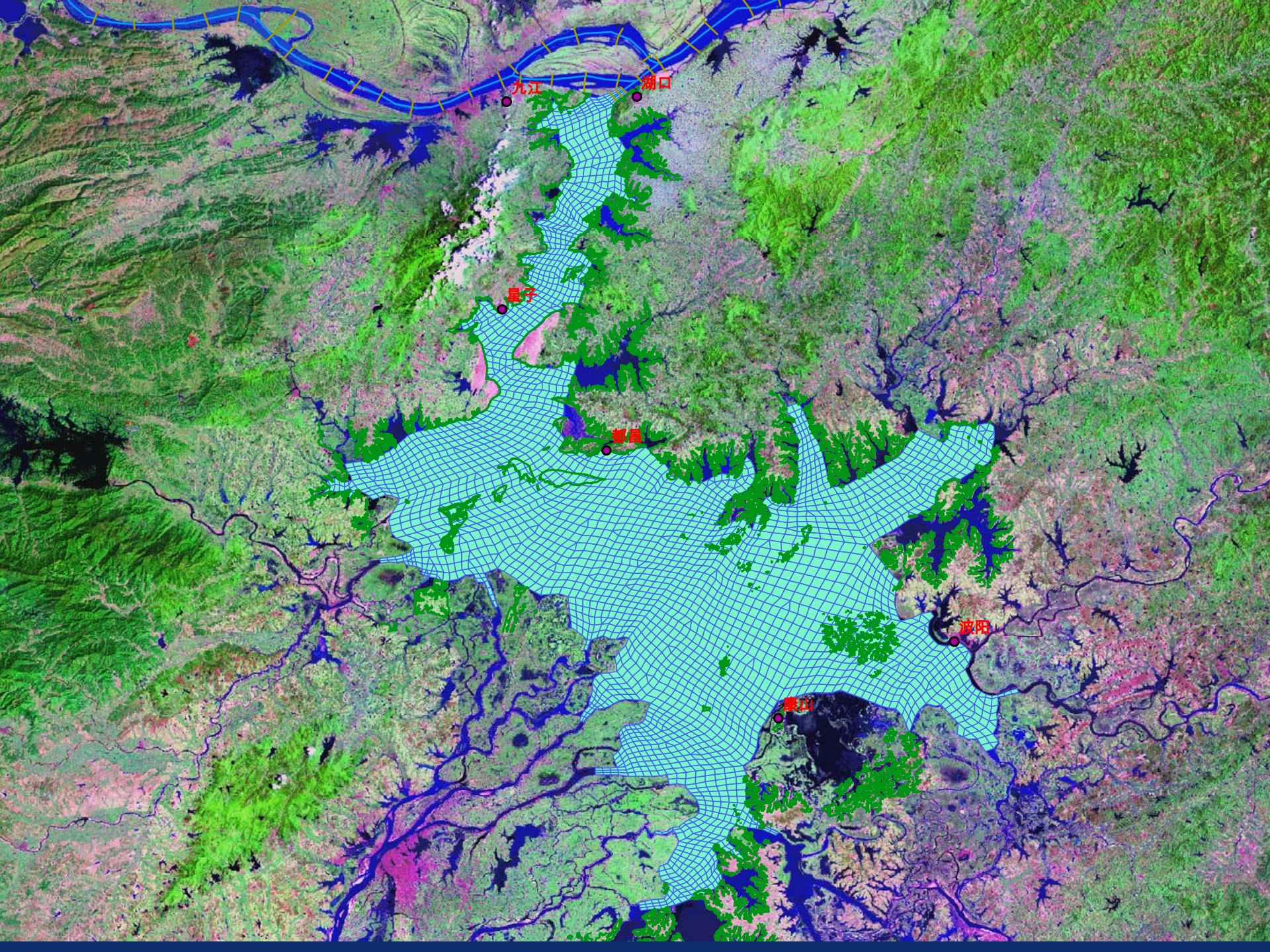


Unstructured grids

Fluxes are computed using HLLC Scheme

$$F_{HLLC} = \begin{cases} F_L & \text{if } 0 \leq S_L \\ F_{*L} & \text{if } S_L \leq 0 \leq S_* \\ F_{*R} & \text{if } S_* \leq 0 \leq S_R \\ F_R & \text{if } S_R \leq 0 \end{cases}$$





九江

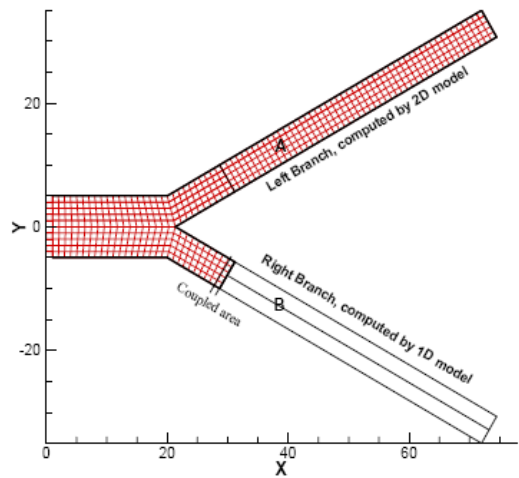
湖口

星子

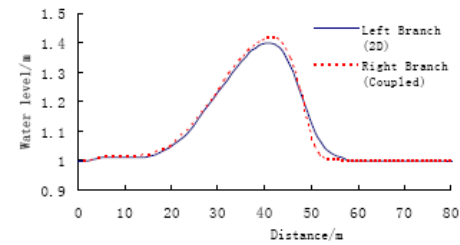
都昌

波阳

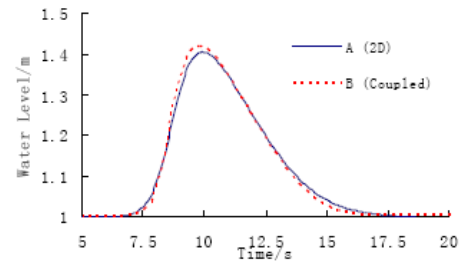
彭泽



(a) River bifurcation



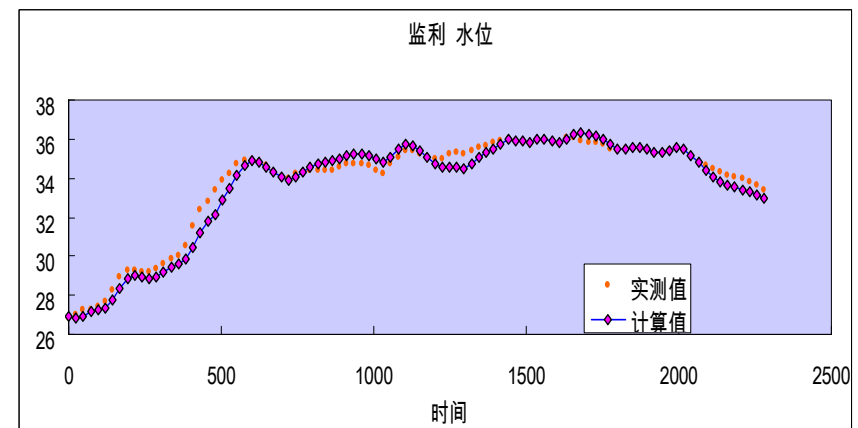
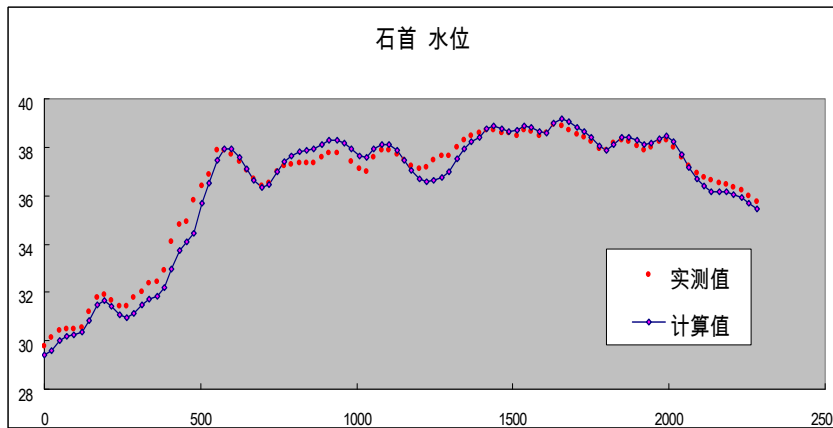
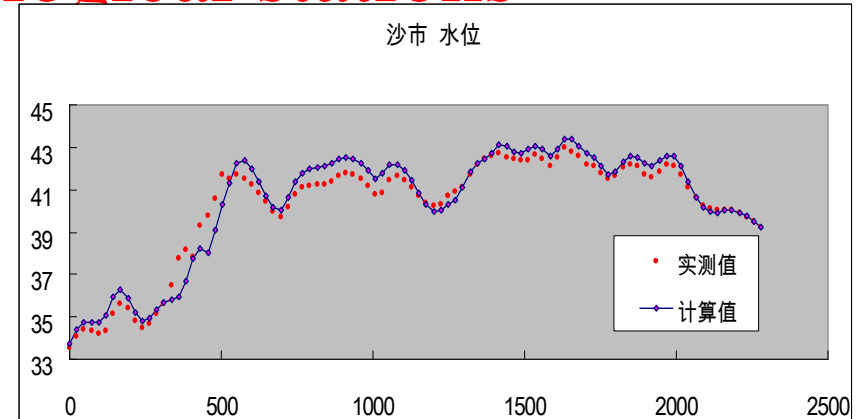
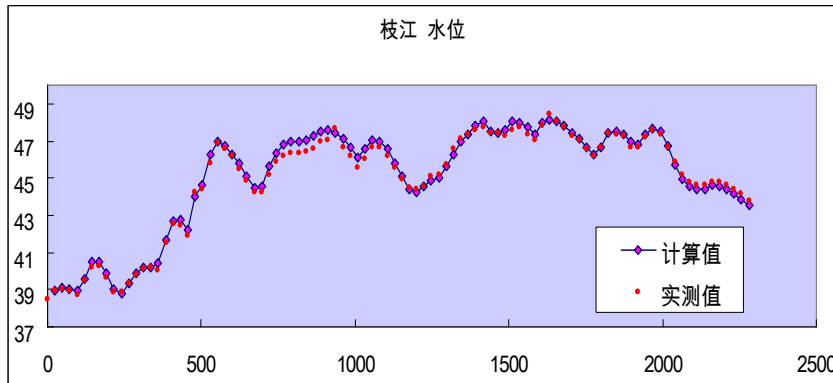
(b) water surface along the centerline at t=10s



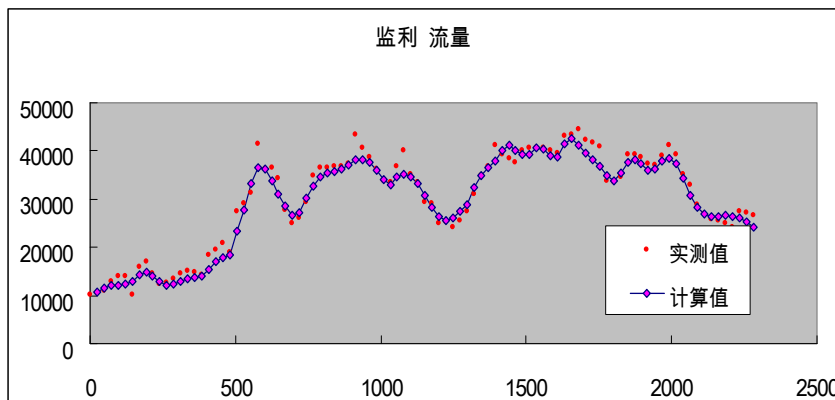
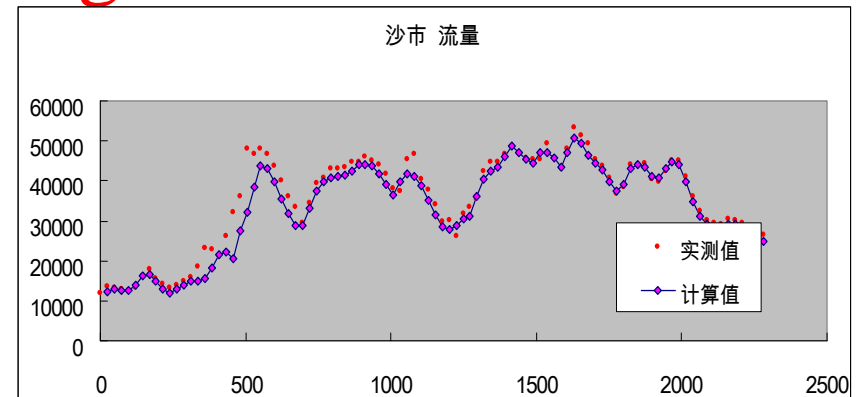
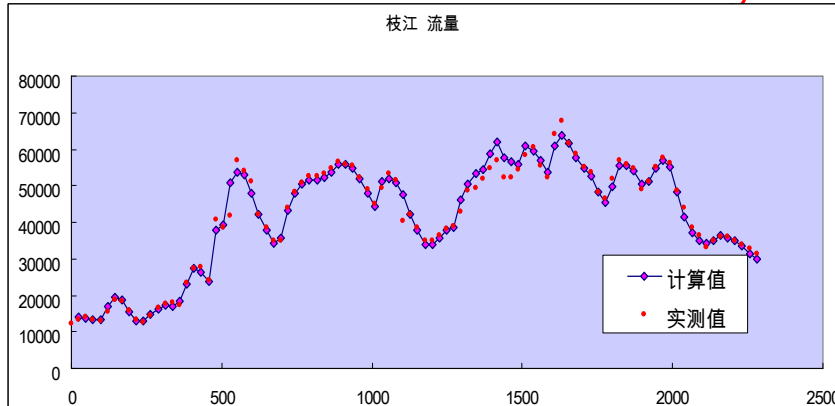
(c) water level hydrograph at A and B

Validation of the model

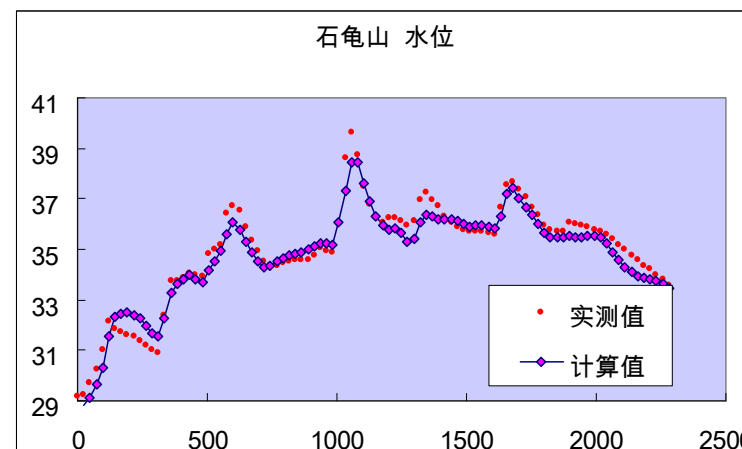
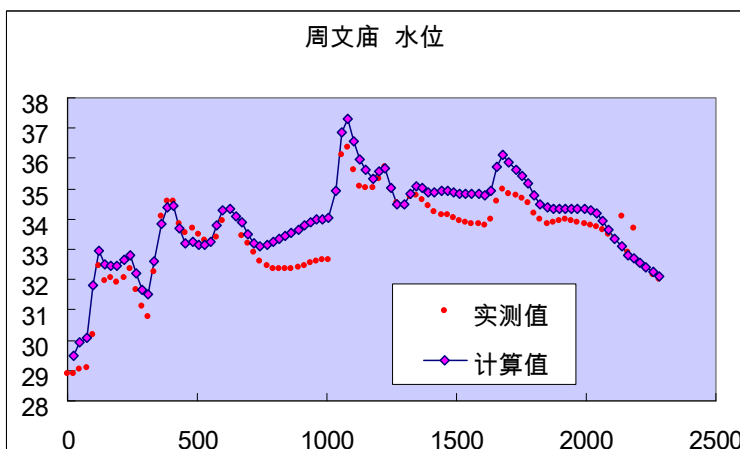
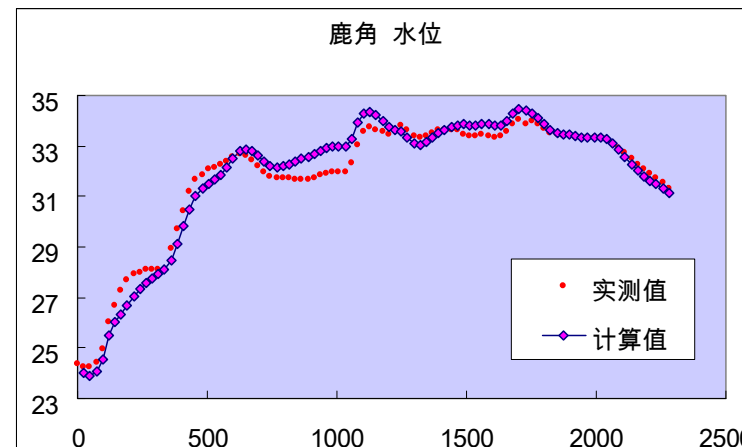
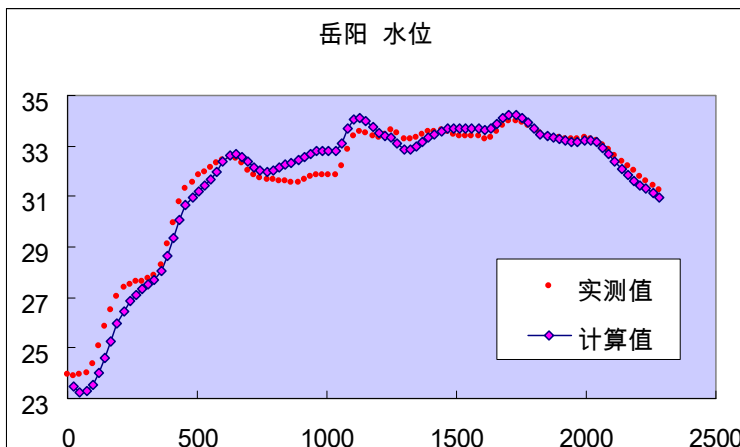
Simulation results on water level for some hydrological stations



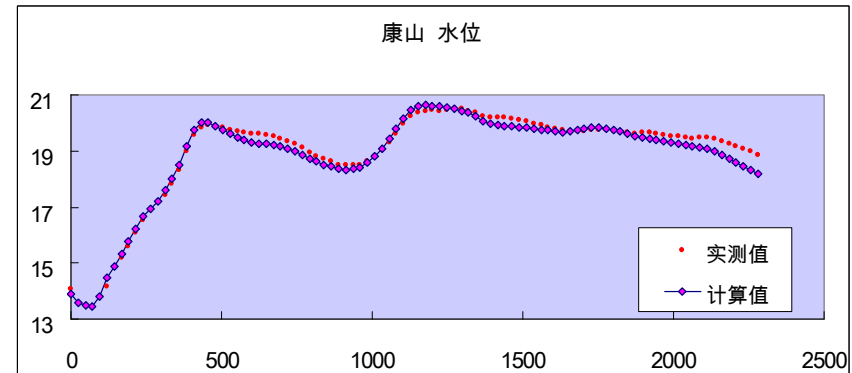
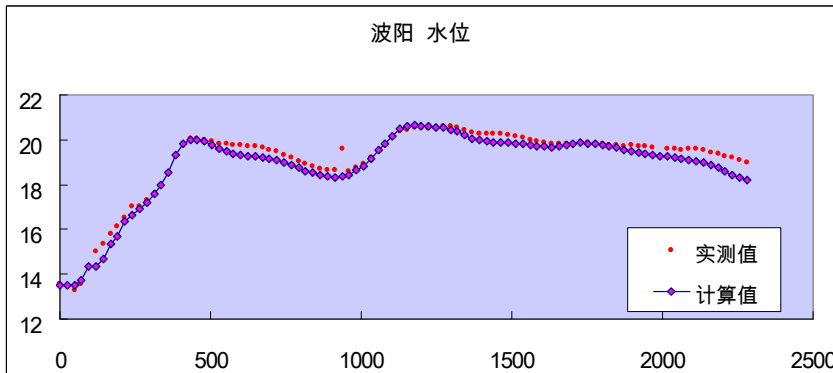
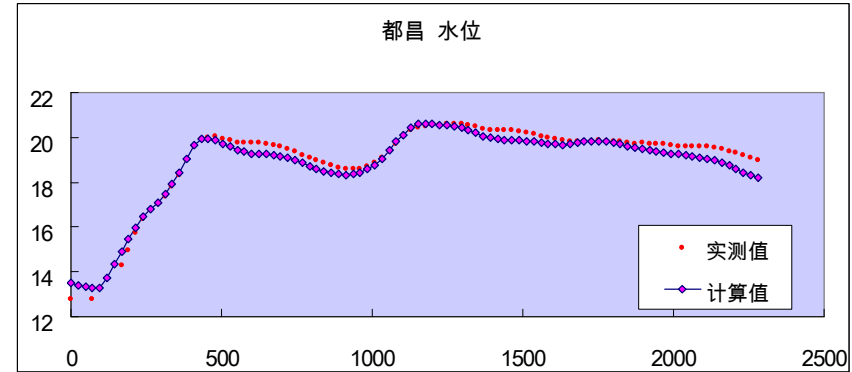
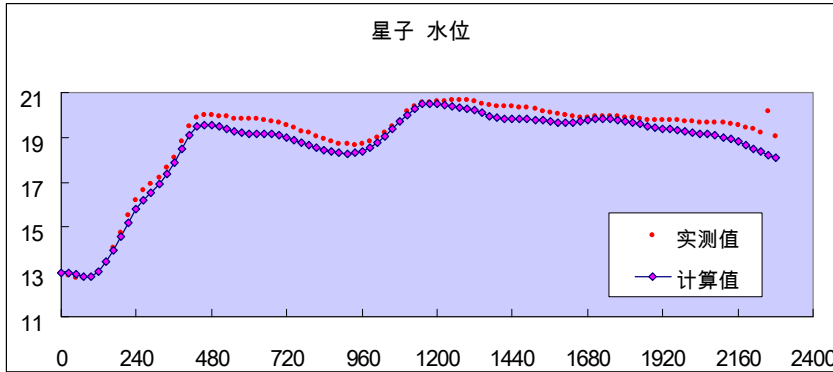
Simulation result on discharge for some hydrological stations



Water level simulation for Dongting Lake

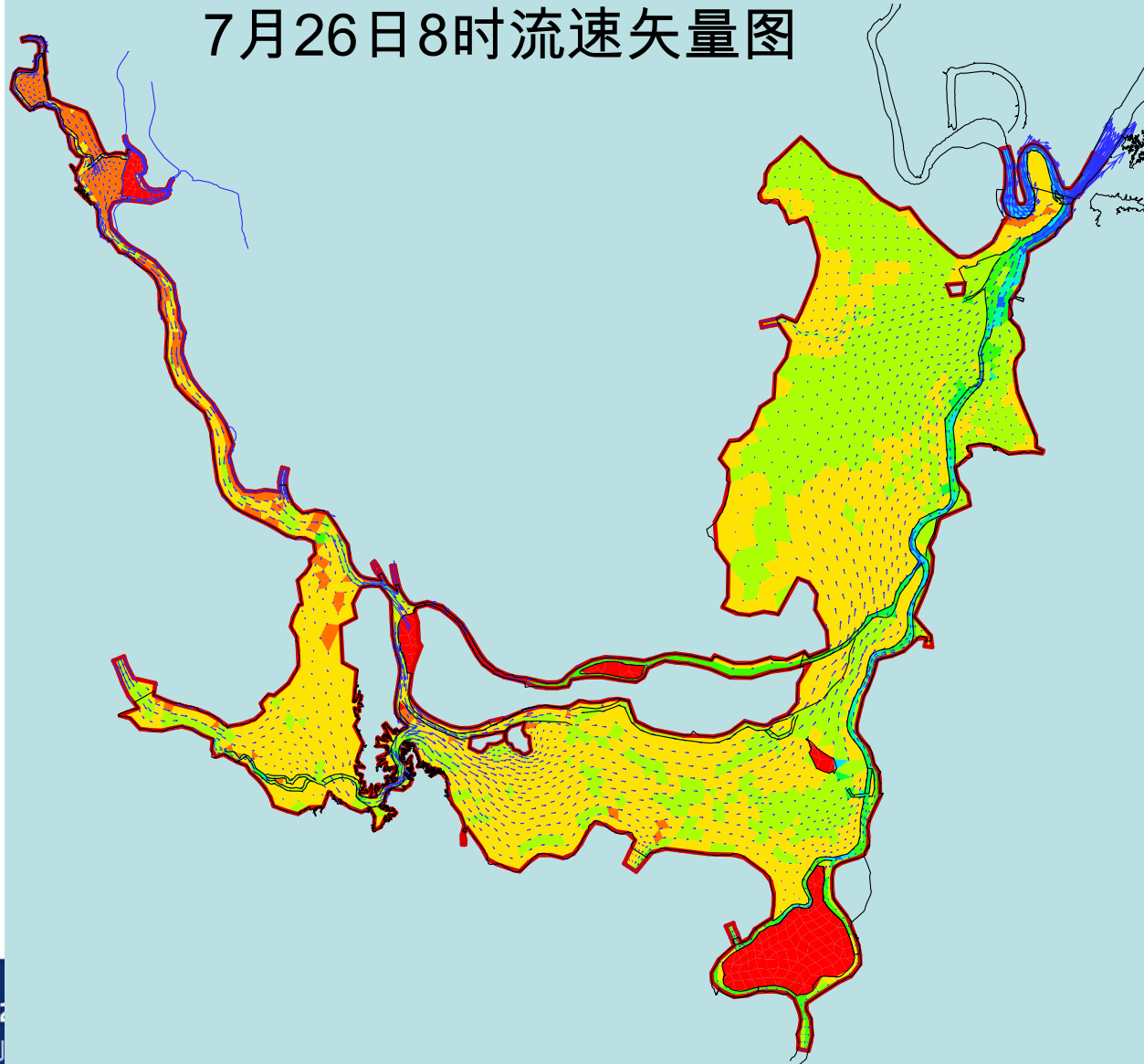


Water level simulation for Poyang Lake

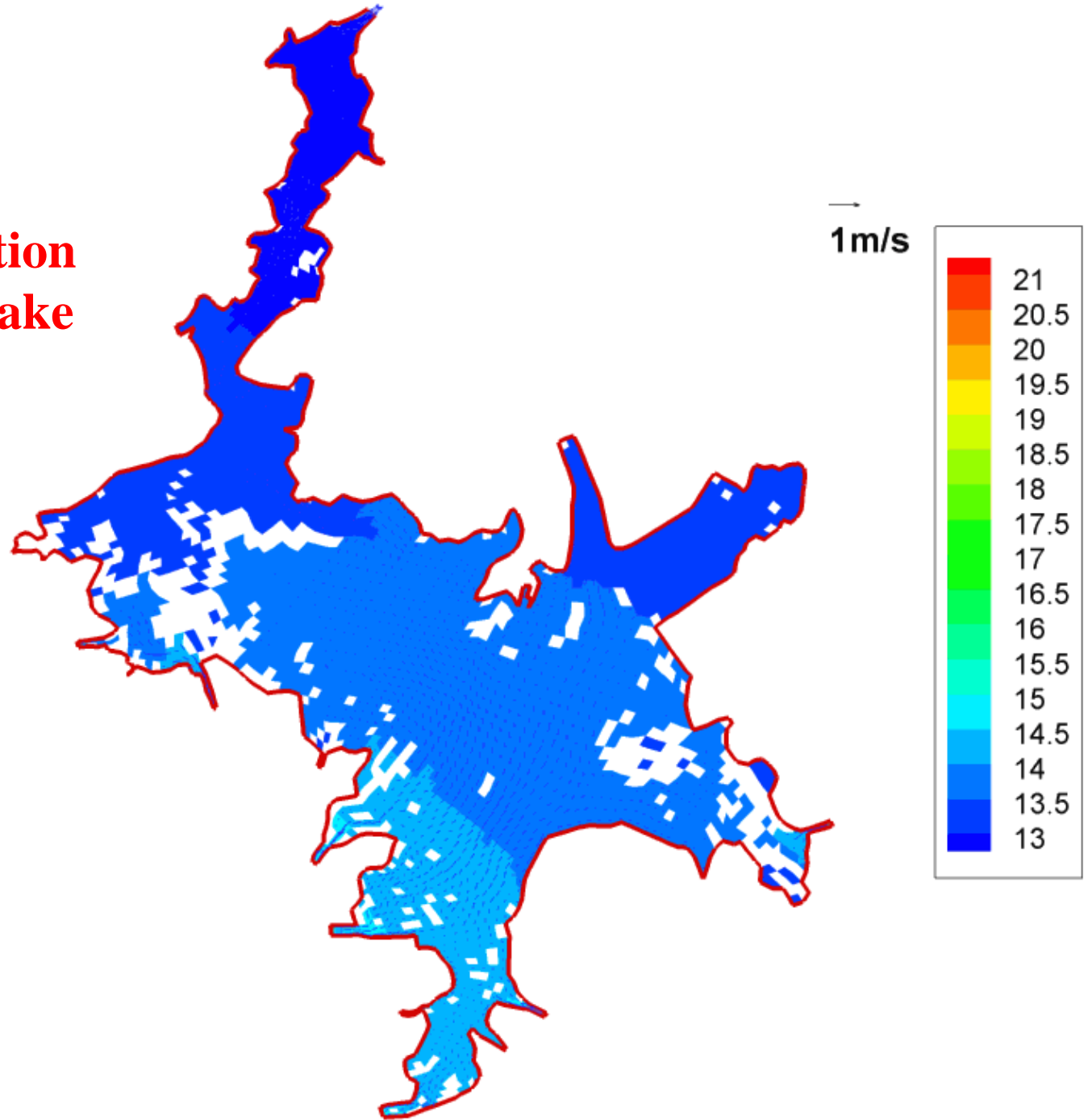


Flow field simulation For Dongting Lake

7月26日8时流速矢量图



Flow field simulation for the Poyang Lake

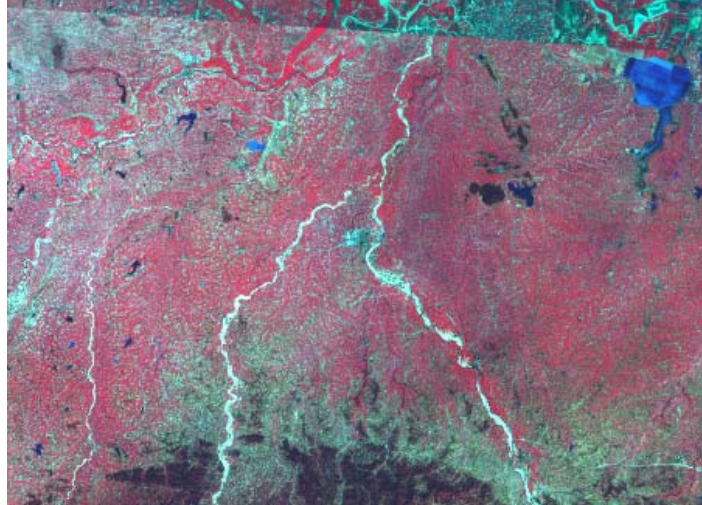
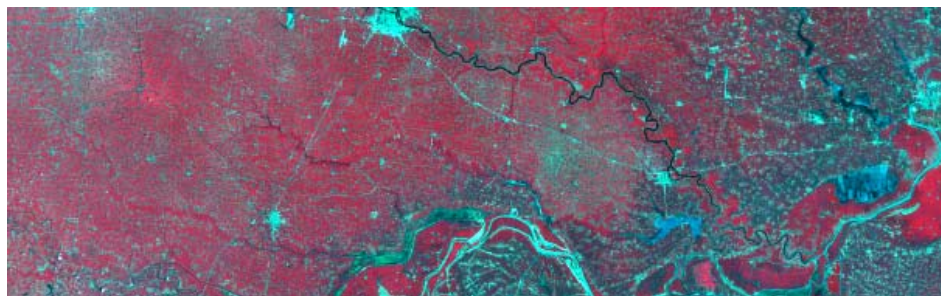




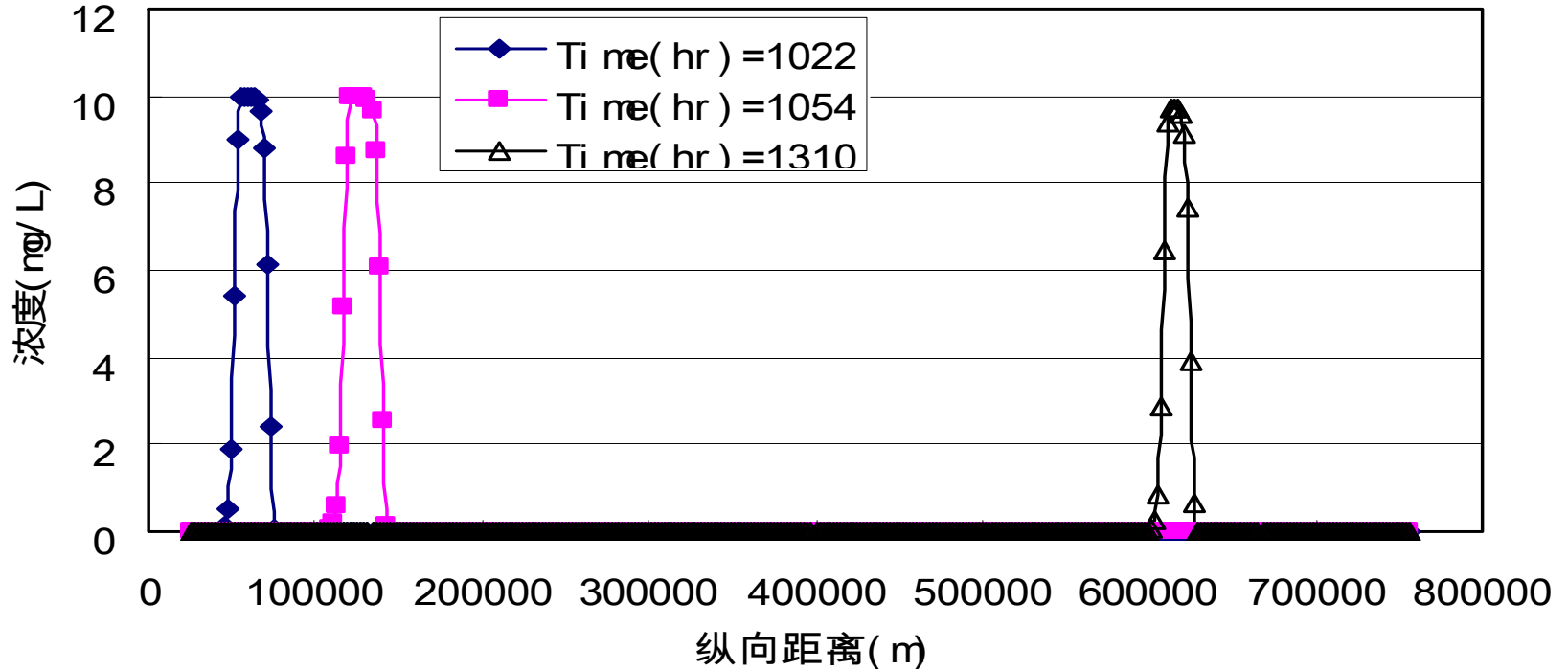
Regulation rule of Three Gorge Reservoir

- **During flood season, when storage is unnecessary, water level is controlled as 144m (limitation water level for flood control), inflow is basically equal to outflow.**
- **When storage is necessary, the highest water level is 175m, and decreased gradually to 144m after flood.**
- **In general case, storage begins after flood season, water level increased to 156m (172m) at the end of Oct. also considering water use on navigation and water supply for middle and downstream.**
- **From Nov. to next May, water level decreases gradually to 144m if water level is 156m at the end of flood season or to 152m if water level is 172m at the end of flood season according to the requirement of power generation and navigation.**

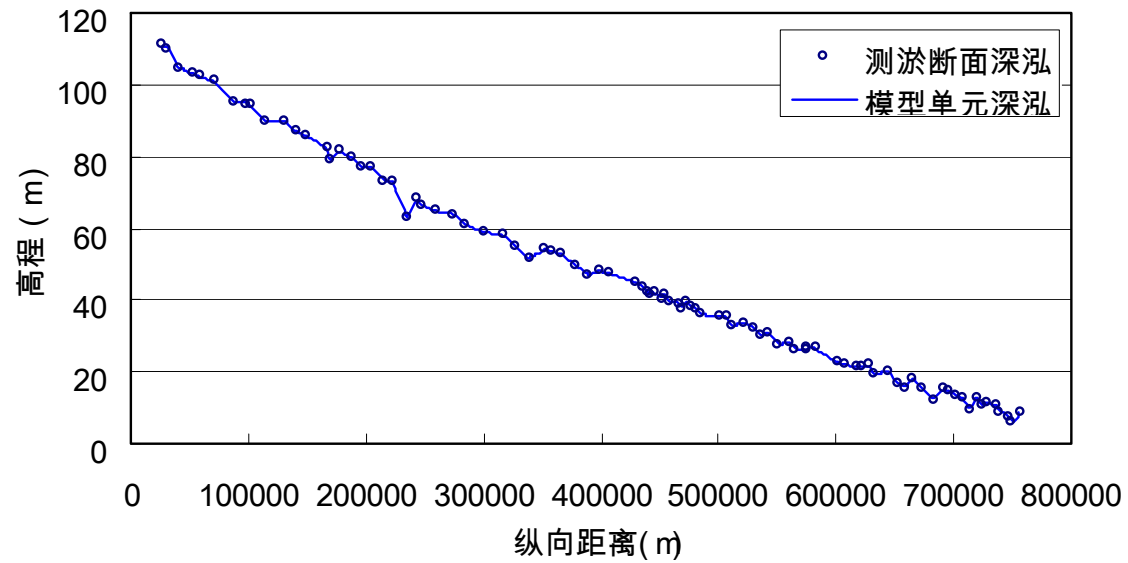
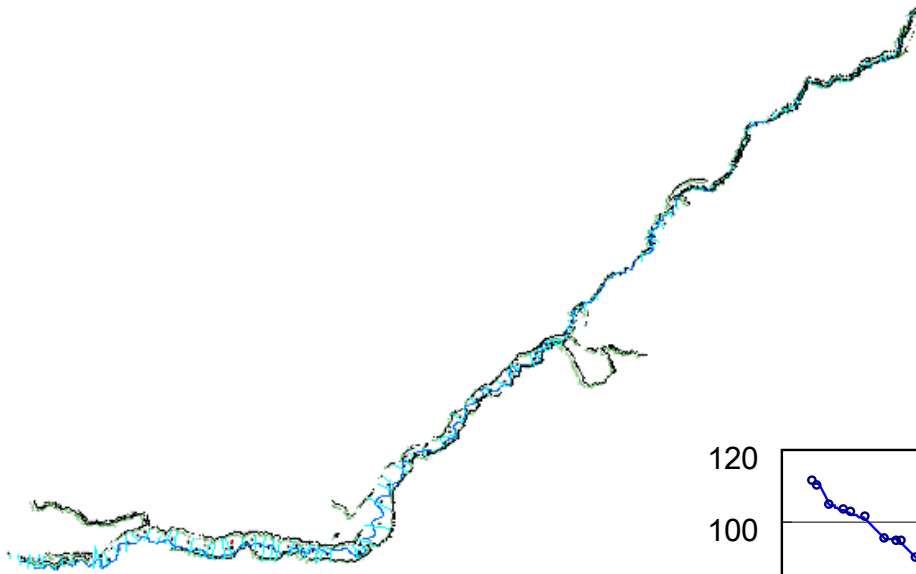
4) Water pollution monitoring and assessment



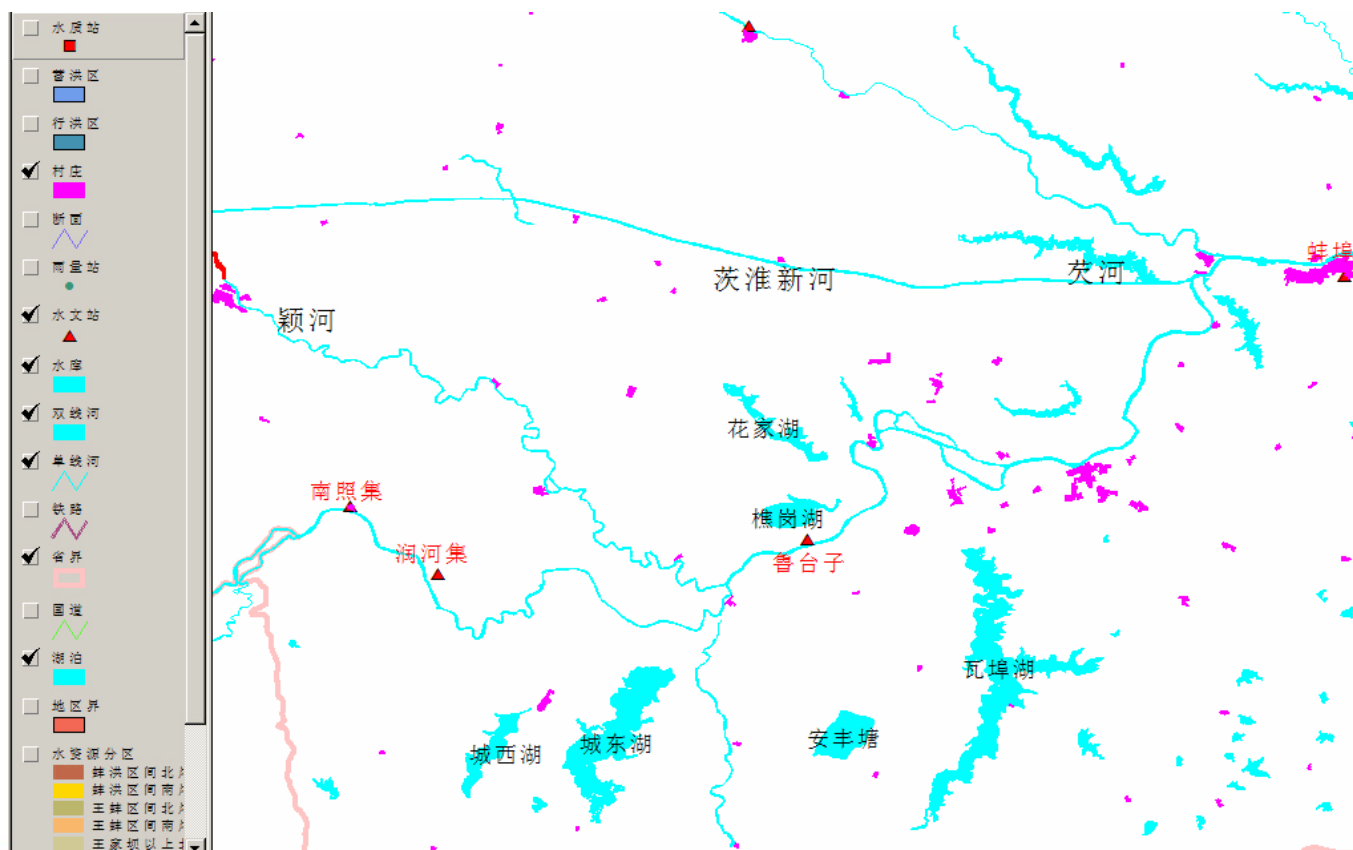
对流项离散的TVD格式采用SUPERBEE格



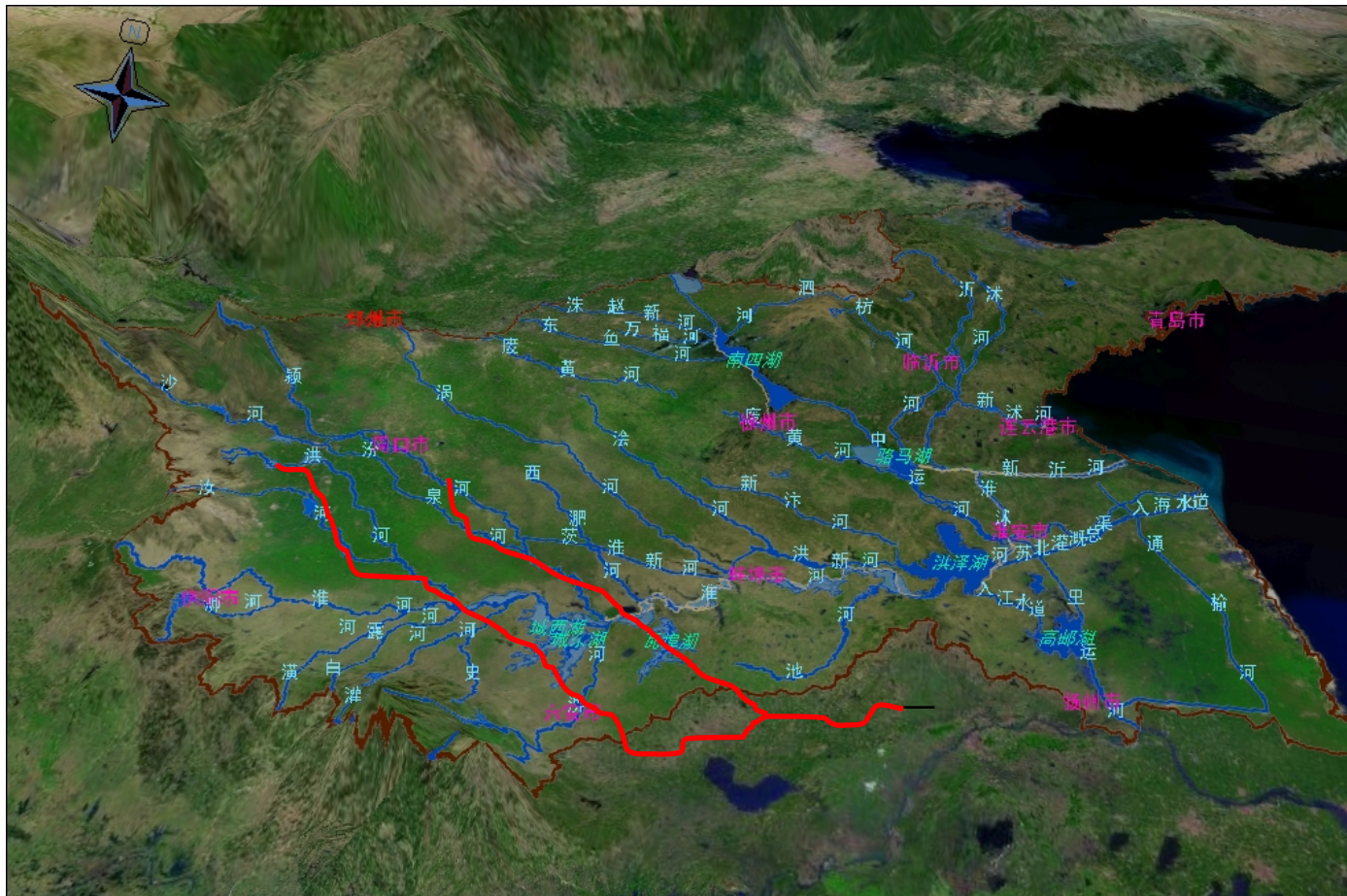
● Section every 2 km



2-D visual display



3-D visual display

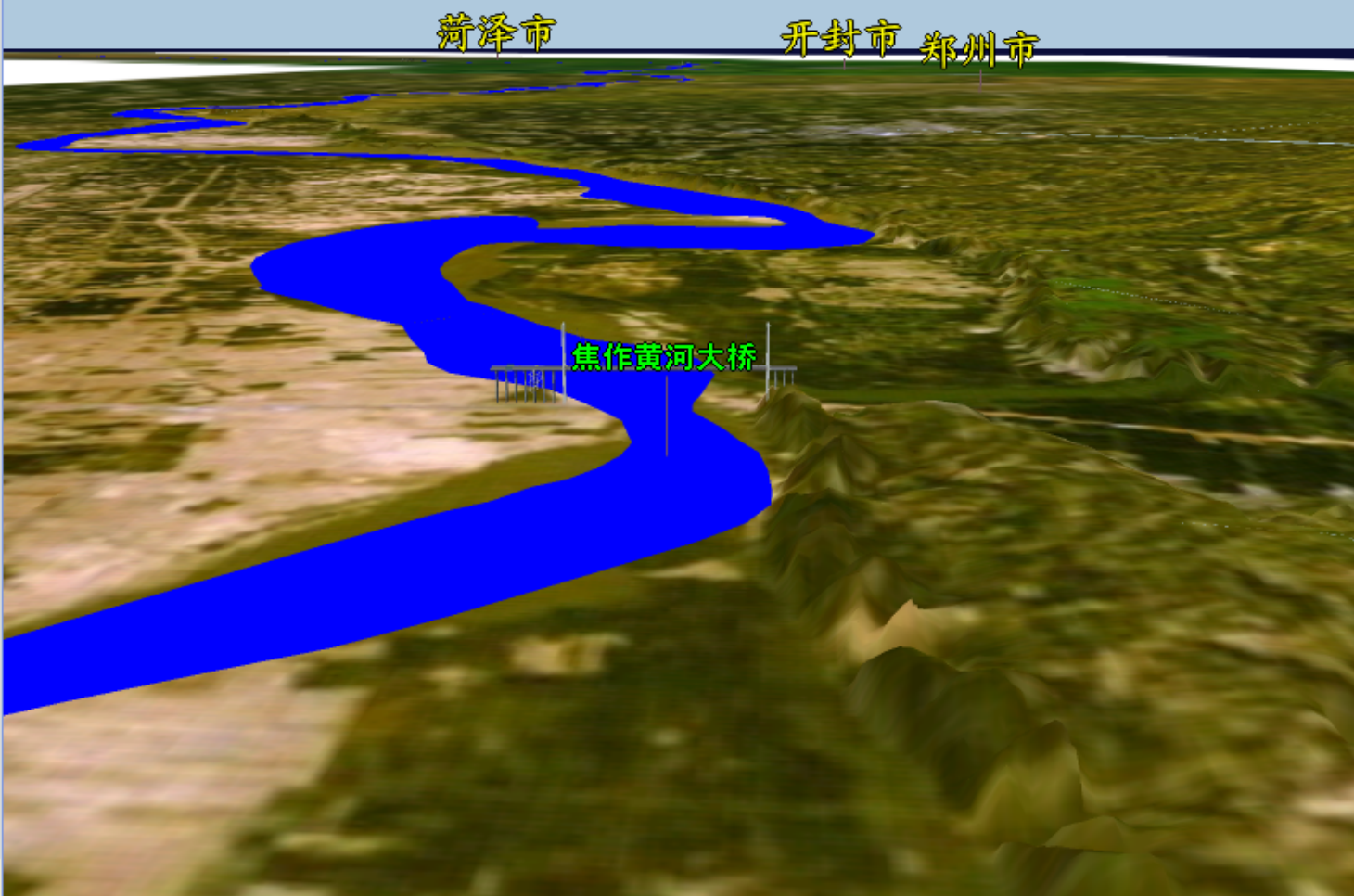


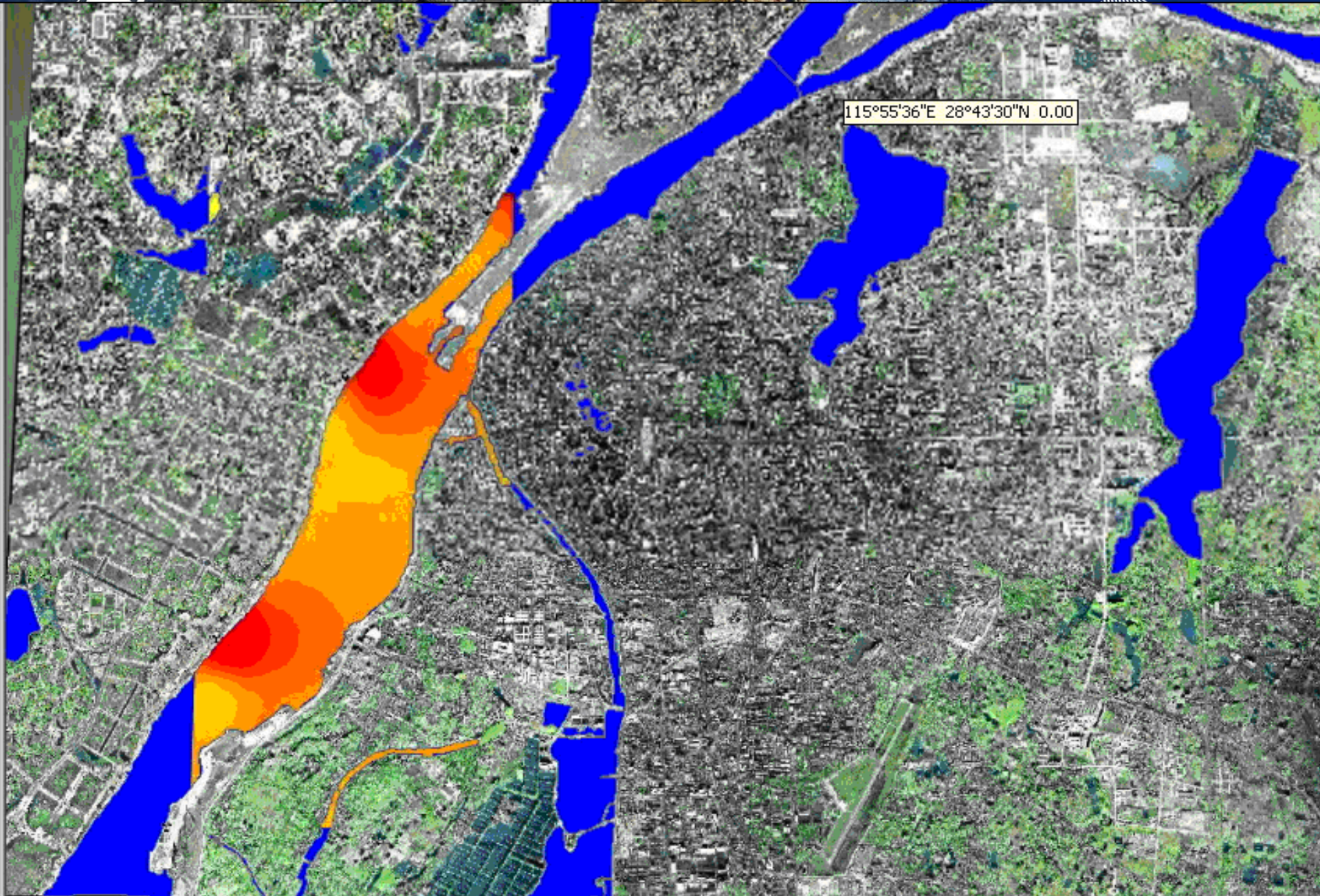
工程窗口

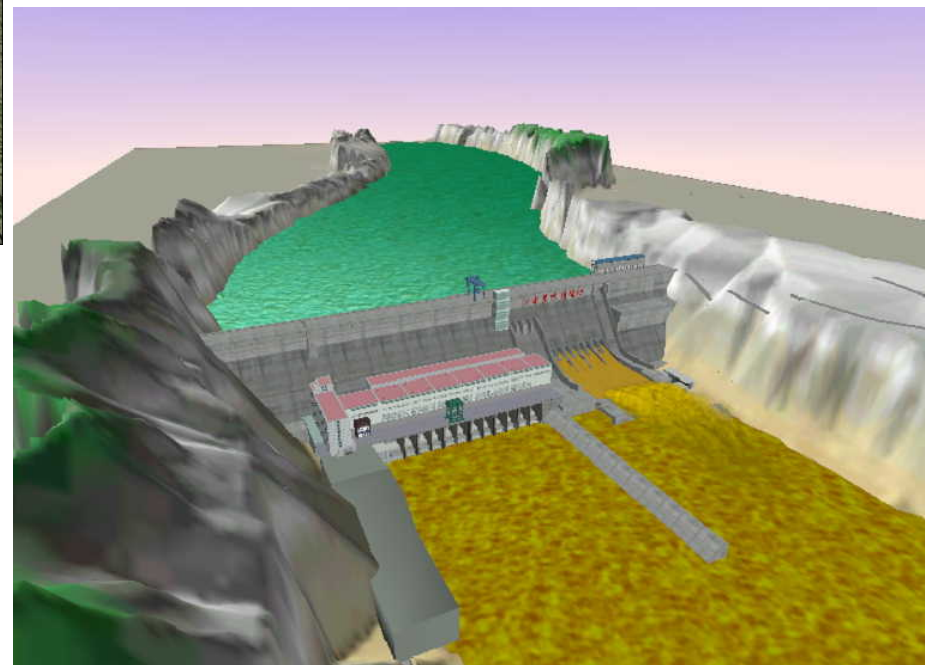
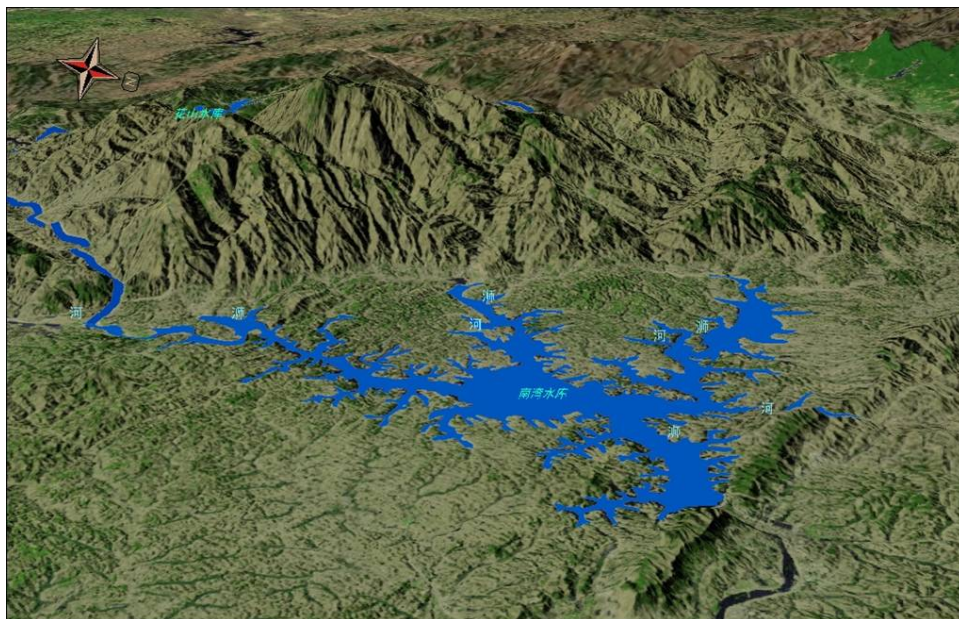
动态演示
当前时间: 1918.00
计算文件: YELLOW_OUT.310
演示速度(秒):
浓度值设定: 0
动态演示 结束

污水团特性
断面个数: 0
河段长度: 0千米

浓度值最高断面
断面名称:
断面位置: 米
浓度值: .0000(mg/L)







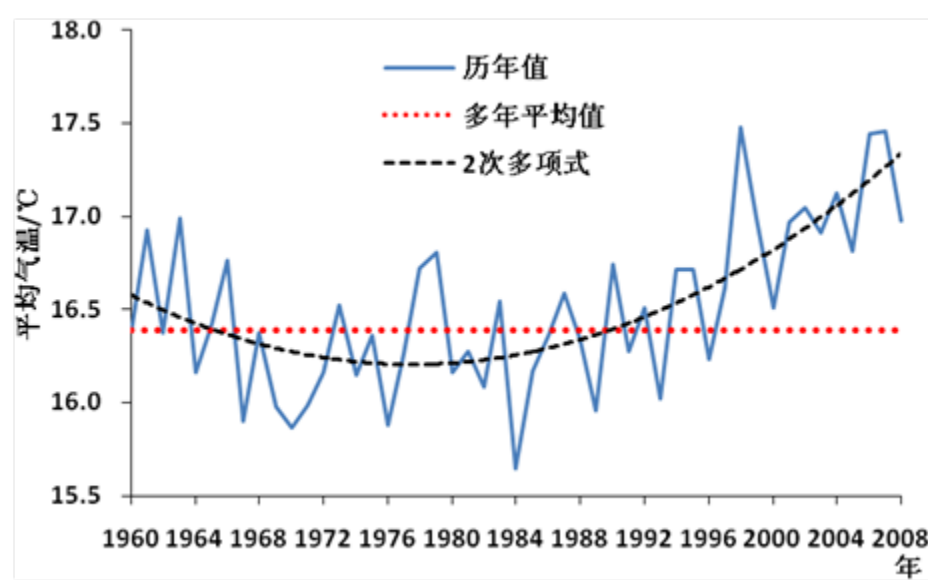
Thank you for your attention

Response of Dongting Lake Environmental Changes to Climate Fluctuations and Three Gorges dam in China IWHR

Climate change of Dongting Lake basin by using meteorological data from 1960 to 2008

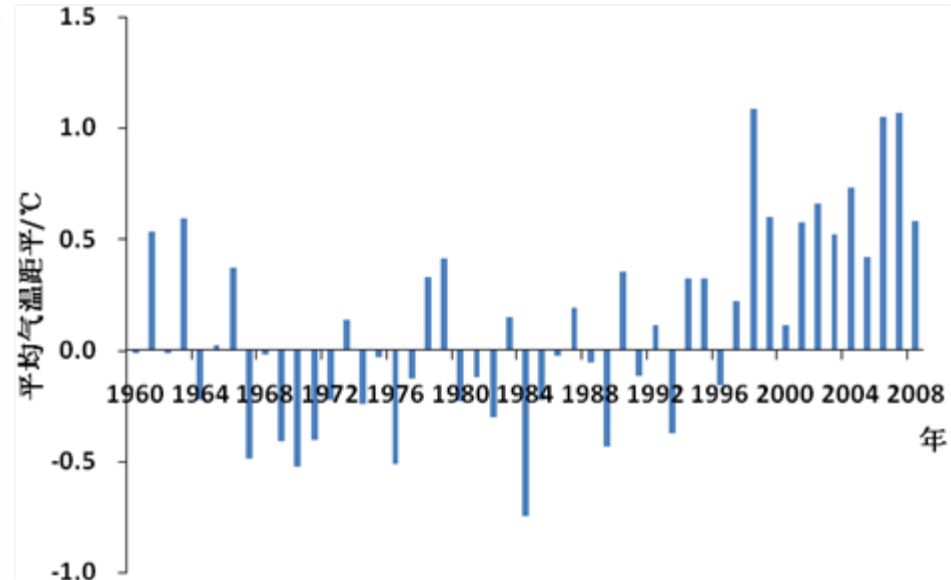
Temperature

Yearly mean temperature



(year)

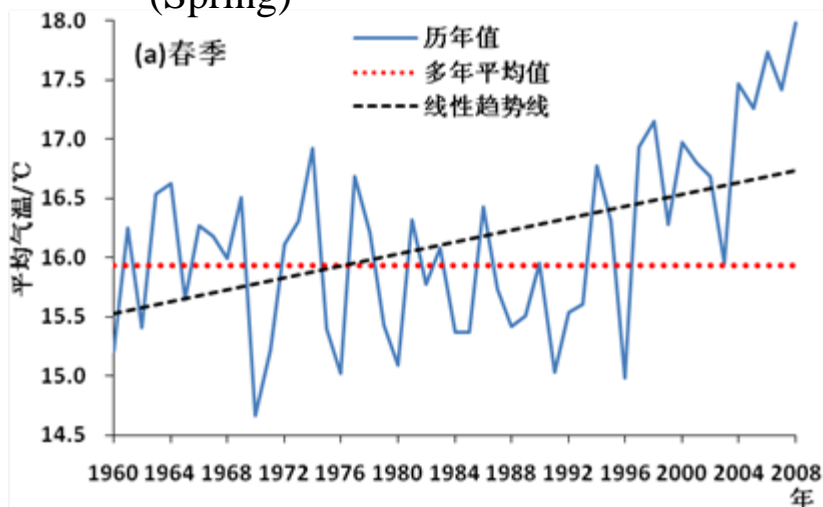
Yearly mean temperature anomaly



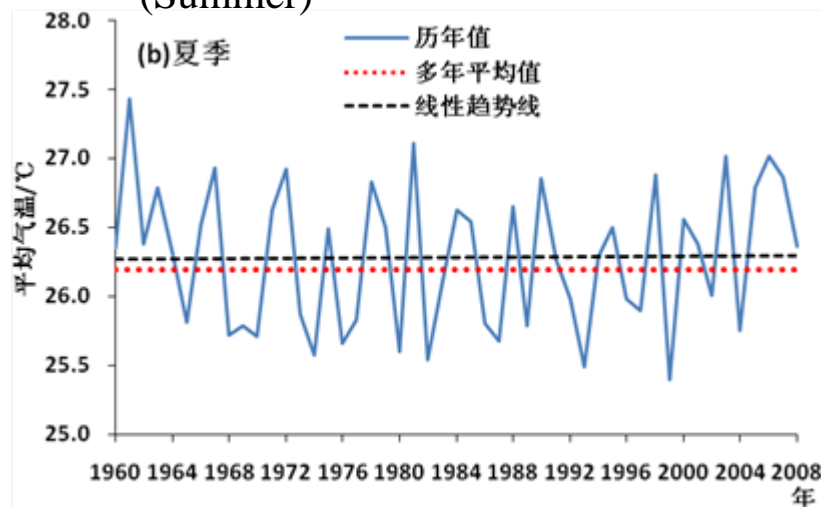
(year)

Temperature

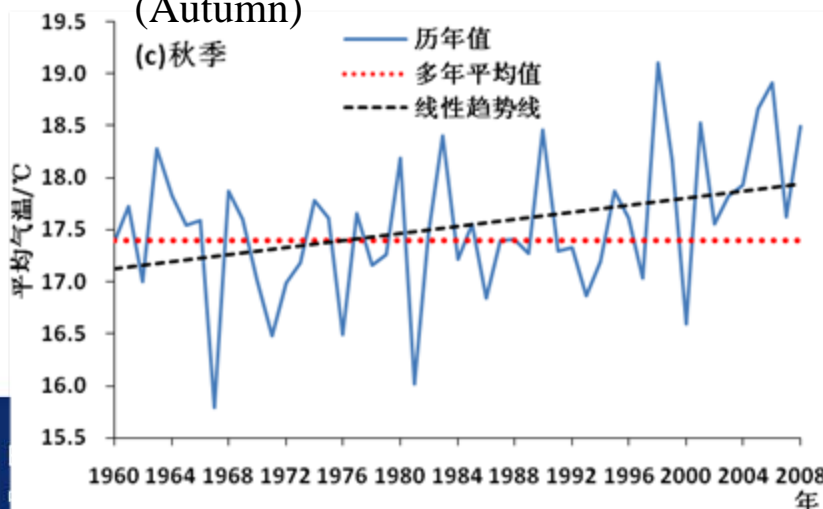
(Spring)



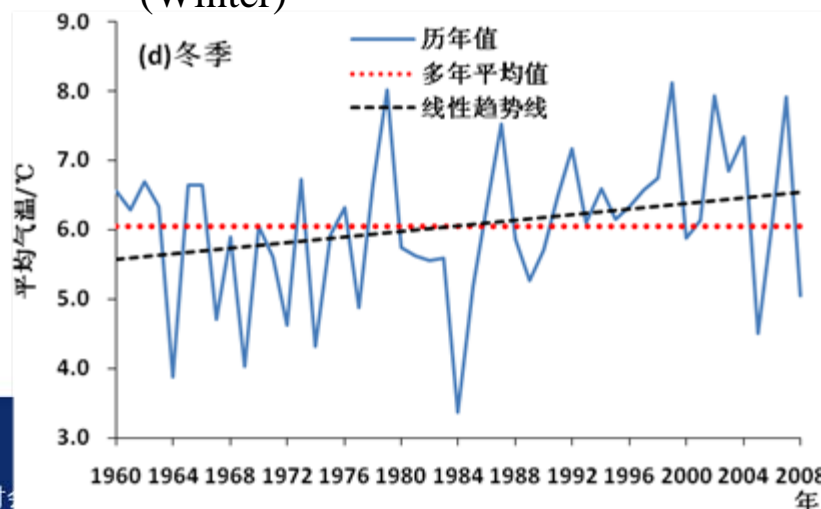
(Summer)



(Autumn)

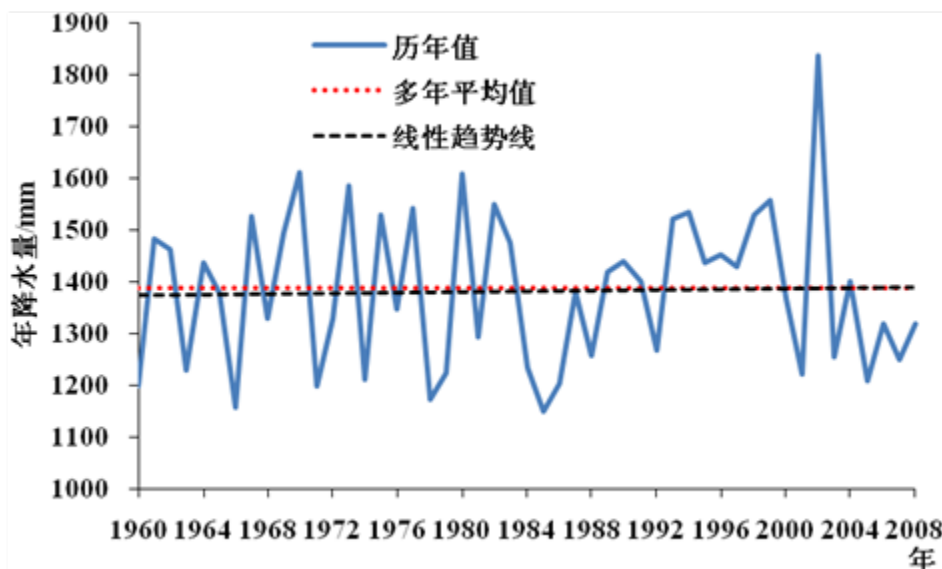


(Winter)



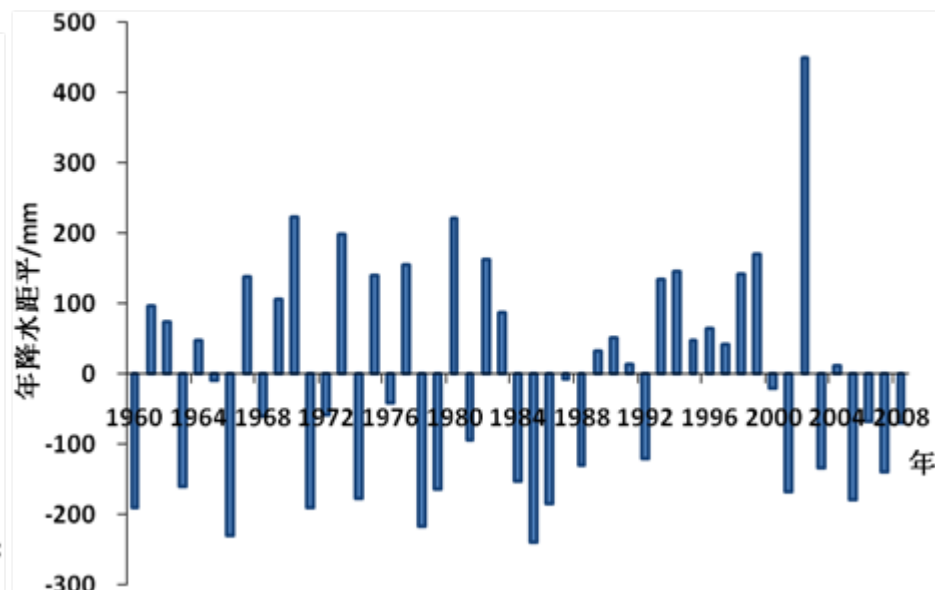
Precipitation

Annual precipitation



(year)

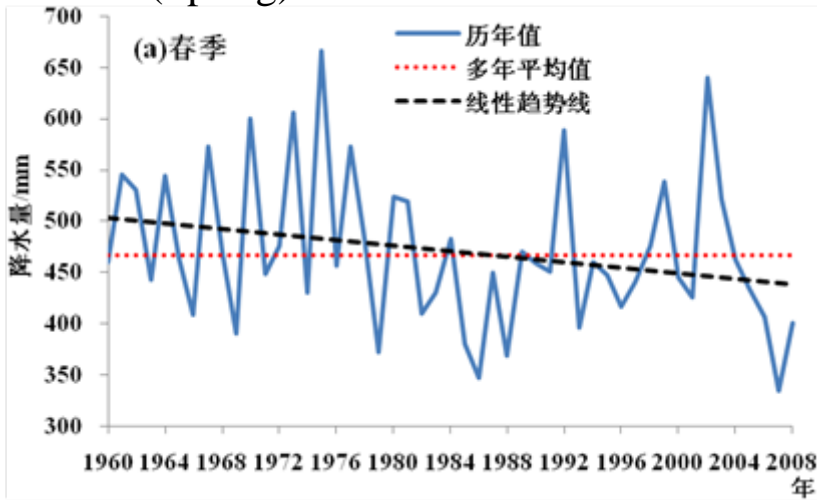
Annual precipitation anomaly



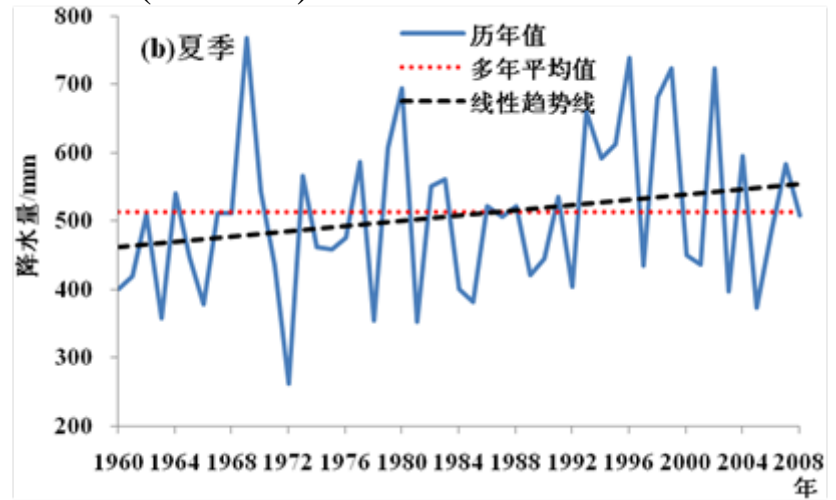
(year)

Precipitation

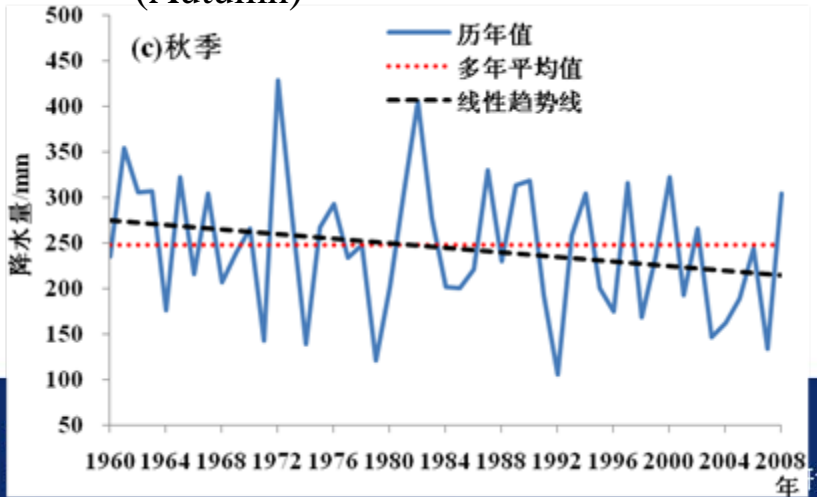
(Spring)



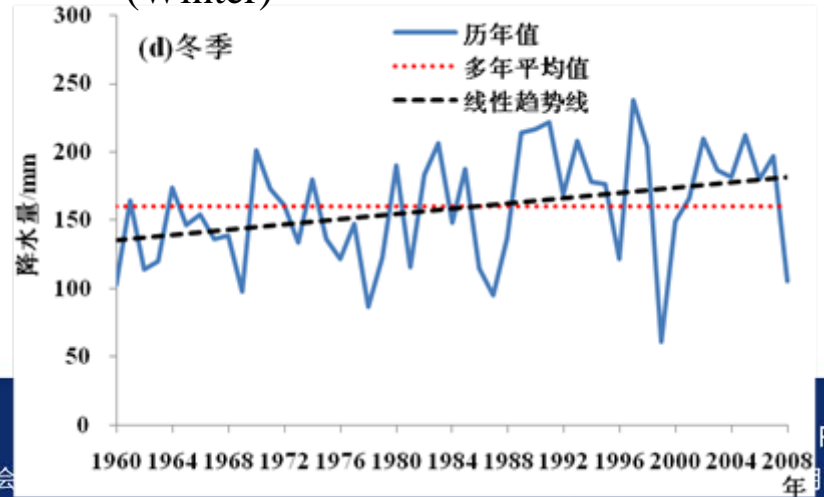
(Summer)



(Autumn)

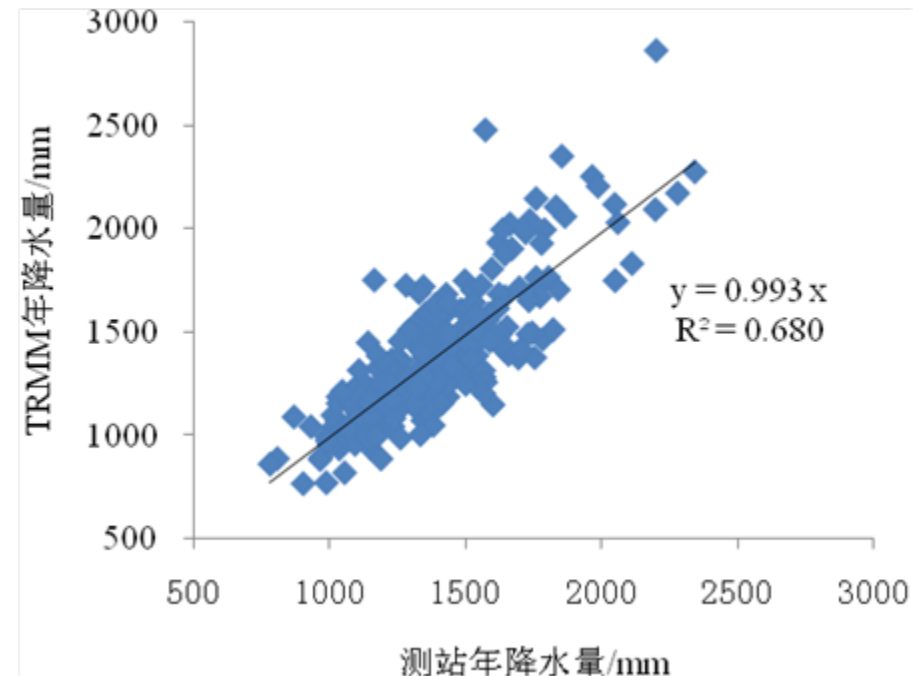
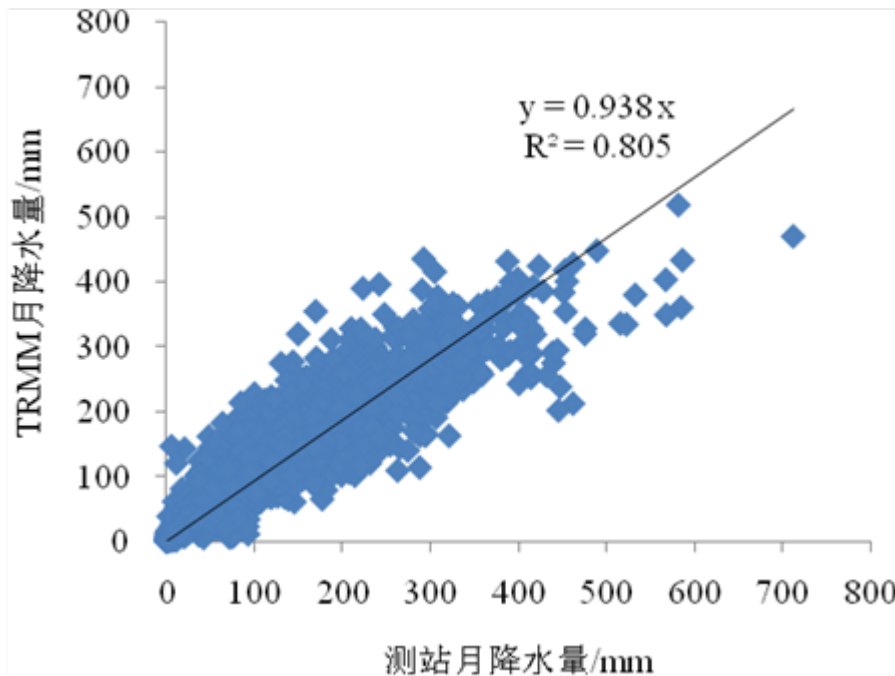


(Winter)



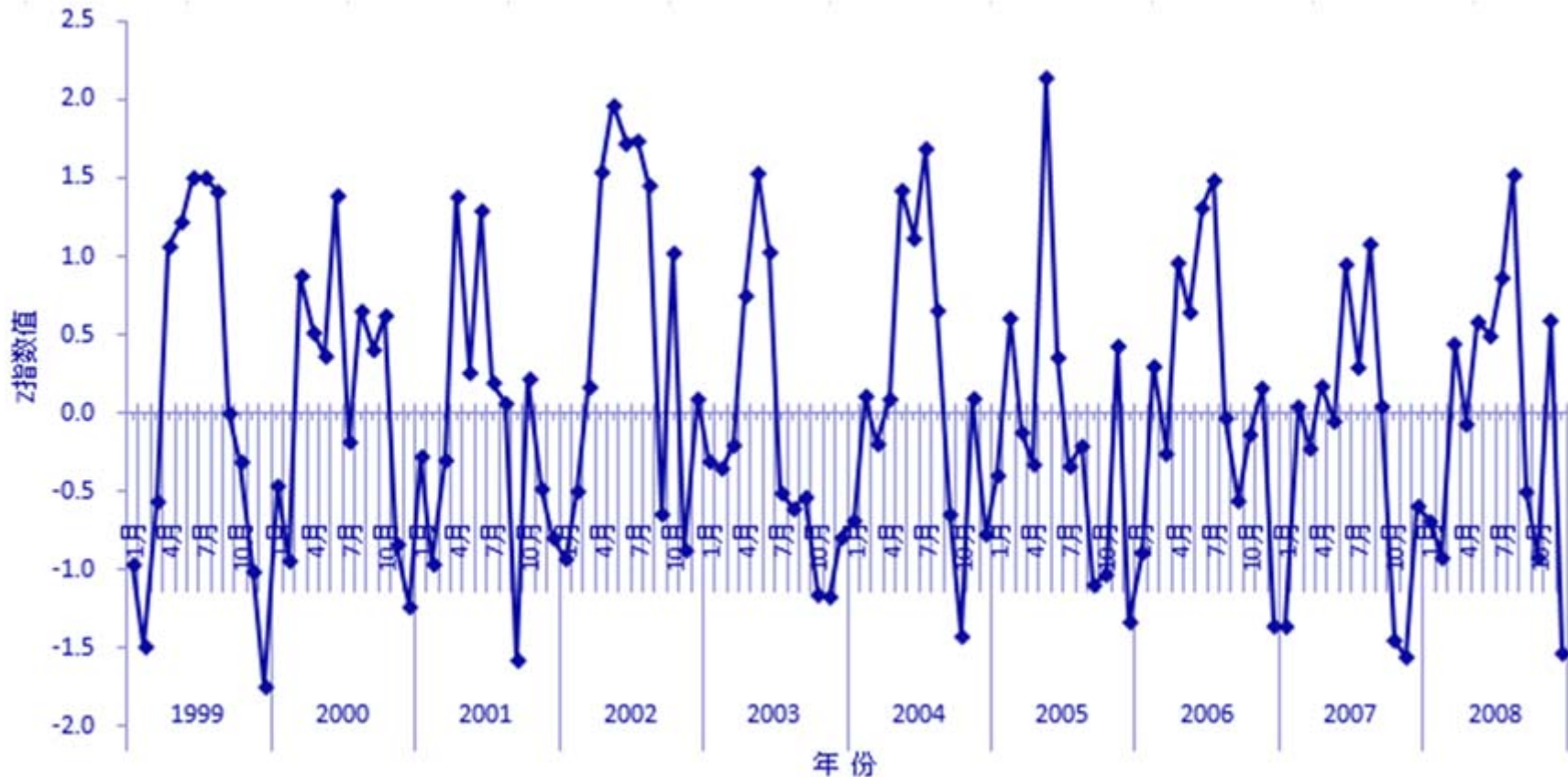
Flood/drought over the Dongting Lake basin based on TRMM precipitation data and regional integrated Z-index from 1999 to 2008

Data: TRMM 3B43, from NASA website



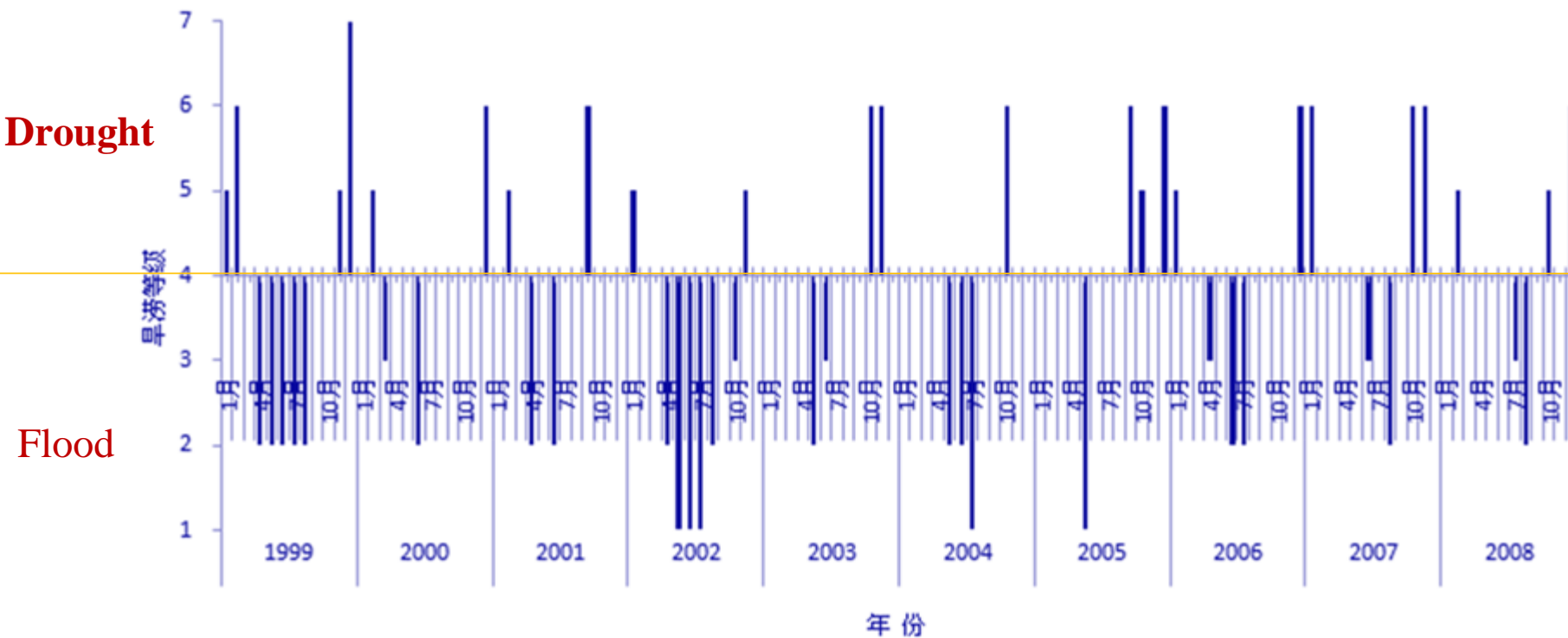
Monthly and annual precipitation scatter diagram of TRMM and rain gauges from 1999 to 2008

Regional integrated Z-index



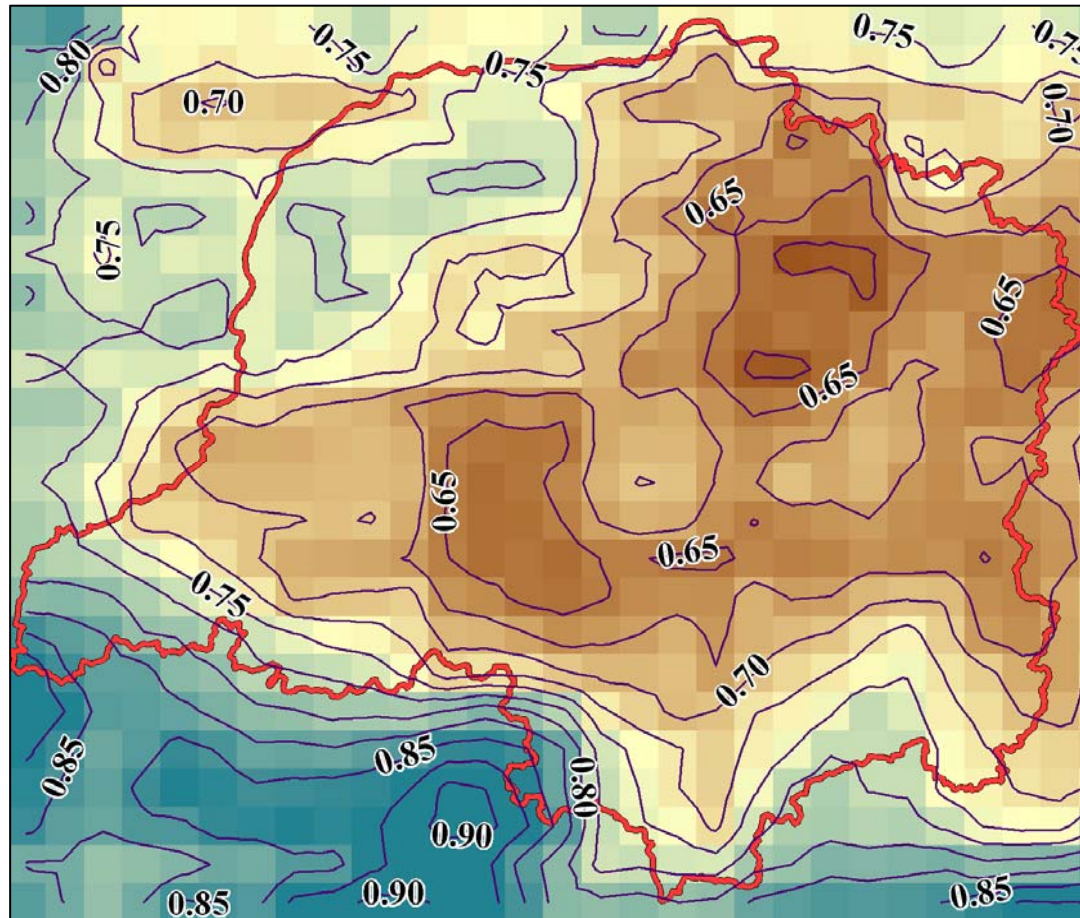
Monthly regional integrated Z-index in the Dongting Lake basin from January 1999 to December 2008

Basin flood/drought grades



Monthly integrated flood/drought grades in the Dongting Lake basin from January 1999 to December 2008

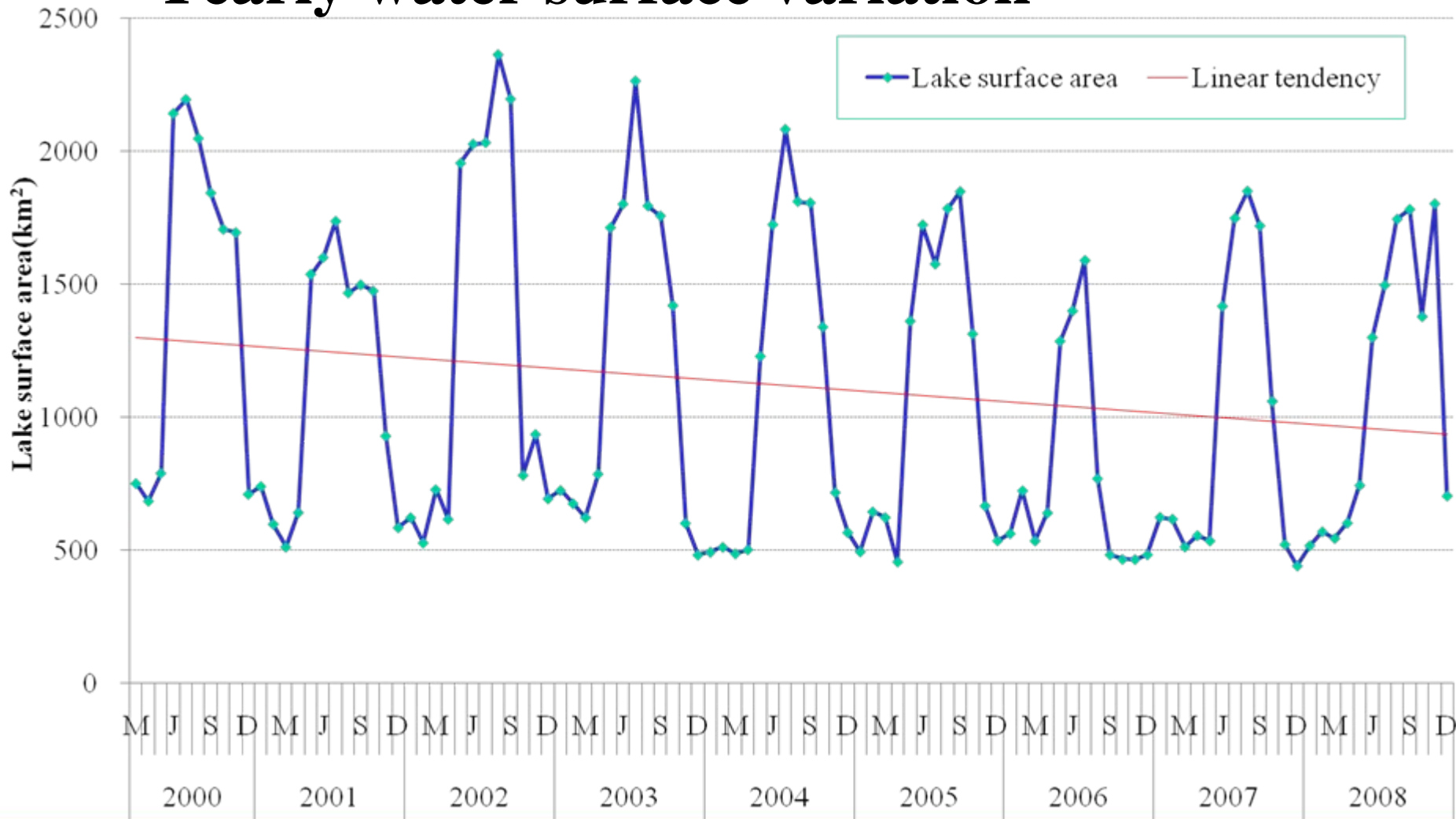
Precipitation variation coefficients



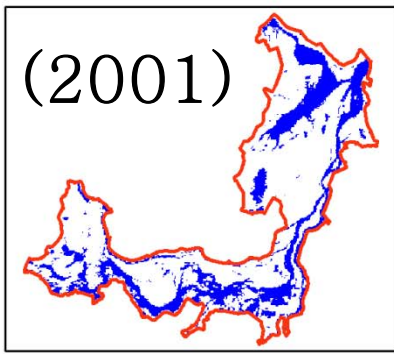
Distribution of the precipitation variation coefficients in the Dongting Lake basin
(The contour interval is 0.025)

Dynamic Monitoring of Water Area Variations in Dongting Lake from 2000 to 2008 Using Terra/MODIS Time Series

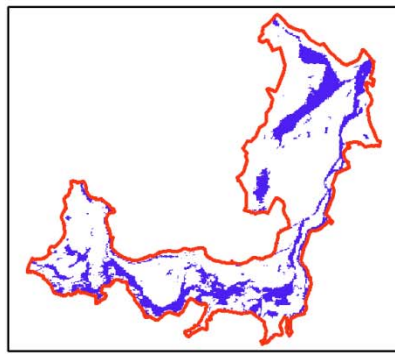
Yearly water surface variation



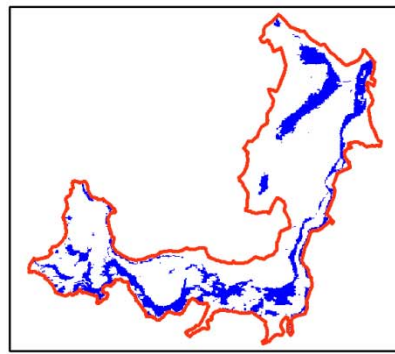
(2001)



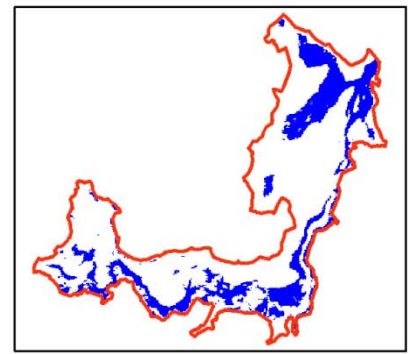
Jan.



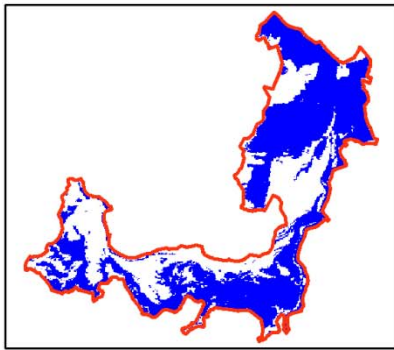
Feb.



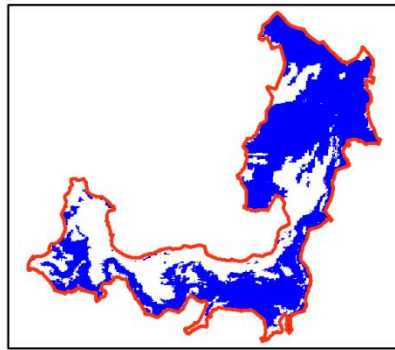
Mar.



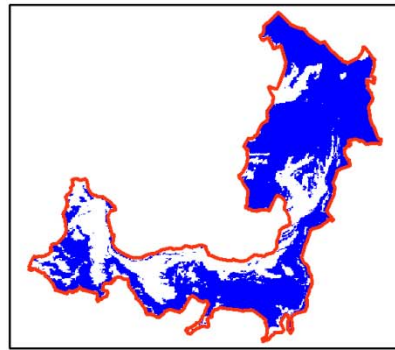
Apr.



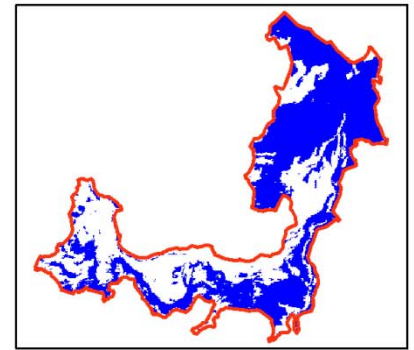
May



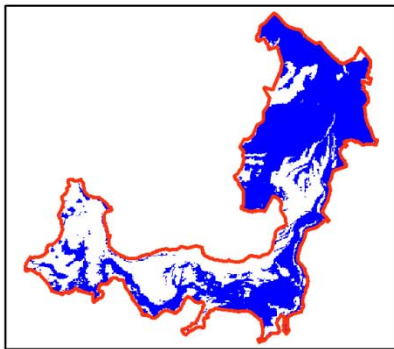
Jun.



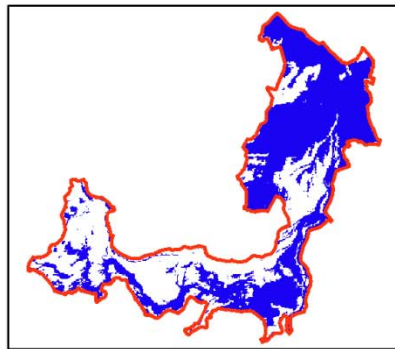
Jul.



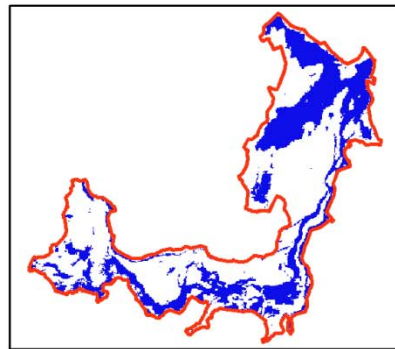
Aug.



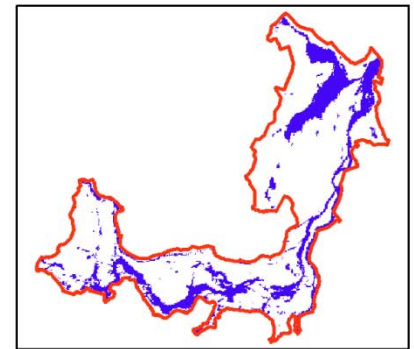
Sept.



Oct.



Nov.

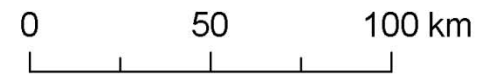


Dec.

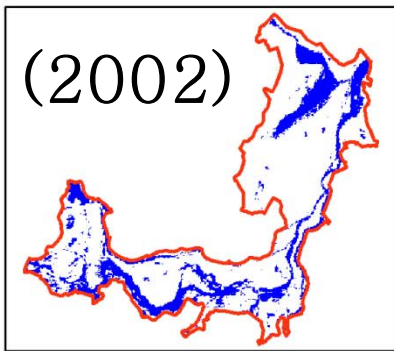


 Lake boudary

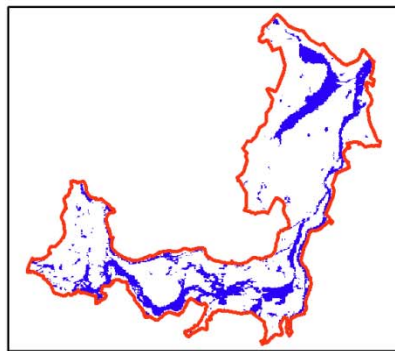
 Water area



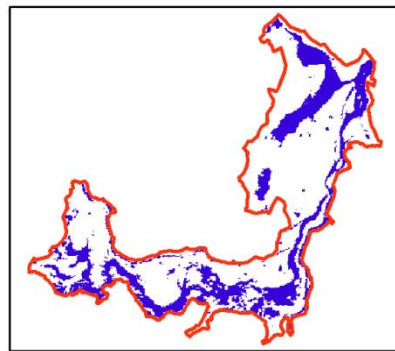
(2002)



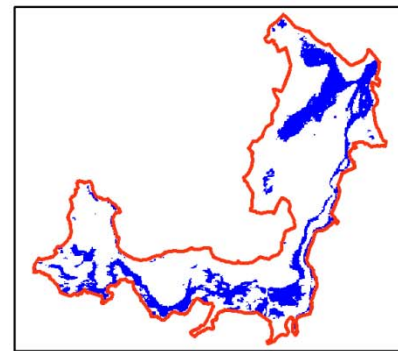
Jan.



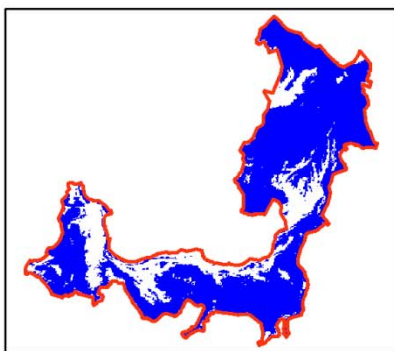
Feb.



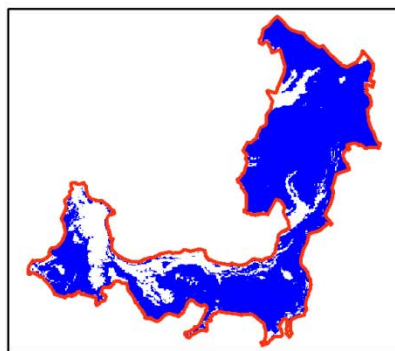
Mar.



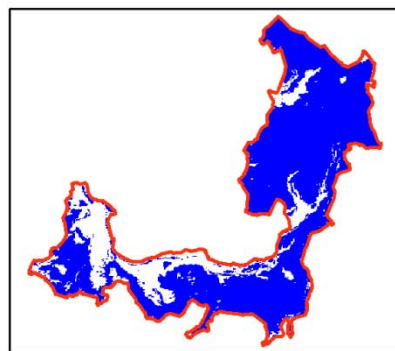
Apr.



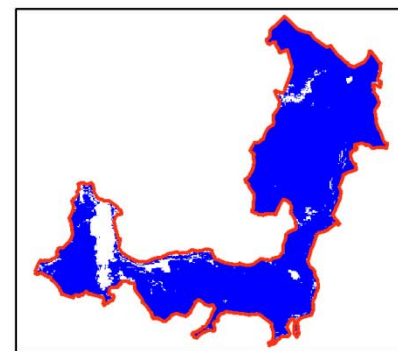
May



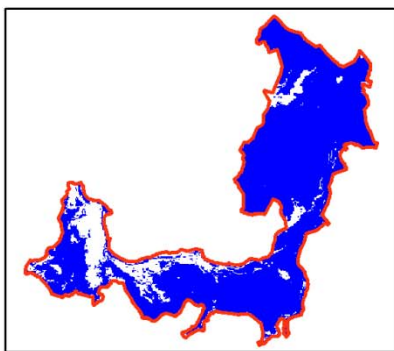
Jun.



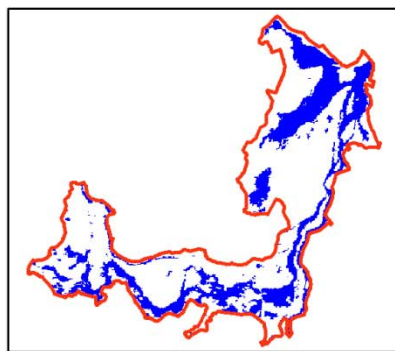
Jul.



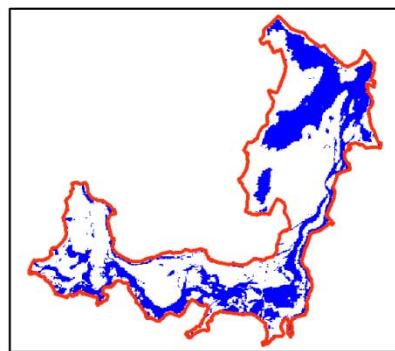
Aug.



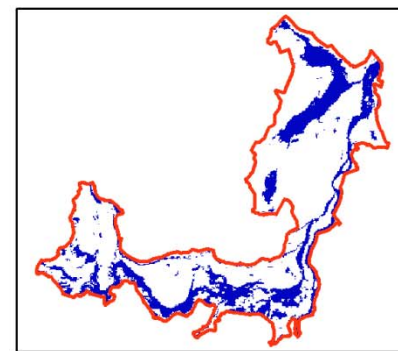
Sept.



Oct.



Nov.

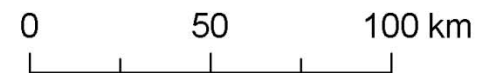


Dec.

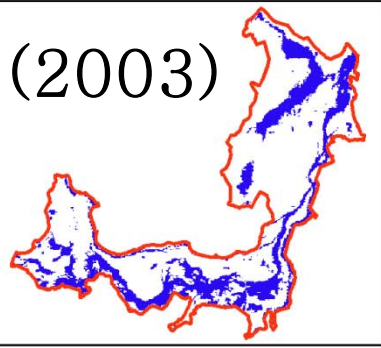


— Lake boudary

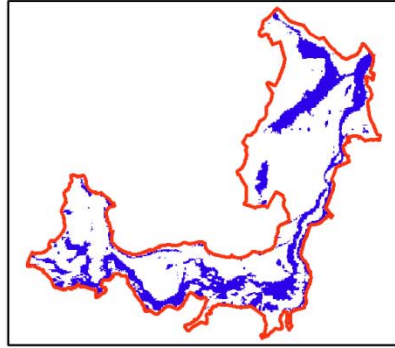
■ Water area



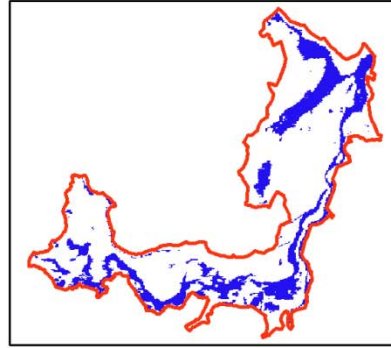
(2003)



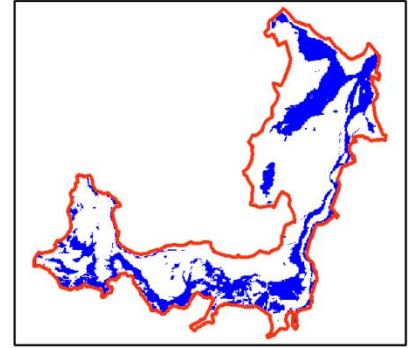
Jan.



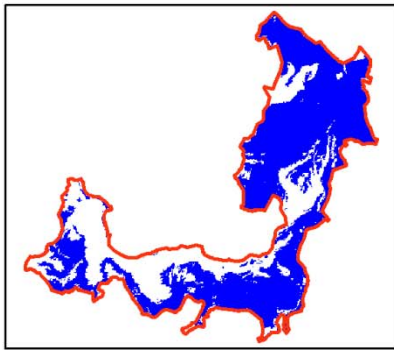
Feb.



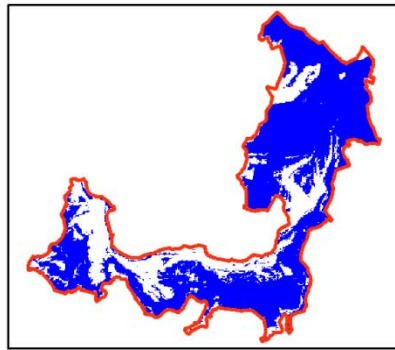
Mar.



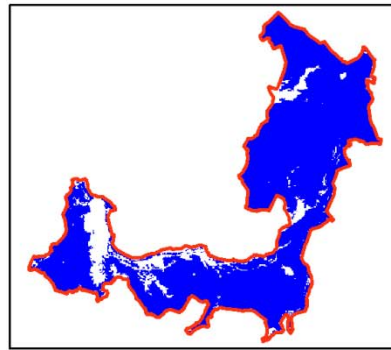
Apr.



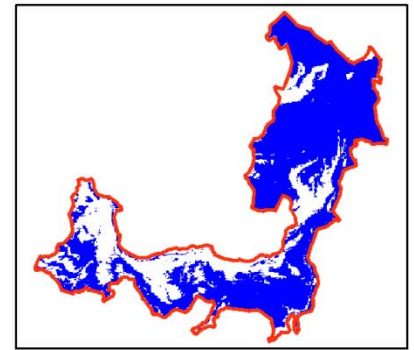
May



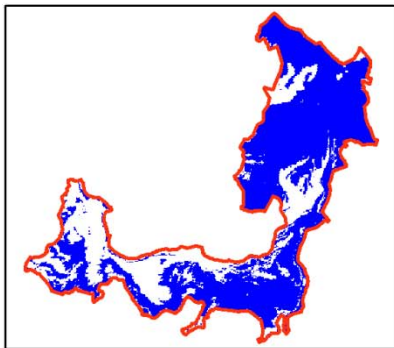
Jun.



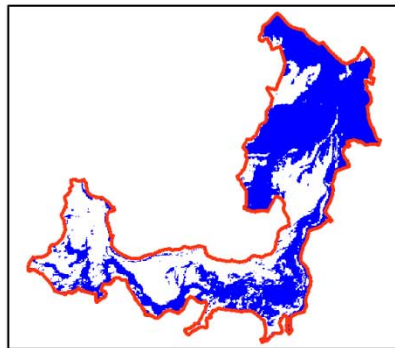
Jul.



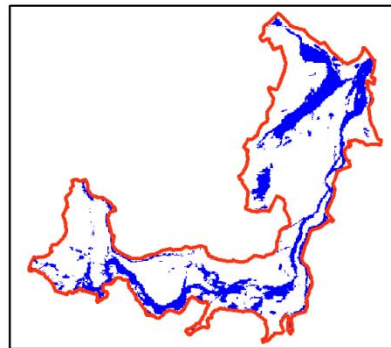
Aug.



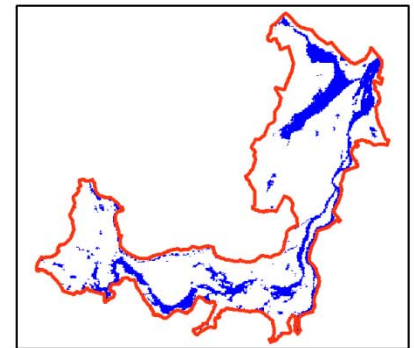
Sept.



Oct.



Nov.

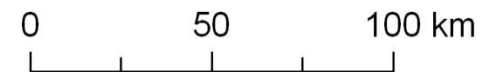


Dec.

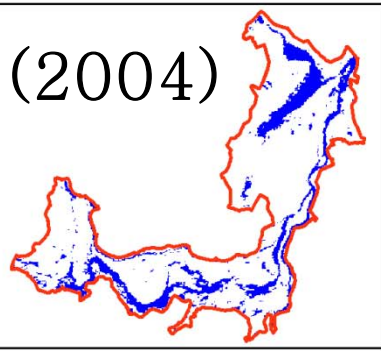


— Lake boudary

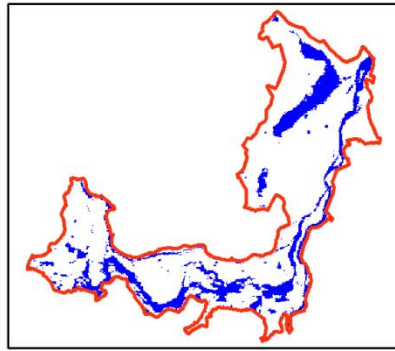
— Water area



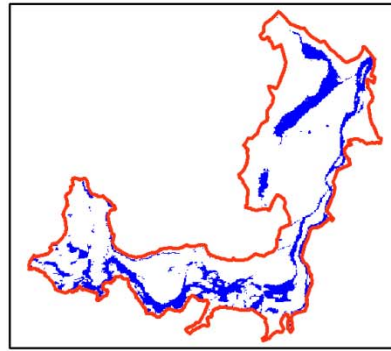
(2004)



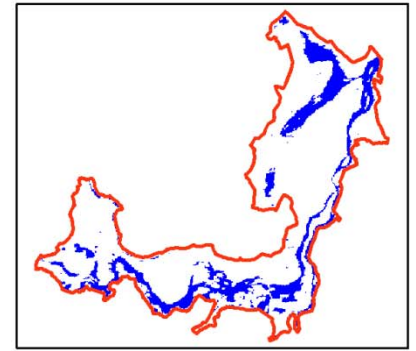
Jan.



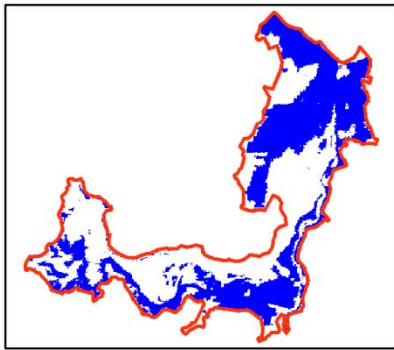
Feb.



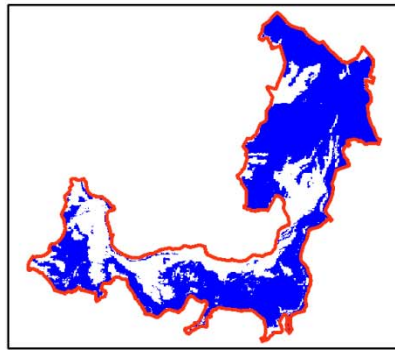
Mar.



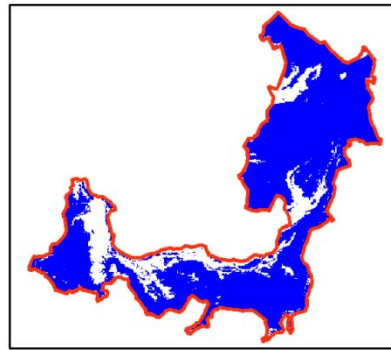
Apr.



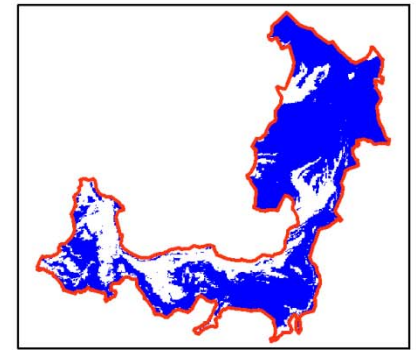
May



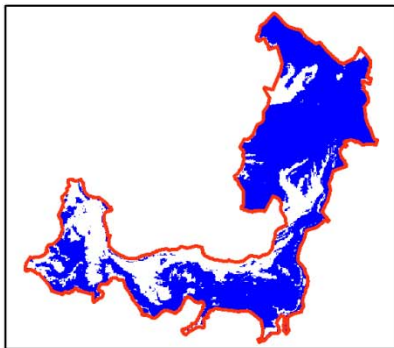
Jun.



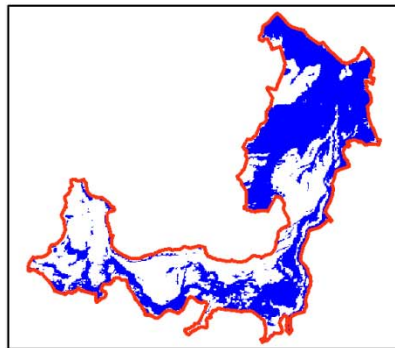
Jul.



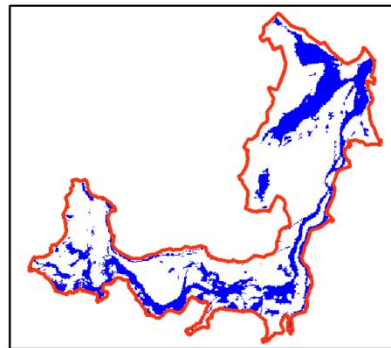
Aug.



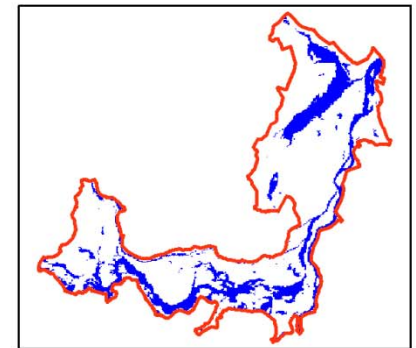
Sept.



Oct.



Nov.

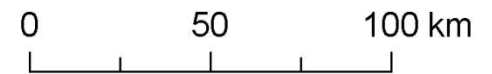


Dec.

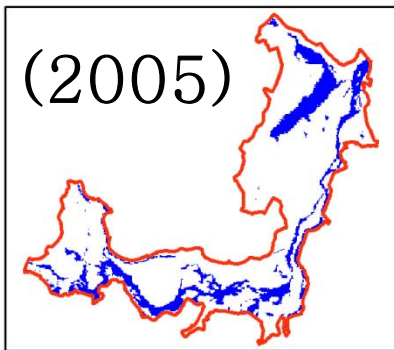


— Lake boundary

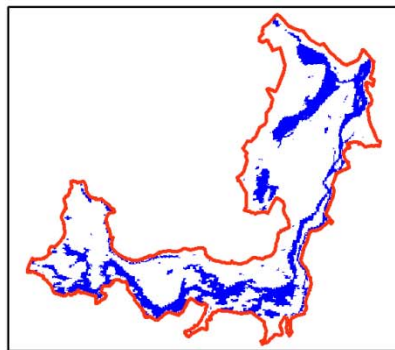
— Water area



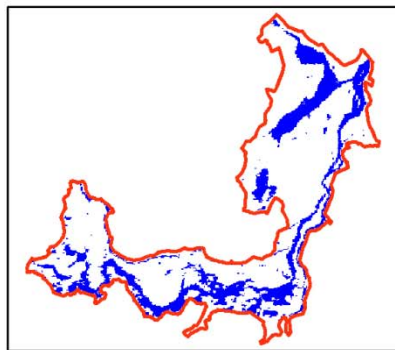
(2005)



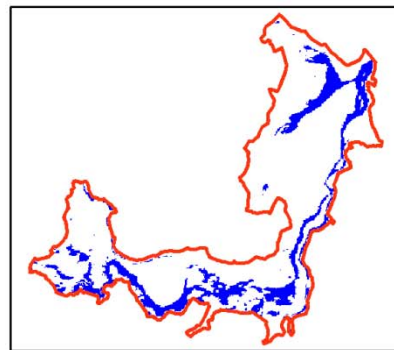
Jan.



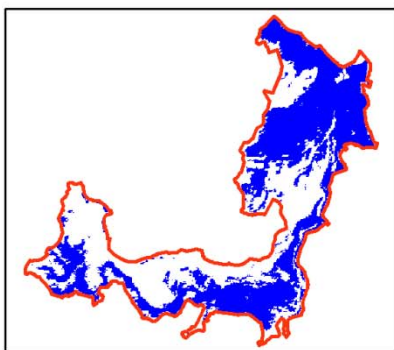
Feb.



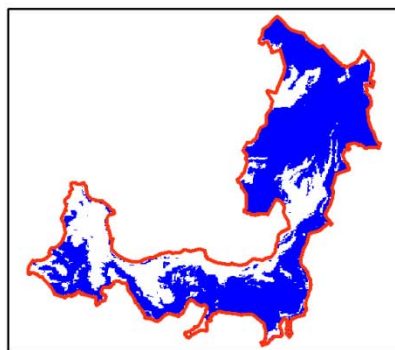
Mar.



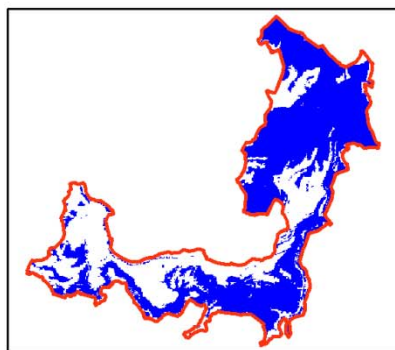
Apr.



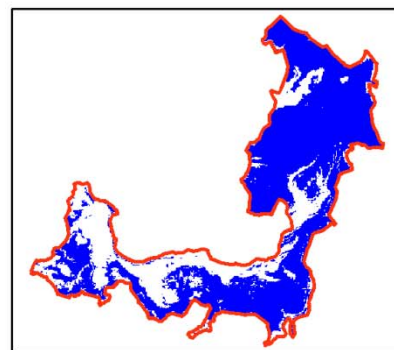
May



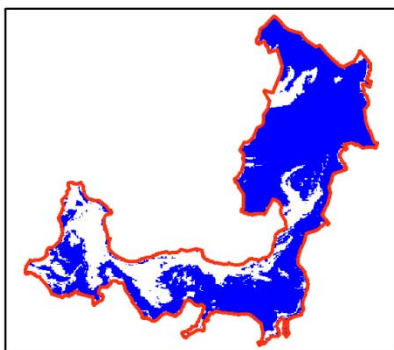
Jun.



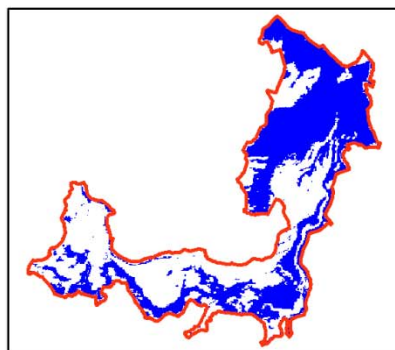
Jul.



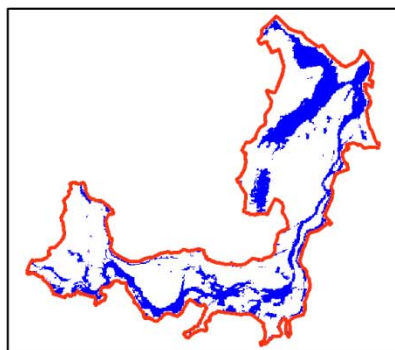
Aug.



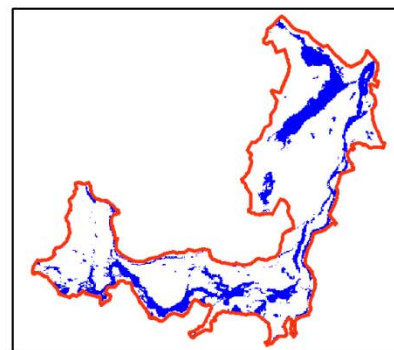
Sept.



Oct.



Nov.

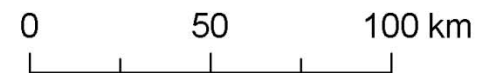


Dec.

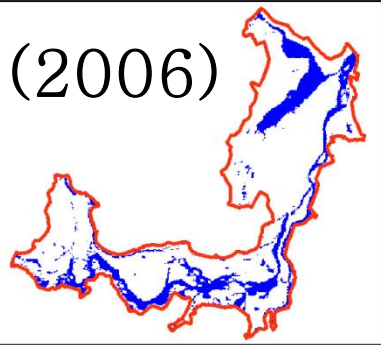


 Lake boudary

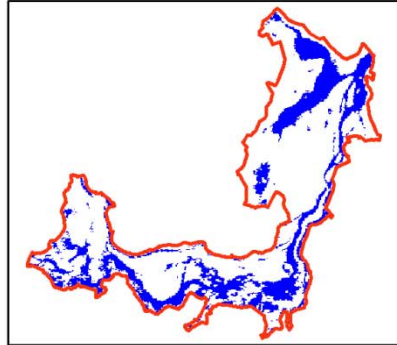
 Water area



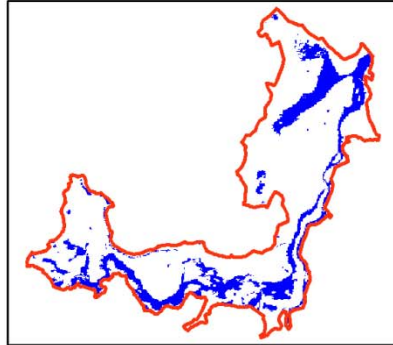
(2006)



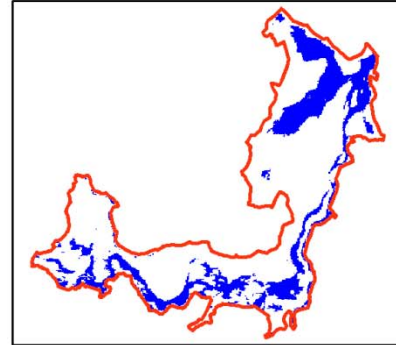
Jan.



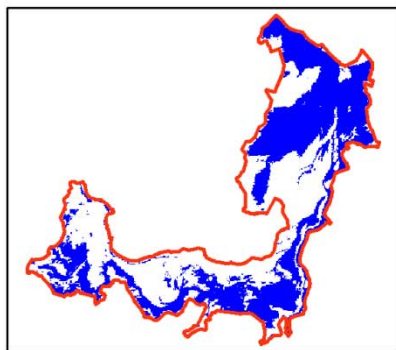
Feb.



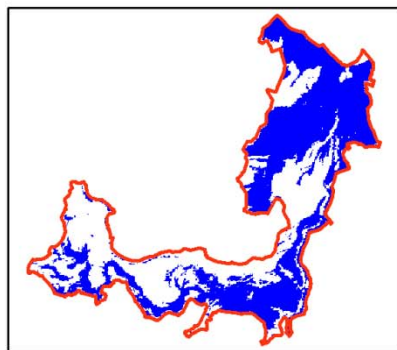
Mar.



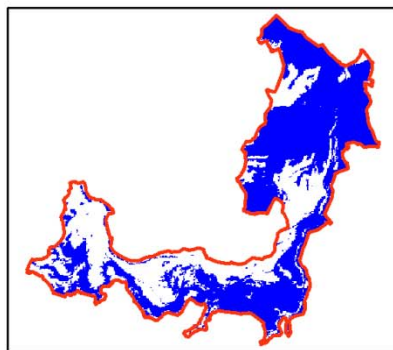
Apr.



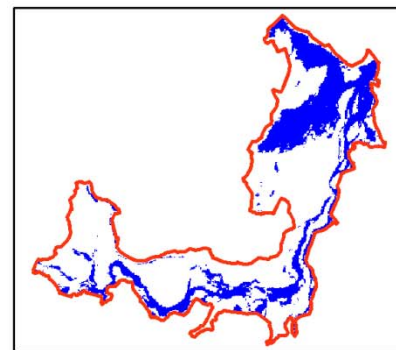
May



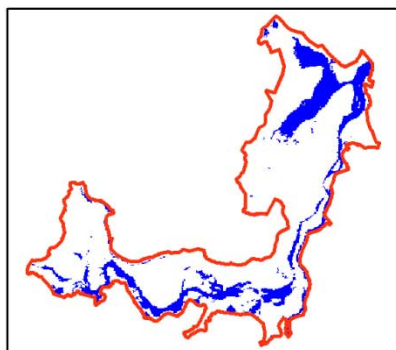
Jun.



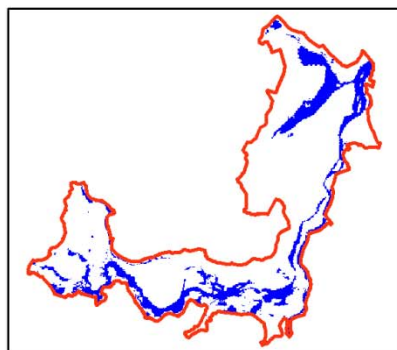
Jul.



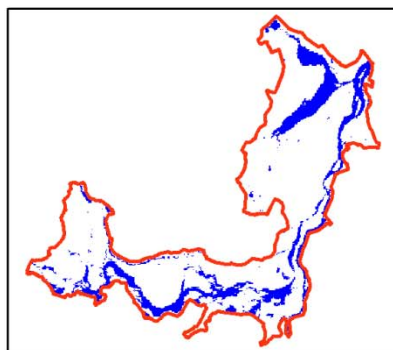
Aug.



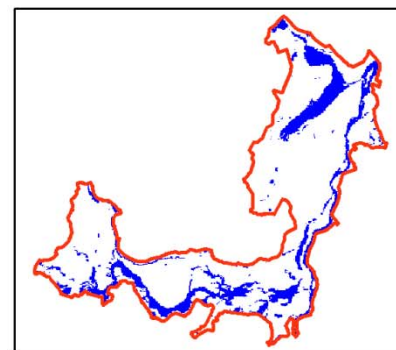
Sept.



Oct.



Nov.

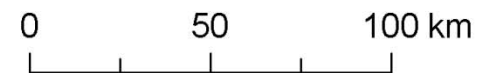


Dec.

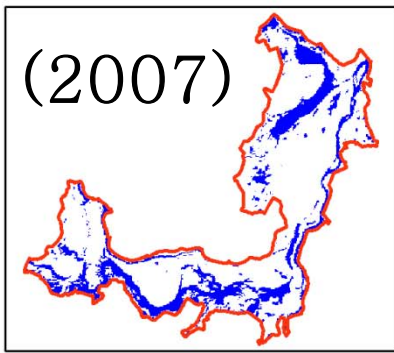


— Lake boudary

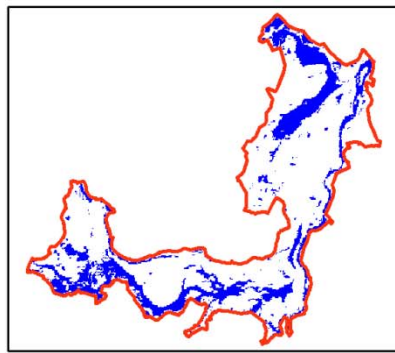
— Water area



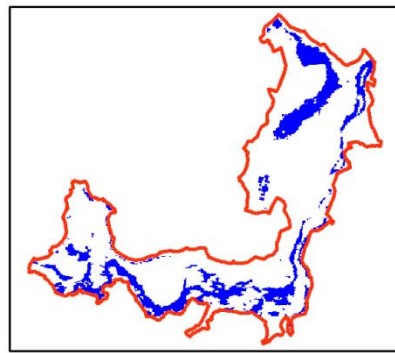
(2007)



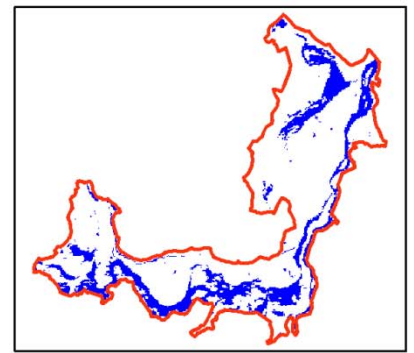
Jan.



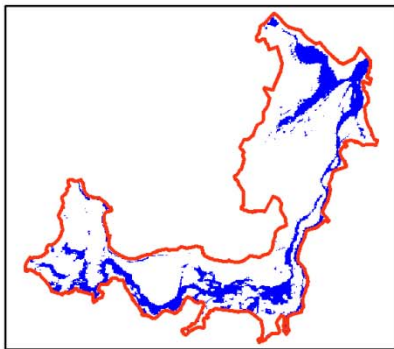
Feb.



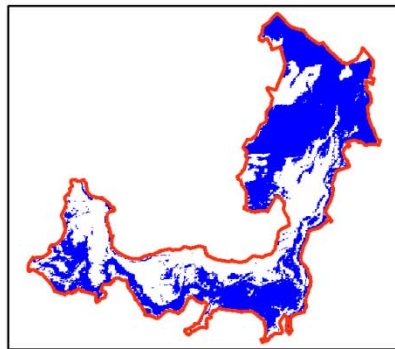
Mar.



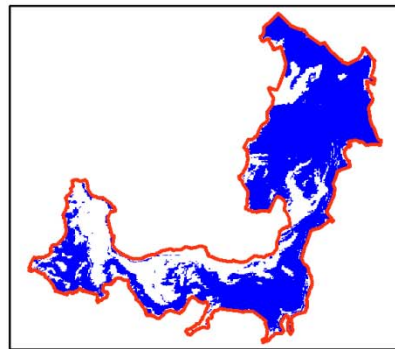
Apr.



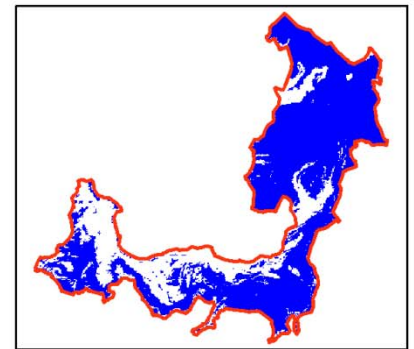
May



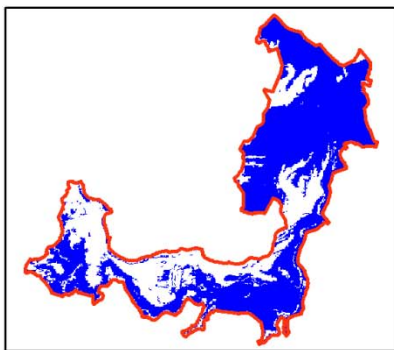
Jun.



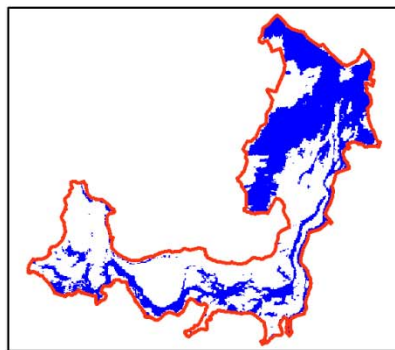
Jul.



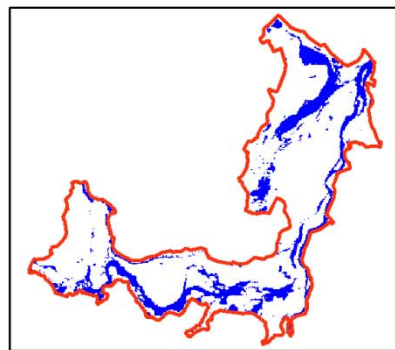
Aug.



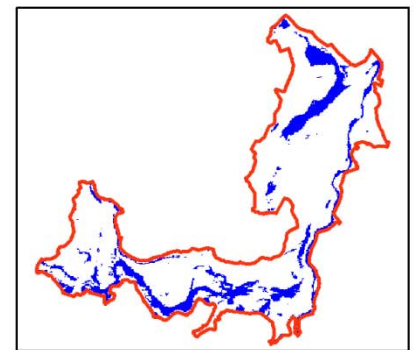
Sept.



Oct.



Nov.

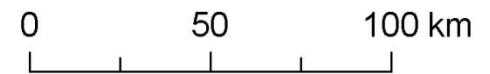


Dec.

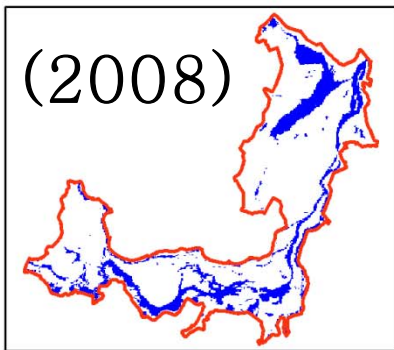


— Lake boundary

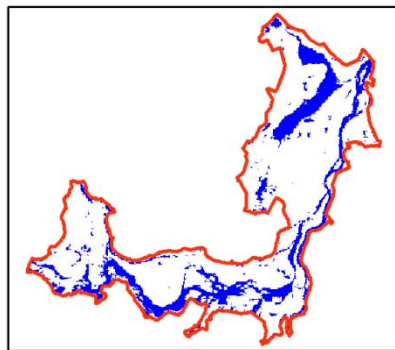
— Water area



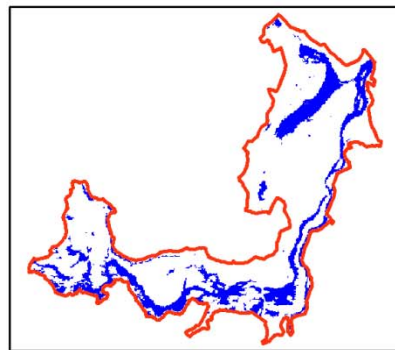
(2008)



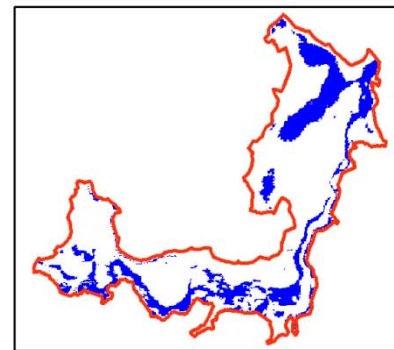
Jan.



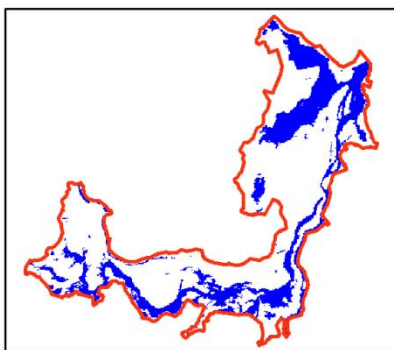
Feb.



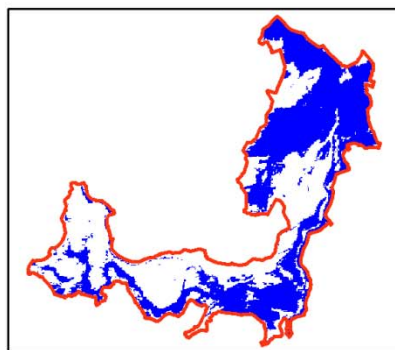
Mar.



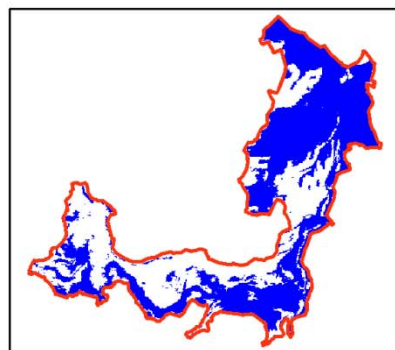
Apr.



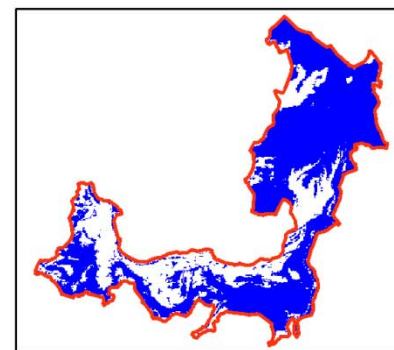
May



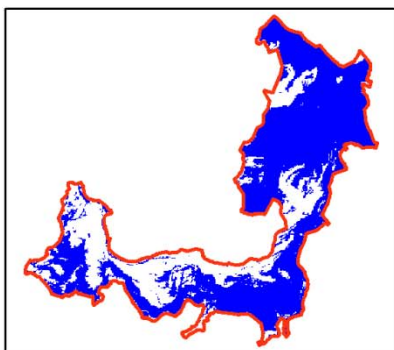
Jun.



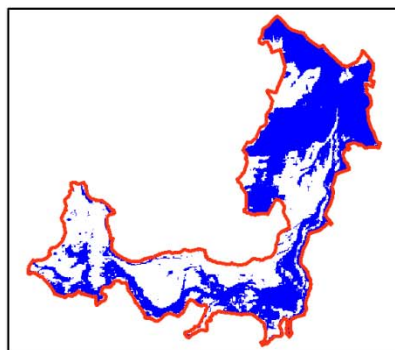
Jul.



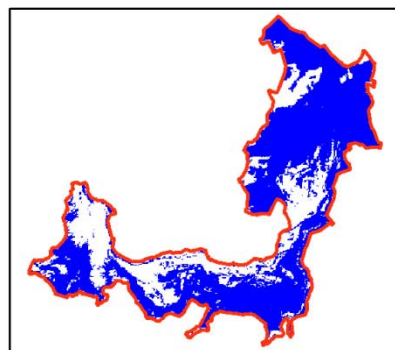
Aug.



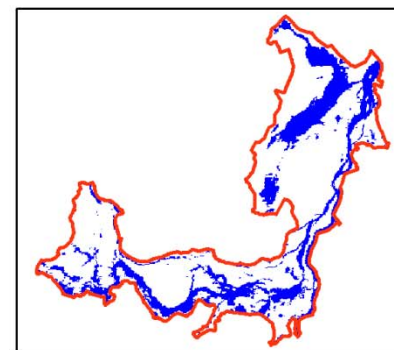
Sept.



Oct.



Nov.

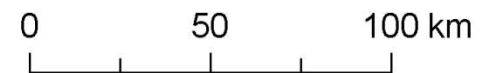


Dec.



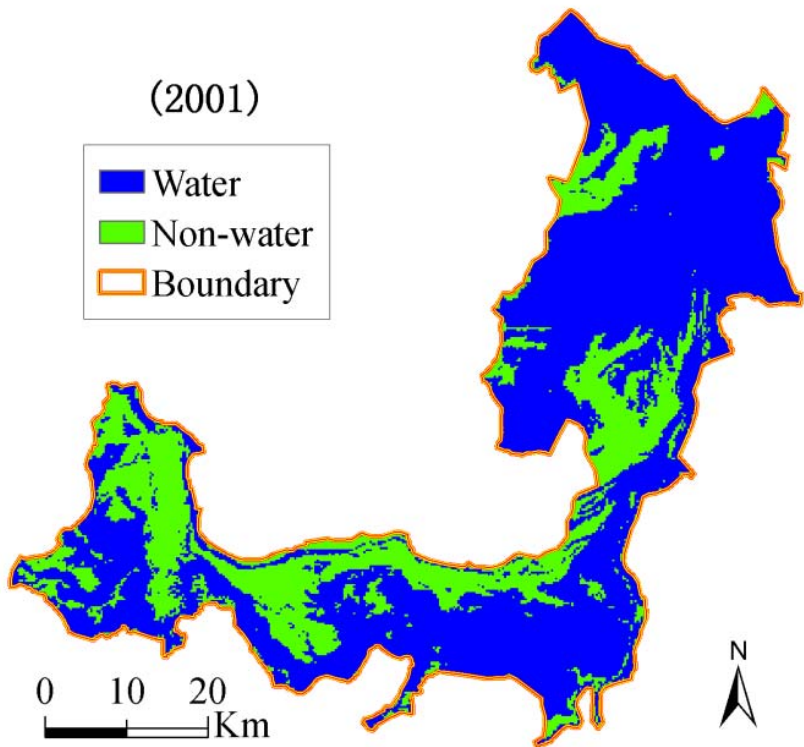
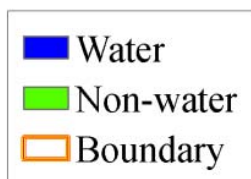
 Lake boudary

 Water area



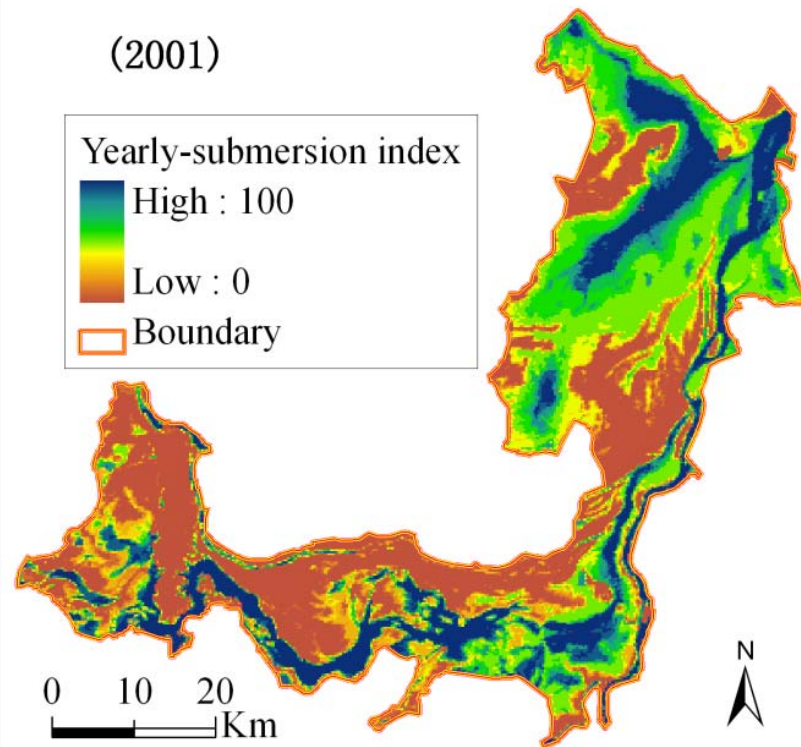
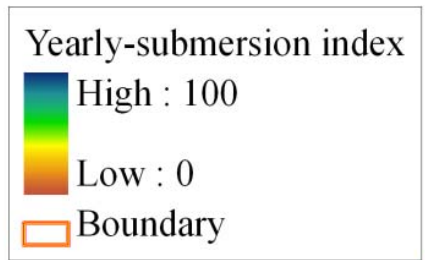
Water maximal extent (2001–2008)

(2001)



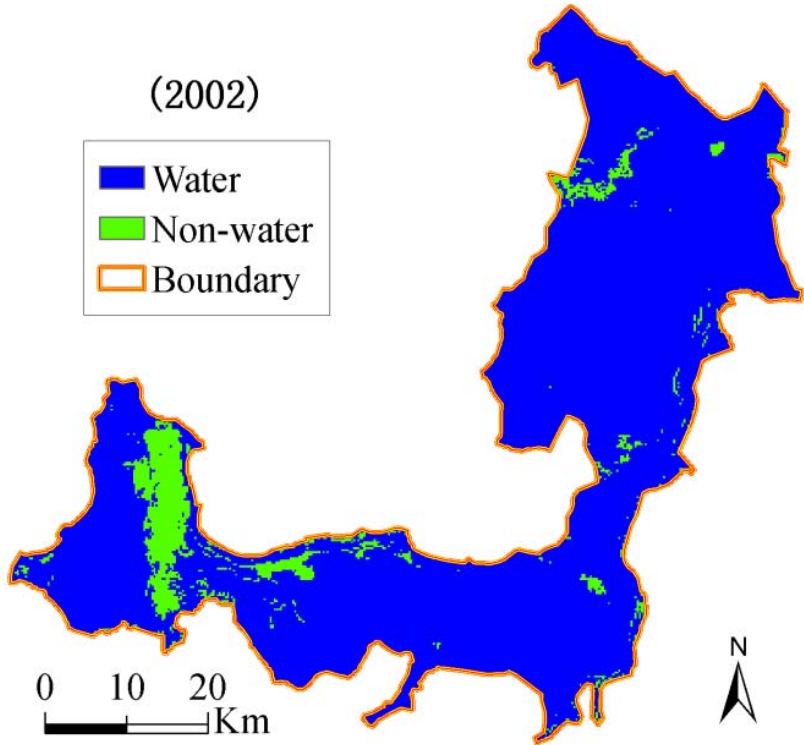
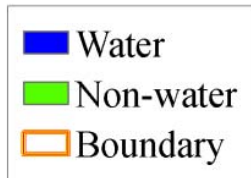
Water duration estimate (2001–2008)

(2001)



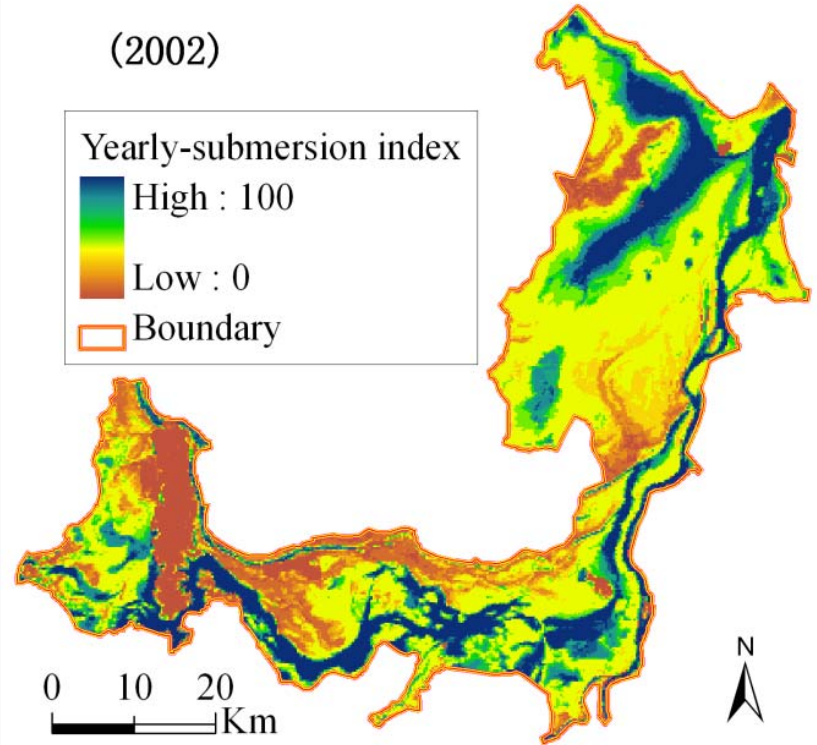
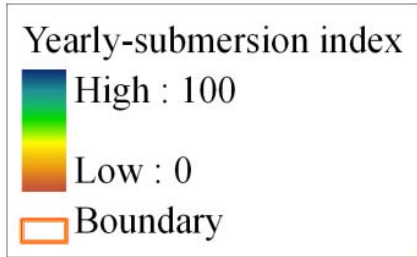
Water maximal extent (2001–2008)

(2002)



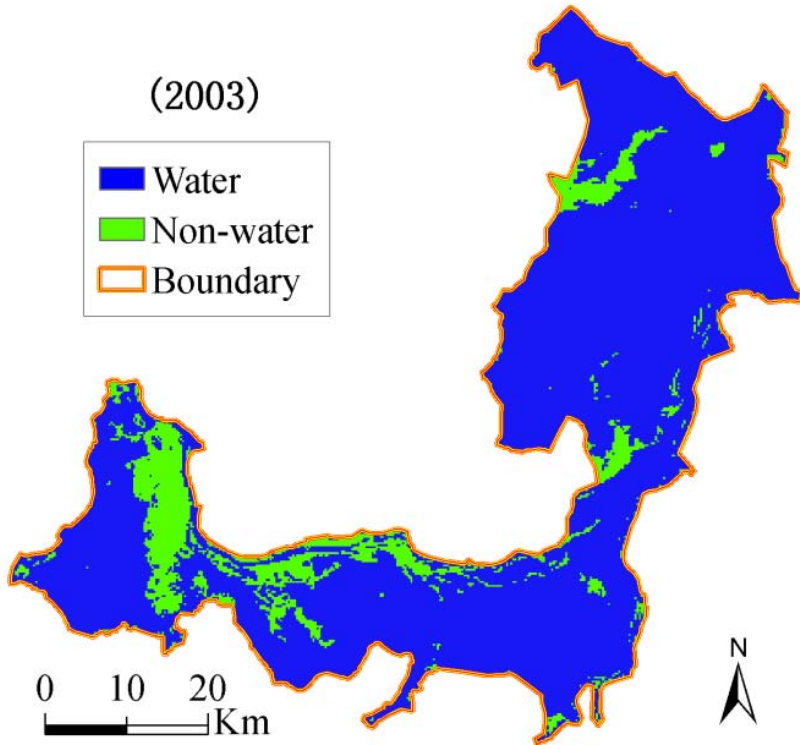
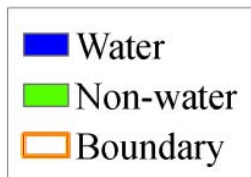
Water duration estimate (2001–2008)

(2002)



Water maximal extent (2001–2008)

(2003)



Water duration estimate (2001–2008)

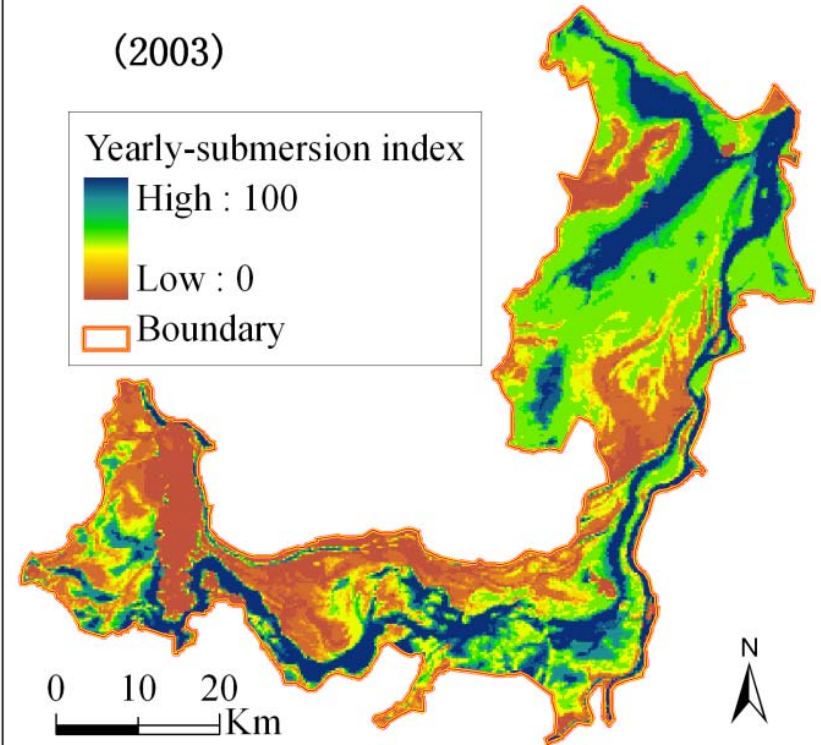
(2003)

Yearly-submersion index

High : 100

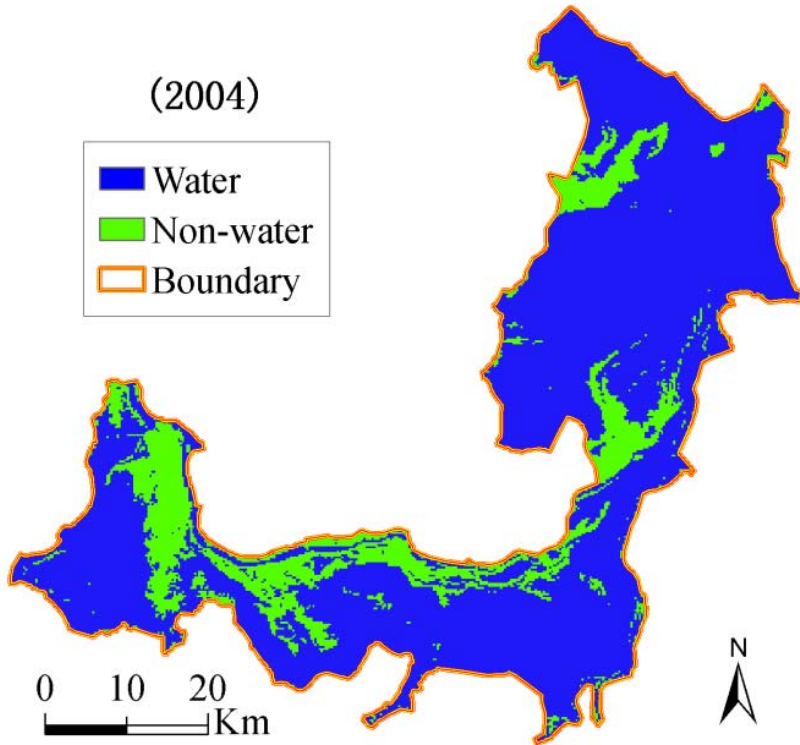
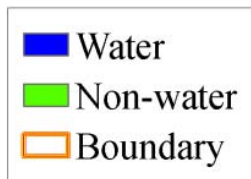
Low : 0

Boundary



Water maximal extent (2001–2008)

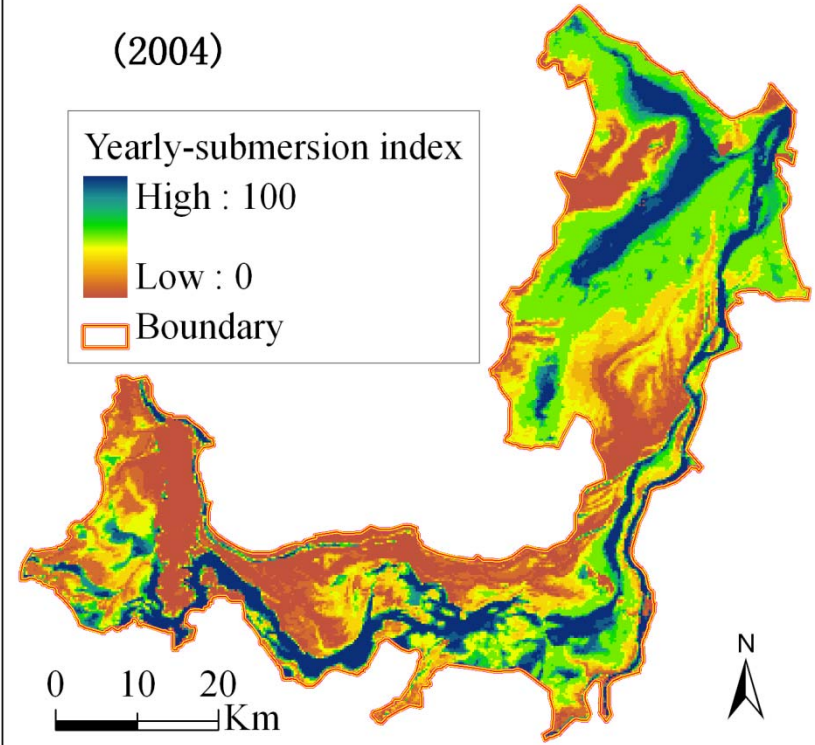
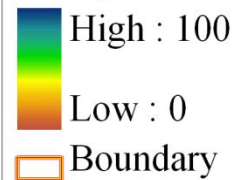
(2004)



Water duration estimate (2001–2008)

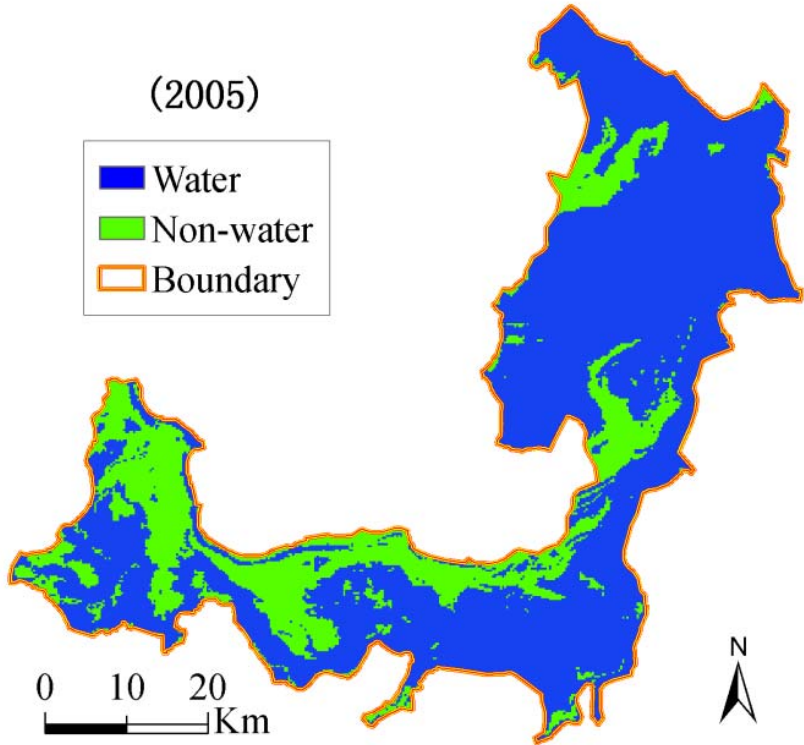
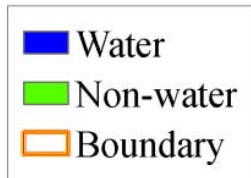
(2004)

Yearly-submersion index



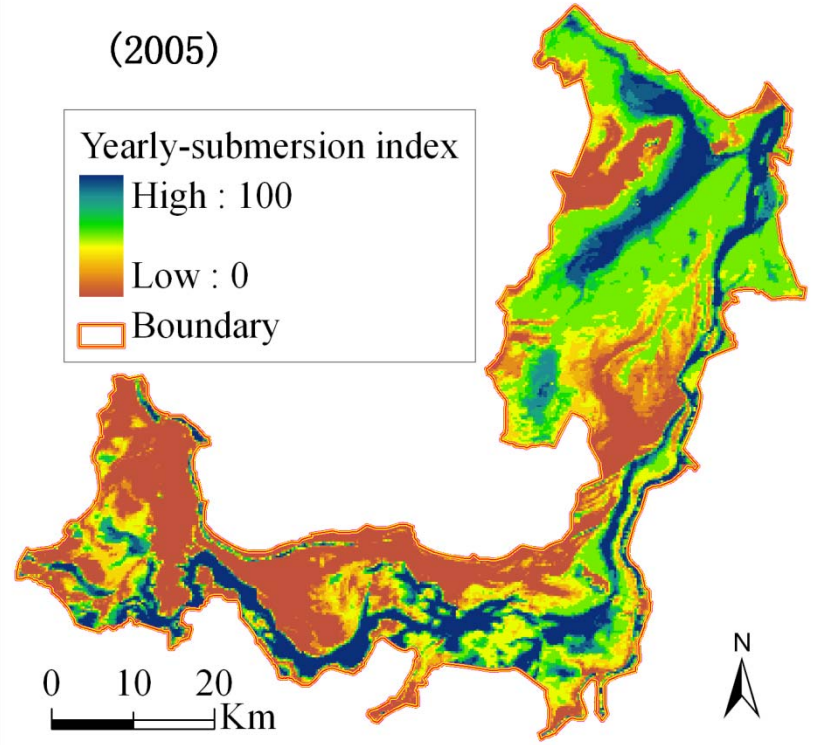
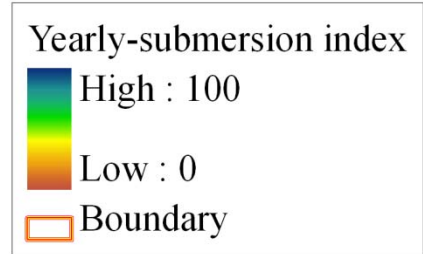
Water maximal extent (2001–2008)

(2005)



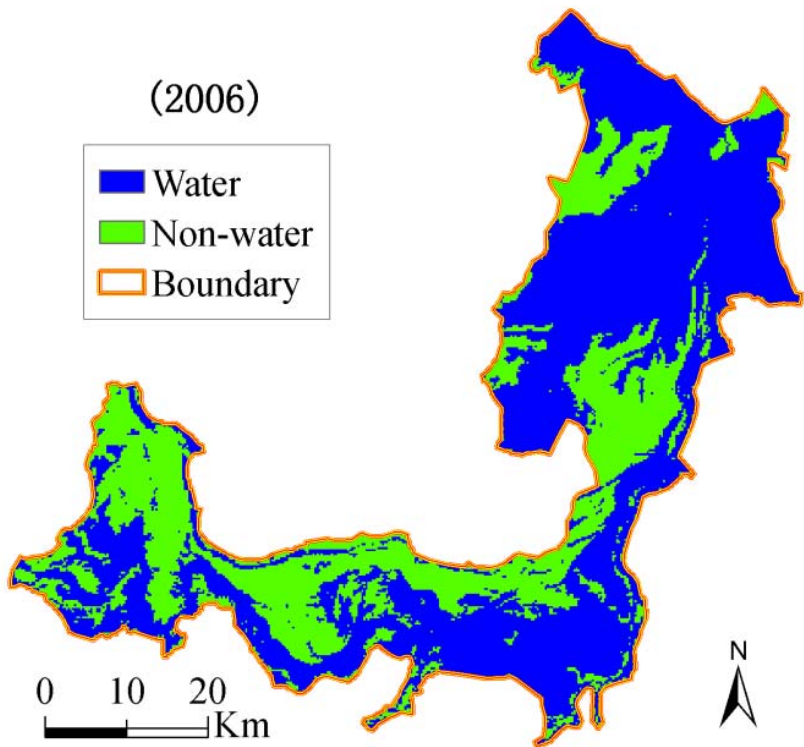
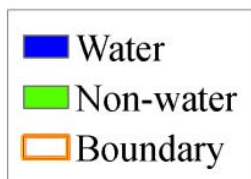
Water duration estimate (2001–2008)

(2005)



Water maximal extent (2001–2008)

(2006)



Water duration estimate (2001–2008)

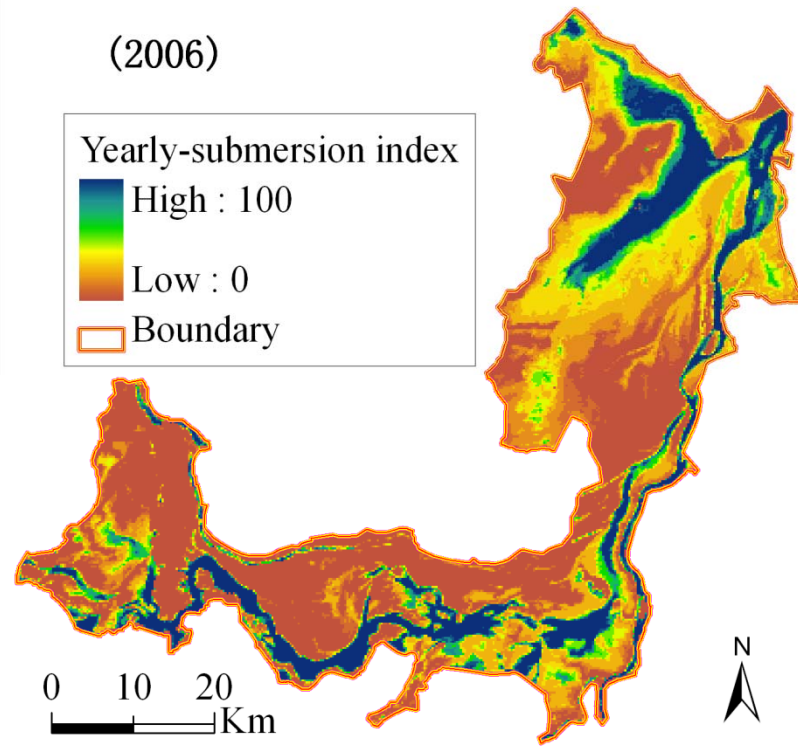
(2006)

Yearly-submersion index

High : 100

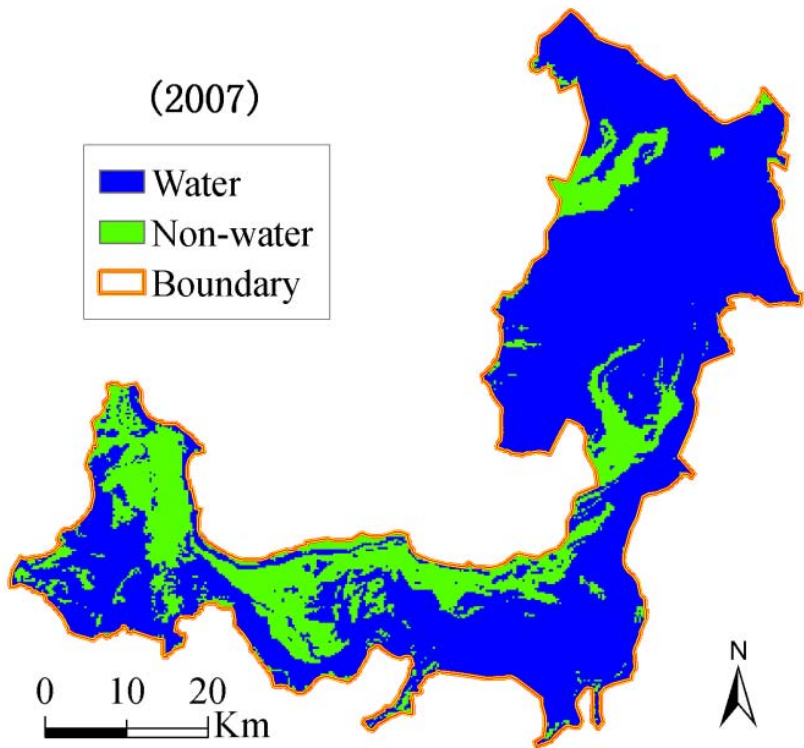
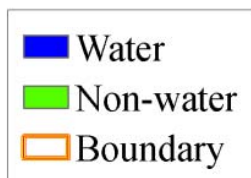
Low : 0

Boundary



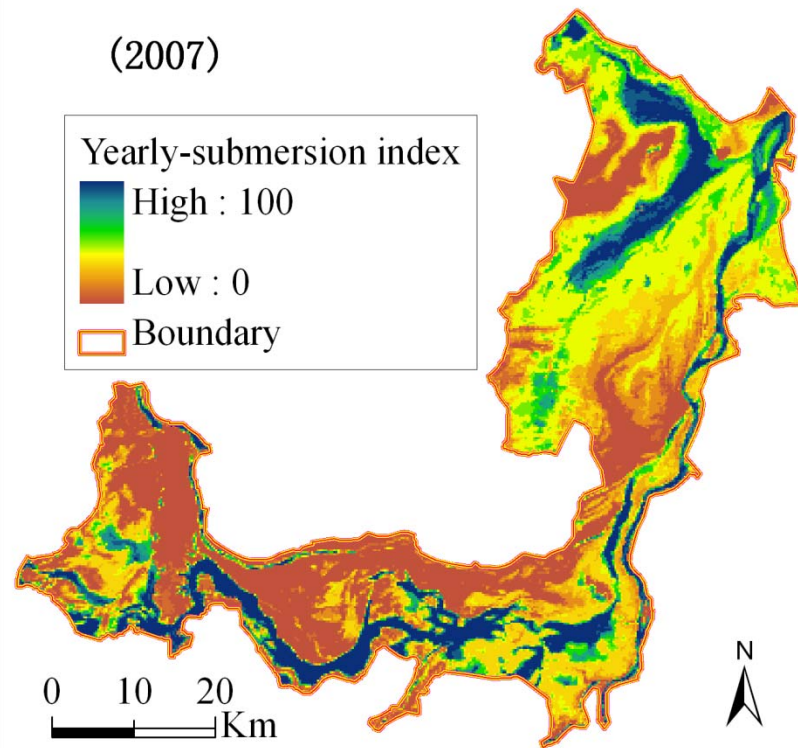
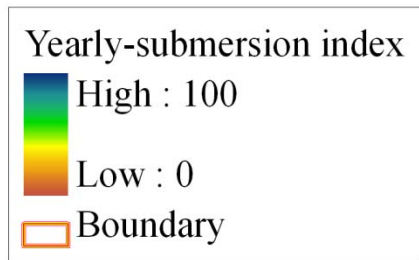
Water maximal extent (2001–2008)

(2007)



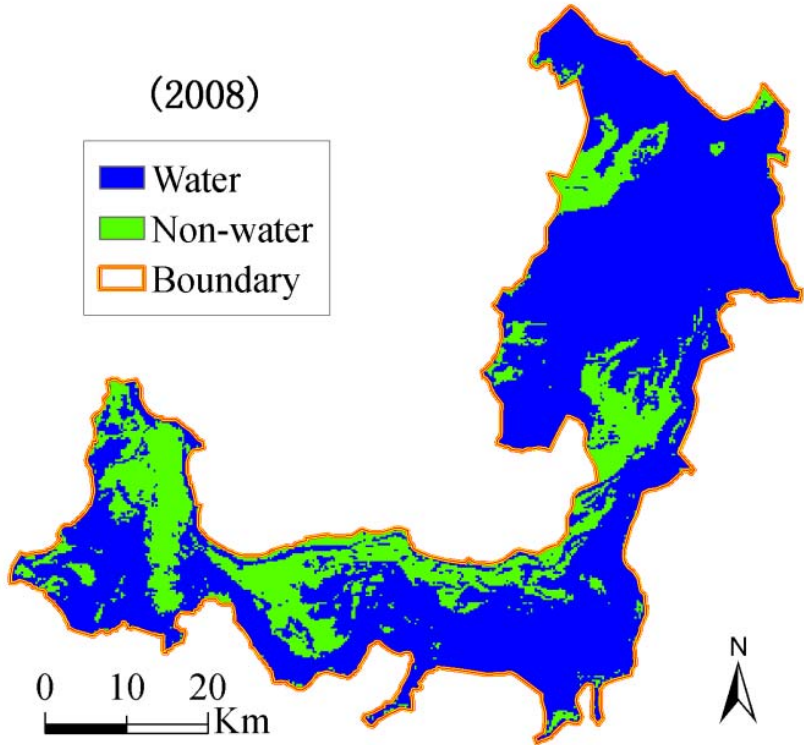
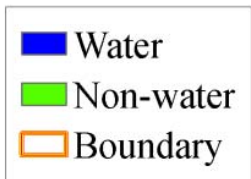
Water duration estimate (2001–2008)

(2007)



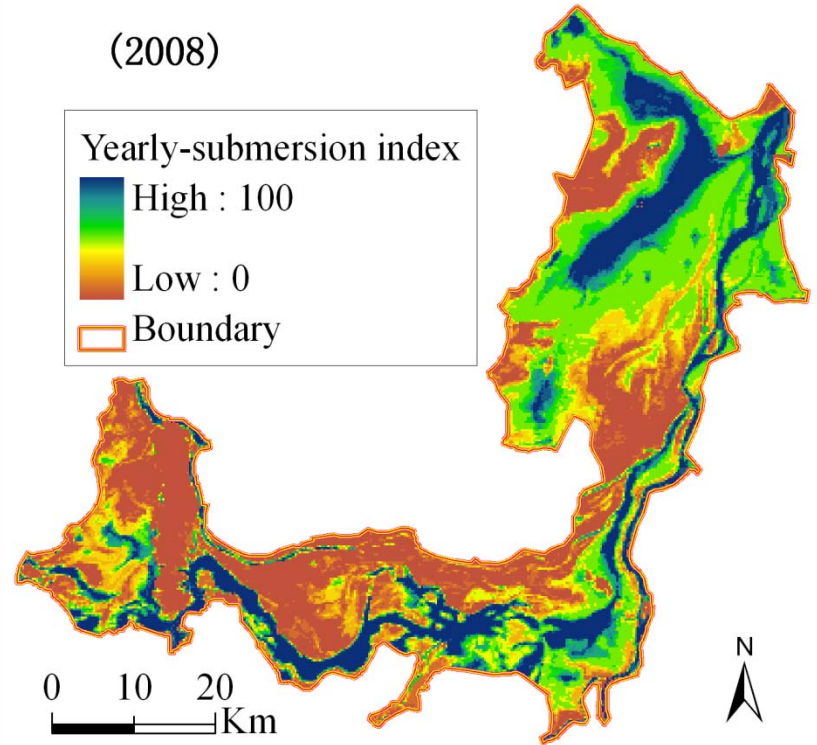
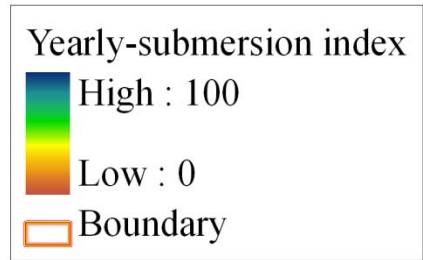
Water maximal extent (2001–2008)

(2008)



Water duration estimate (2001–2008)

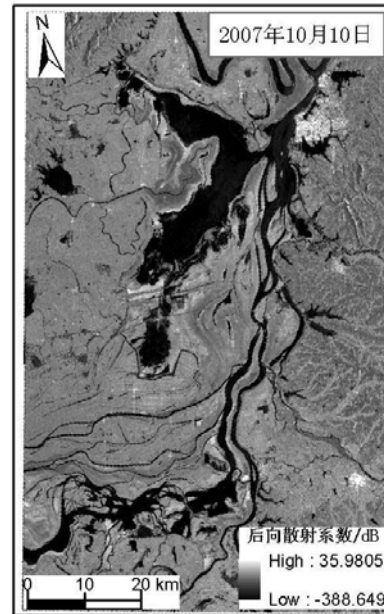
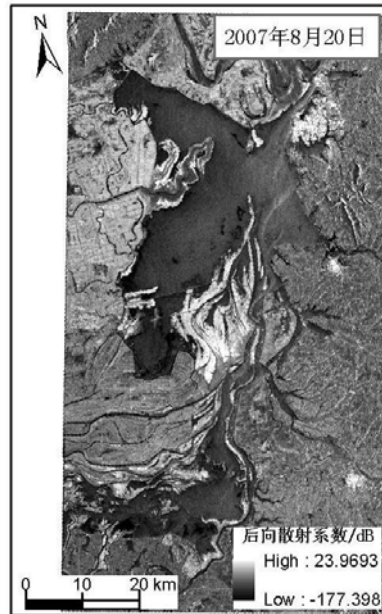
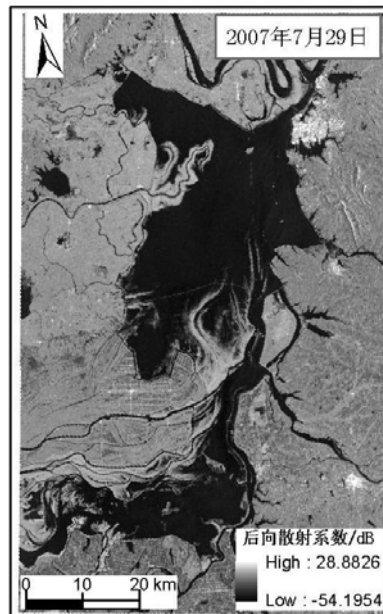
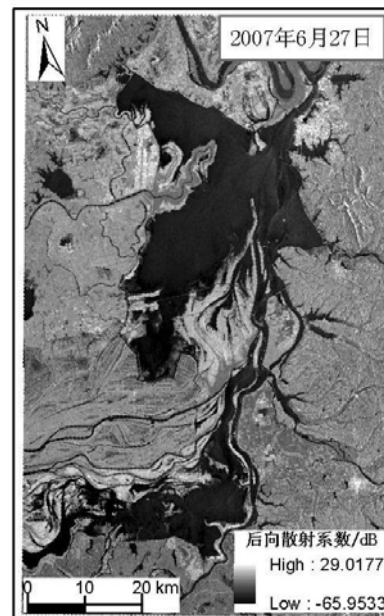
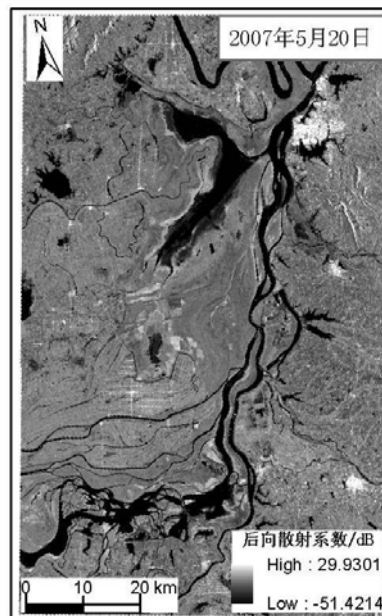
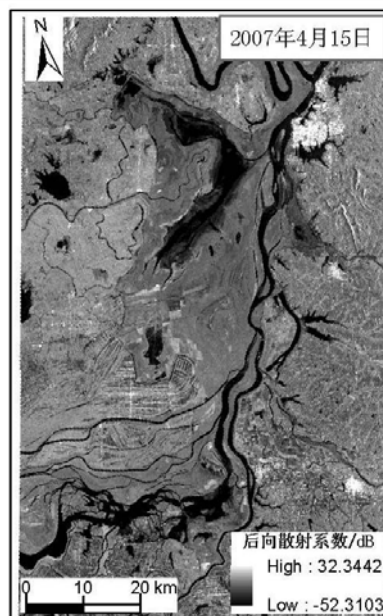
(2008)



Water Body Extraction from ENVISAT ASAR Images Based on a Modified Otsu thresholding Method

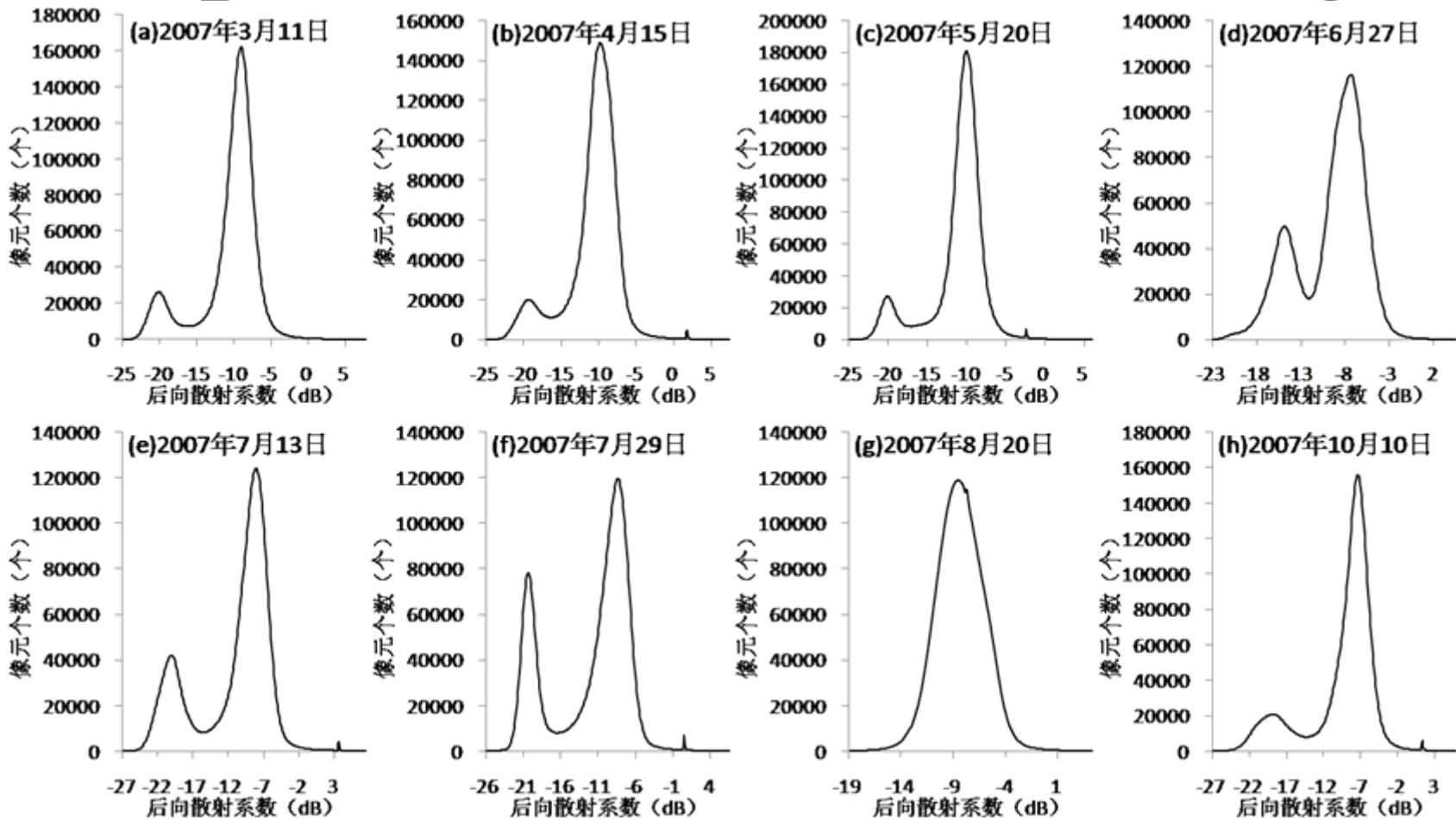
- * Eight scenes ENVISAT/ASAR APP-1P imageries during the low and high water season of 2007 year were use to monitor the flood of Dongting Lake.

ID	Acquire time	Data level	Polarization mode	Incidence angle	Space resolution	ascending /descending
1	2007-3-11	IMP_1P	H/H	IS5	30m	descending
2	2007-4-15	IMP_1P	H/H	IS5	30m	descending
3	2007-5-20	IMP_1P	H/H	IS5	30m	descending
4	2007-6-27	IMP_1P	V/V	IS3	30m	descending



Results of the ASAR data preprocessed

Optimal threshold searching

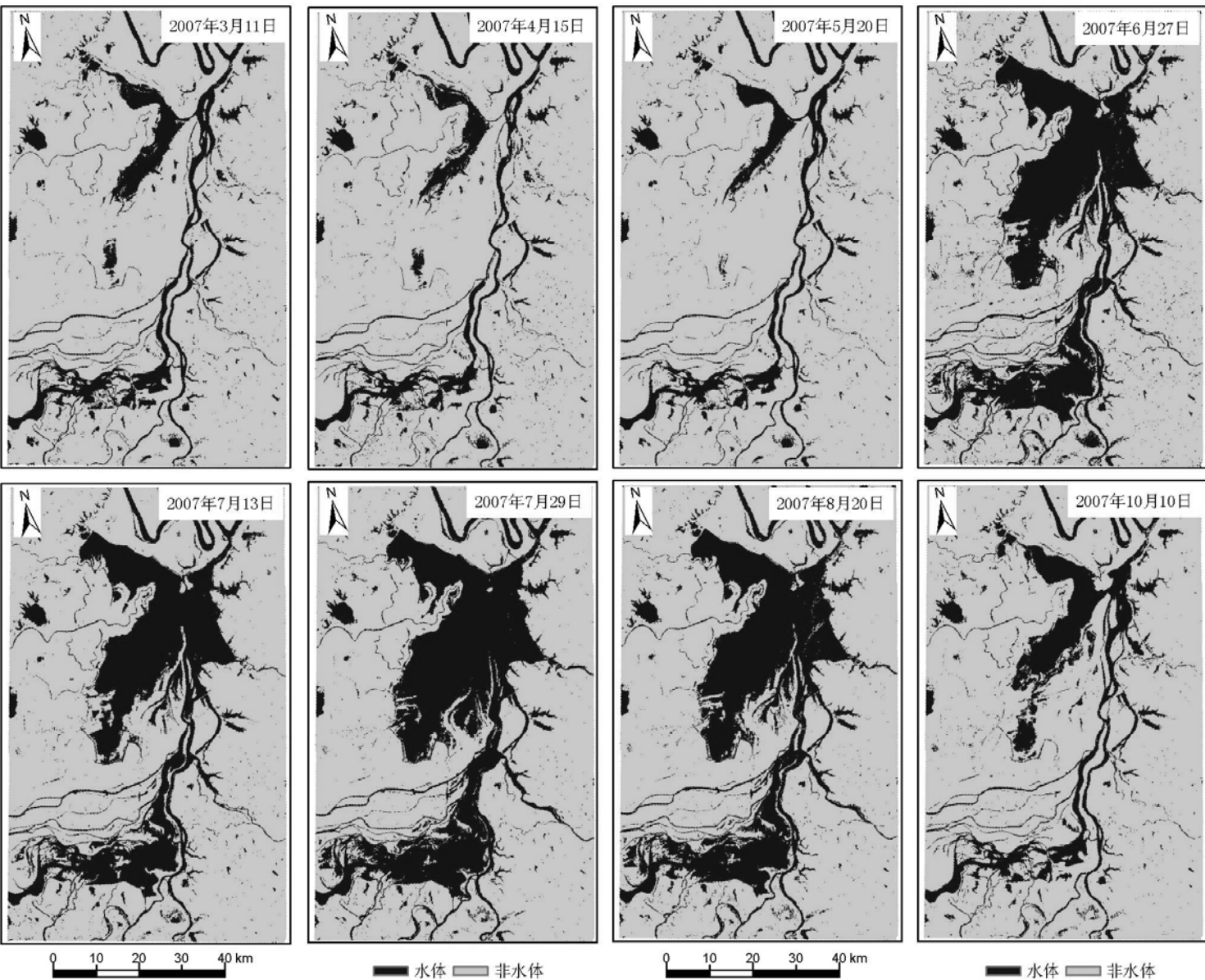


The histogram of the backscattering coefficient for the eight preprocessed ASAR images

Optimal threshold searching results by the modified Otsu method

Time	Left-peak	Right-peak	Inter-peak valley	optimal threshold
2007-3-11	-20.0367	-9.03671	-16.5367	-15.8367
2007-4-15	-19.5498	-10.0498	-16.6498	-15.3499
2007-5-20	-20.0834	-9.98340	-17.0834	-16.4834
2007-6-27	-15.2501	-7.75012	-12.5501	-12.2501
2007-7-13	-19.8435	-7.74347	-15.6435	-15.2435
2007-7-29	-20.5582	-8.55821	-16.5582	-15.6582
2007-8-20	—	—	—	—
2007-10-10	-19.2492	-7.54919	-14.5492	-14.0492

Note: The histogram of the backscattering coefficient for 2007-8-20 ASAR data has only one peak, so the modified Otsu method is not applicable.



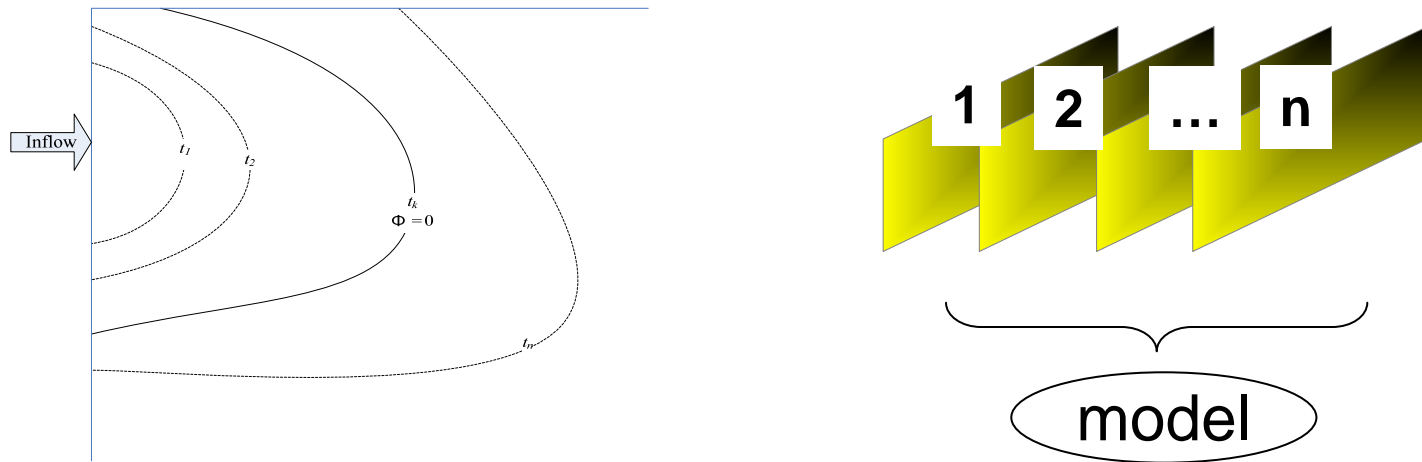
The water extracted results based the optimal threshold from the modified Otsu method

Assimilation of remotely sensed flood extent

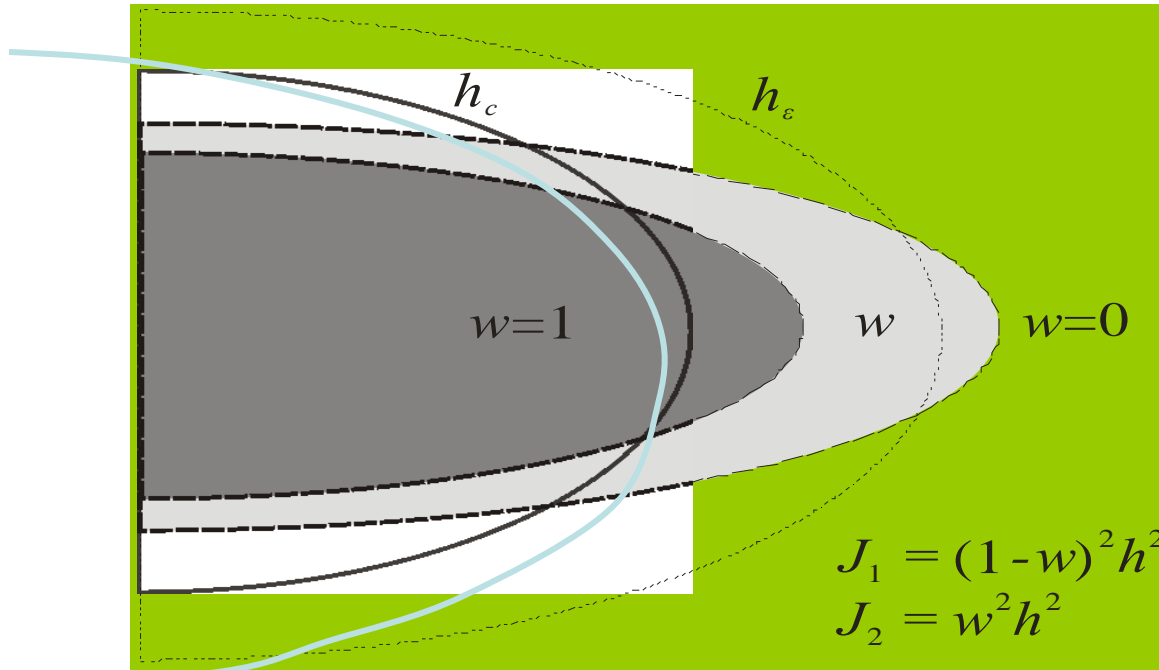
- Objective: To quantitatively utilize the rich remotely sensed data from satellite imageries in the analysis or prediction of flood routing processes, a variational data assimilation (4D-Var) method is proposed to assimilate the flood extent data into a two-dimensional (2D) flood dynamic model.
- State-of-art of flood assimilation: Based on the proposed 4D-Var method, the water levels derived from RADARSAT-1 image of a Mosel River flood event (1997, France) was assimilated into 2D flood model and was proved to be capable of enhancing model calibration. However, water levels from satellite imagery are indirectly retrieved by estimating the waterline elevations using the remotely observed flood extent and topographic map (or a digital elevation model). The accuracies of available water levels are low, typically 40~50 cm. Additional step, i.e. the water level retrieval could be found when we conduct the assimilation of remotely sensed water levels into hydraulic model.

5) Assimilation of remotely sensed for flood extent

- As direct observations, the remotely flood extent can be directly derived from satellite imagery and with close spatial resolution (like, 30m of Envisat ASAR and 250m MODIS data) comparing with the mesh size normally applied in flood modeling. Therefore, we would like to answer a question if we can assimilate flood extent data directly into the model by identifying the parameters using the 4D-Var and then improve the flood prediction.



Cost function



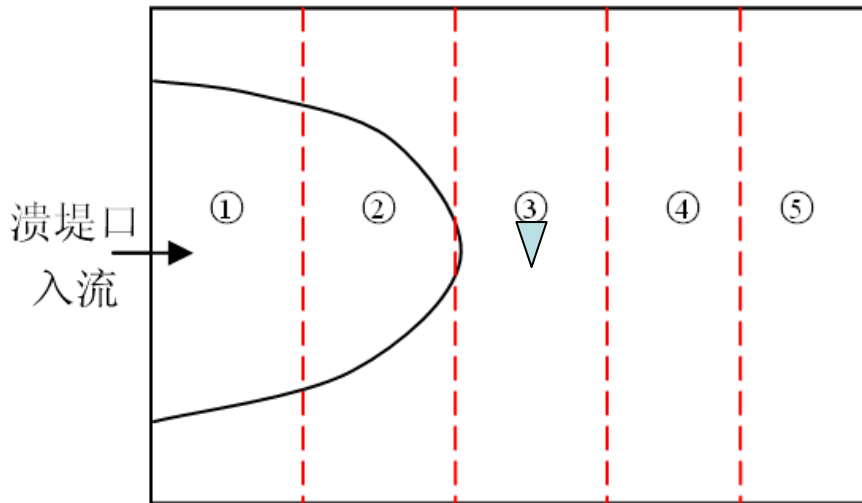
$$J(p) = 0.5 \left(\sum_{\Omega_1} (1-w_i)^2 h_i^2 + \sum_{\Omega_2} w_i^2 h_i^2 \right)$$

Ω_1 outside of the remotely sensed water area but inside of the computed water area

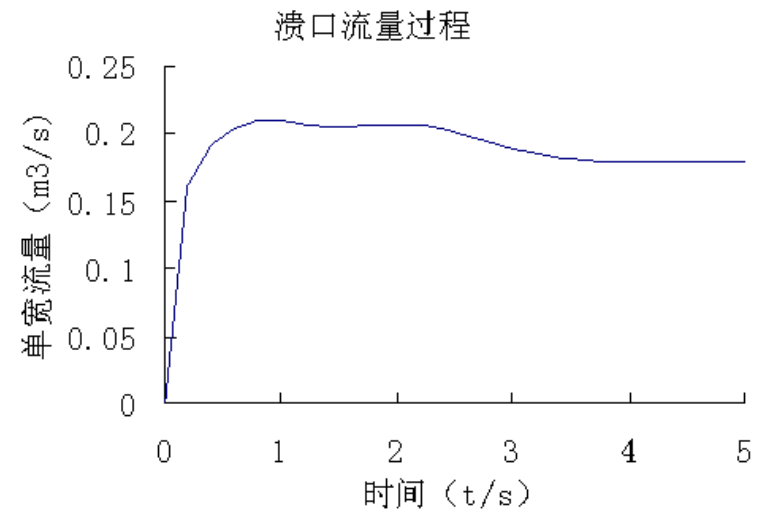
Ω_2 inside the remotely sensed water area but outside of the computed water area

Twin experiments

Dyke-Breach



(a) 算例示意图



(b) 溃口流量过程

Dyke-Breach——Experiments

Twin experiments (synthetic data)

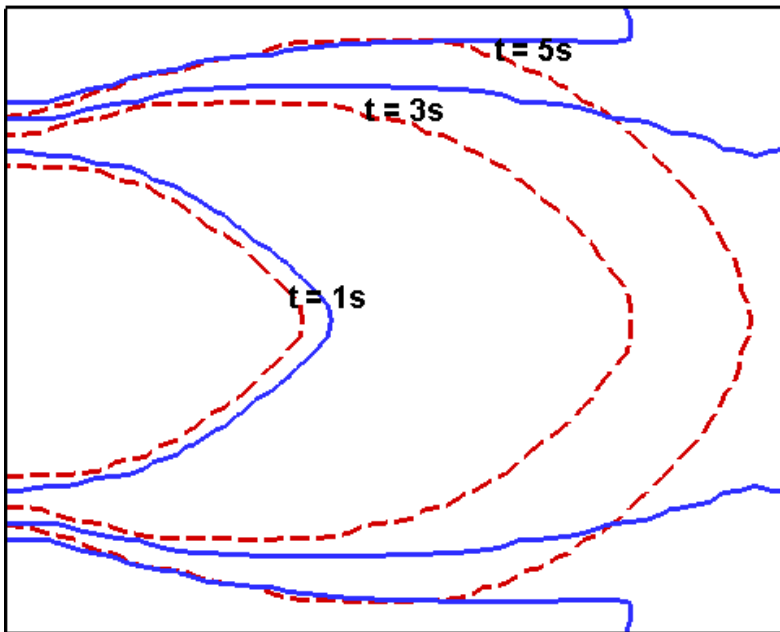
Observations :

- (1) stage hydrograph at central point**
- (2) water extent at different time**

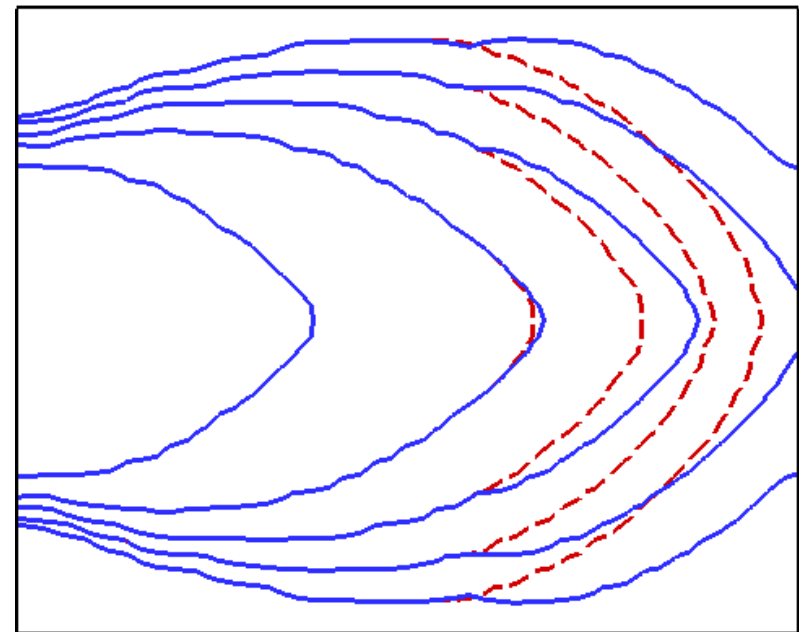
Description of observations

	Description of observations
Group A	One flood extent at $t = 5s$
Group B	Three flood extent at $t = 1, 3$ and $5s$
Group C	$Z(t)$, water level hydrograph at central position of floodplain (measuring time interval is $1s$)
Group D	One flood extent at $t = 5s$ and $Z(t)$
Group E	Three flood extents at $t = 1, 3$ and $5s$ and $Z(t_0)$

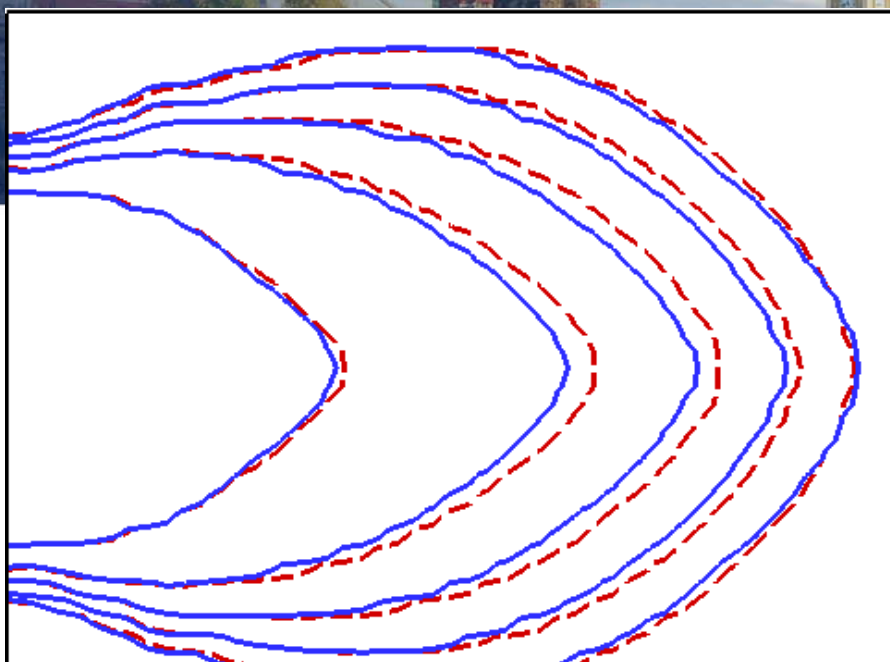
Experiment series A: Identification of the n values



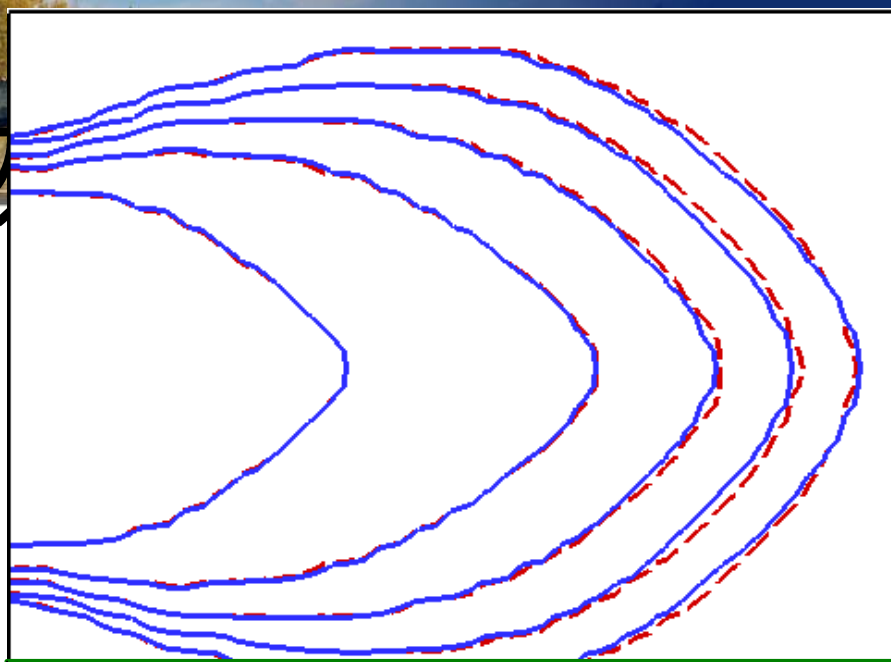
Initl	0.02
-------	------



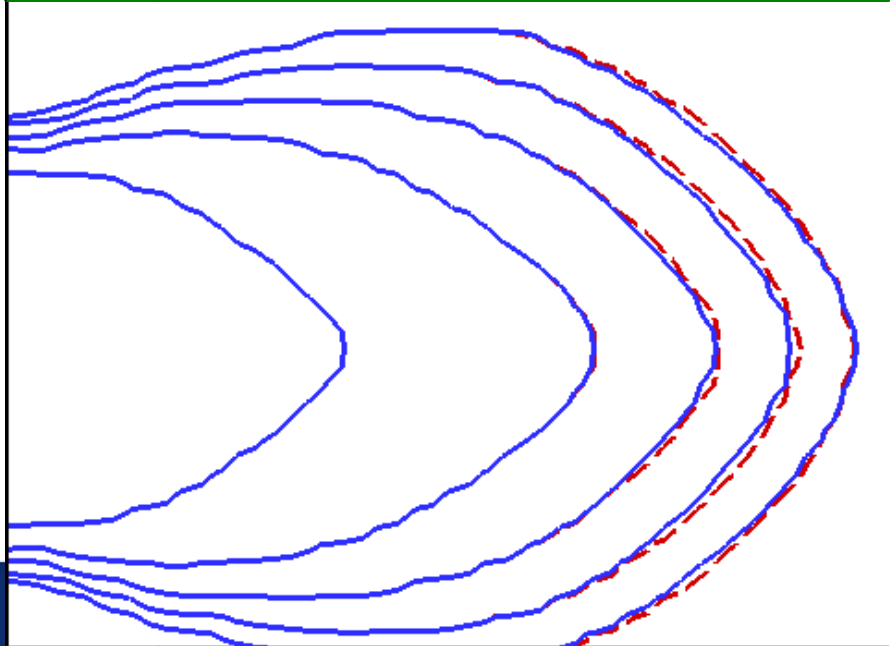
G-C	0.03	0.04	0.05	0.02	0.02
-----	------	------	------	------	------



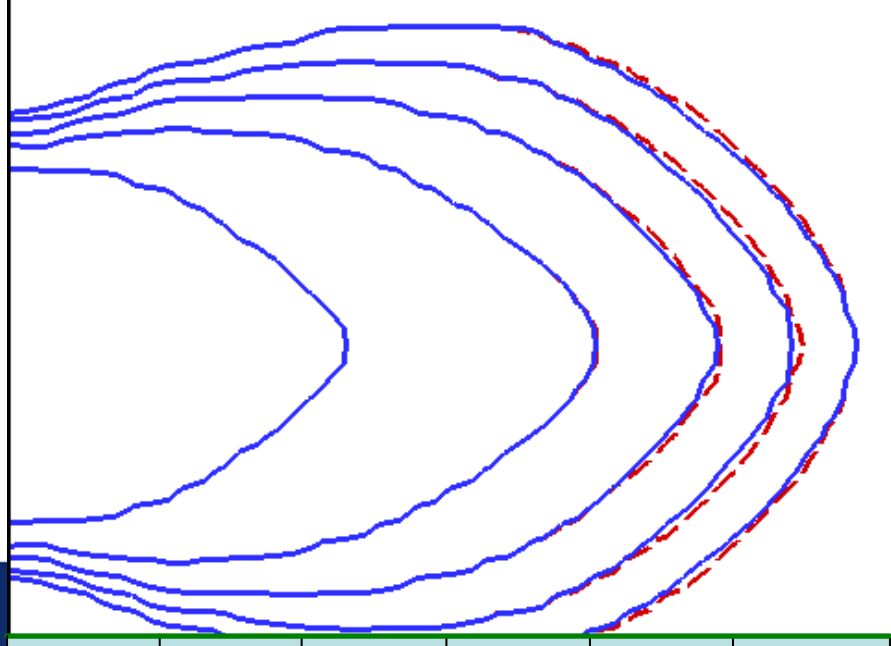
G-A	0.031	0.053	0.053	0.028	0.042
-----	-------	-------	-------	-------	-------



G-B	0.029	0.038	0.057	0.035	0.069
-----	-------	-------	-------	-------	-------

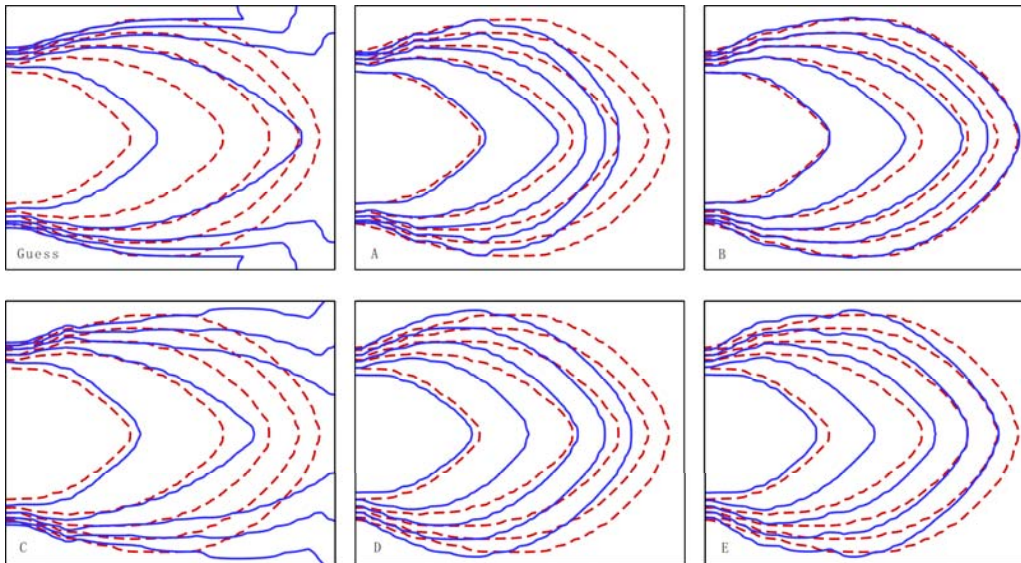


G-D	0.030	0.040	0.050	0.042	0.070
-----	-------	-------	-------	-------	-------

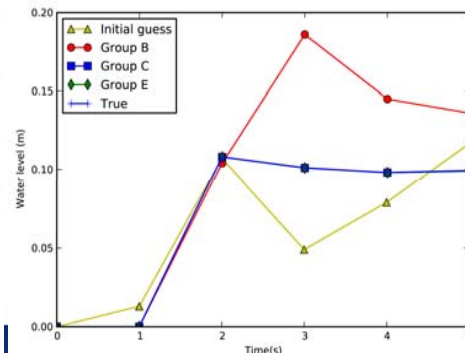
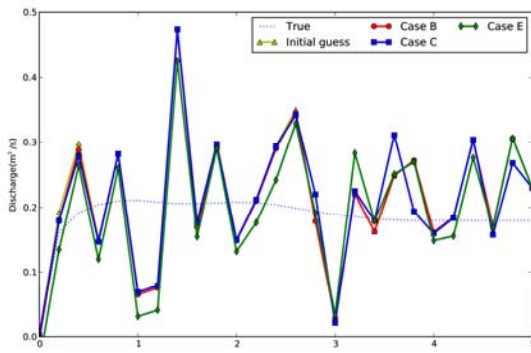


G-E	0.030	0.040	0.050	0.044	0.071
-----	-------	-------	-------	-------	-------

Experiment series C: Identification of the n values and inflow discharge

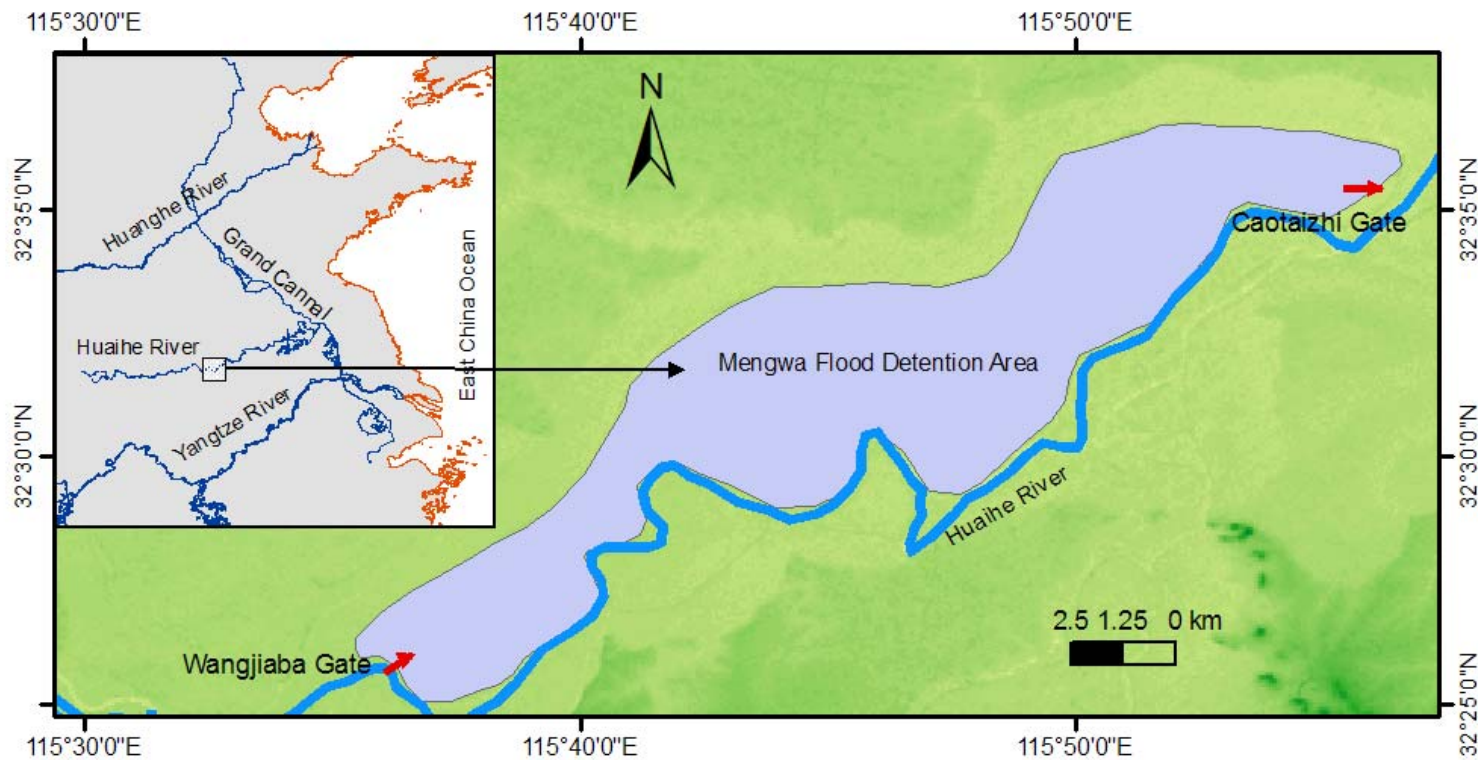


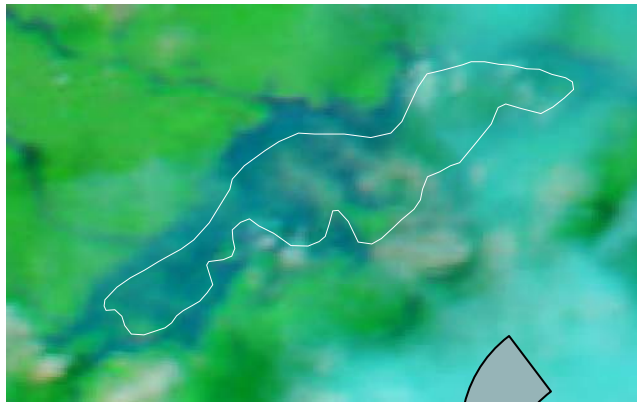
The RMSEs of the runs assimilating observations of Group A, B, C, D and E decrease by 50%, 64%, 45%, 48% and 41%, respectively.



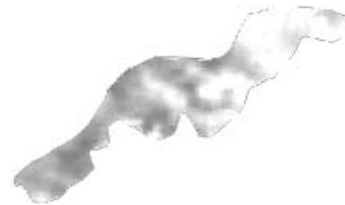
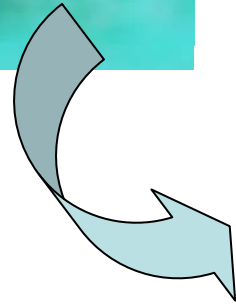
Assimilation of real remotely sensed flood extent

Study area





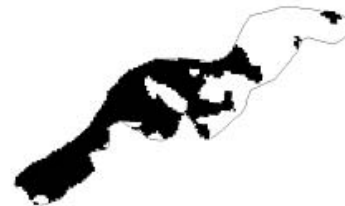
MODIS data with 250m resolution
at 11 July, 2007 over Mengwa Flood Retention Area



luminance



DN = 110



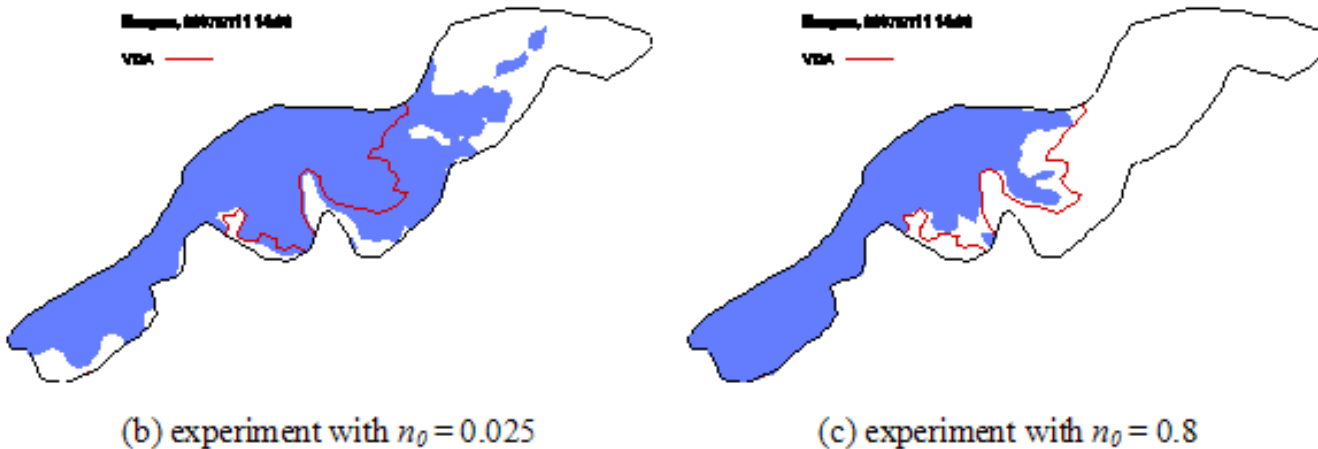
DN = 121



DN = 126

Luminance of MODIS image with Band 7-2-1 and the extracted flood extent with different threshold values of digital number (DN)

Results



- Assimilation of flood extent extracted from MODIS data with 250m resolution into 2D model, the Manning roughness coefficient, n is identified to improve the analysis of flood routing over the Mengwa Flood Retention Area.
- The computed flood extents based on different initial guess n_0 values (blue covered area) are compared with the results with variational data assimilation method (labeled as VDA, red line). We obtained the consistent flood extents (red line) in both experiments as shown in (b) and (c) with different initial guess n_0 values by using the variational data assimilation method

Thank you for your attention!